AXIAL CAPACITY OF PILES SUPPORTED ON INTERMEDIATE GEOMATERIALS

by

Heather Margaret Brooks

A thesis submitted in partial fulfillment
of the requirements for the degree

of

Master of Science

in

Civil Engineering

MONTANA STATE UNIVERSITY
Bozeman, Montana

July 2008

APPROVAL

of a thesis submitted by

Heather Margaret Brooks

This thesis has been read by each member of the thesis committee and has been found to be satisfactory regarding content, English usage, format, citation, bibliographic style, and consistency, and is ready for submission to the Division of Graduate Education.

Robert Mokwa, Ph.D., PE

Approved for the Department of Civil Engineering

Brett Gunnink, Ph.D., PE

Approved for the Division of Graduated Education

Dr. Carl A. Fox

STATEMENT OF PERMISSION TO USE

In presenting this thesis in partial fulfillment of the requirements for a master's degree at Montana State University, I agree that the Library shall make it available to borrowers under rules of the Library.

If I have indicated my intention to copyright this thesis by including a copyright notice page, copying is allowable only for scholarly purposes, consistence with "fair use" as prescribed in the U.S. Copyright Law. Requests for permission for extended quotation from or reproduction of this thesis in whole or in parts may be granted only by the copyright holder.

Heather Margaret Brooks

July 2008

DEDICATION

For my parents, family and friends, the people who have helped me through the difficult times. Thank you all.

TABLE OF CONTENTS

TABLE OF CONTENTS CONTINUED

LIST OF TABLES

LIST OF FIGURES

LIST OF FIGURES CONTINUED

Figure Page

TERMINOLOGY

α	=	adhesion factor
A	=	plugged pile area
A_{open}	=	area of steel within the pile cross section
B_b	=	drilled shaft diameter
BC	=	blow count
C	=	claystone
c_a	=	adhesion
CAPWAP	=	CAse Pile Wave Analysis Program
$CAPWAP_{shaft}$	=	CAPWAP measured shaft resistance
$CAPWAP_{toe}$	=	CAPWAP measured toe resistance
CDOT	=	Colorado Department of Transportation
cIGM	=	cohesive IGM
CN	=	control number
CP	=	closed ended pipe pile
c_u	=	undrained shear strength
D/10	=	static load test failure criteria, load at deflection equal to $B_b/10$
Dav	=	Davison method of static load determination
Drill	=	groundwater level during drilling
Dr/Res	=	groundwater level immediately after drilling
E*	=	total potential energy
E	=	young's modulus of the cushion
Early Refusal	=	pile is driven to a very low set at a depth that is less than the anticipated design length
End-bearing	=	portion of ultimate capacity derived from toe compression resistance
F_{eff}	=	hammer efficiency parameter
FHWA	=	Federal Highway Administration

f_s	=	unit side resistance
FS	=	factor of safety
f_y	=	steel yield strength
H	=	H-pile
ITD	=	Idaho Transportation Department
IGM	=	Intermediate Geomaterial
$Input_{new}$	=	new input for DRIVEN
K_o	=	coefficient of lateral earth pressure at rest
Loc Sc	=	local scour around a pile
LPC	=	Laboratoire des Ponts et Chaussees, static load test failure criteria
LT Sc	=	long term channel scour
M	=	multiple/percentage increase of original MDT inputs
Max	=	maximum load applied to pile
MDT	=	Montana Department of Transportation
MDT_{input}	=	MDT original DRIVEN input
MDT DRIVEN	=	capacity calculated from original MDT inputs
N_{60}	=	adjusted SPT N-value
N_c	=	penetration resistance
N_{shaft}	=	normalized CAPWAP shaft resistance
N_{slayer}	=	normalized shaft resistance calculated with DRIVEN IGM layer predicted shaft resistance
N_t	=	normalized CAPWAP toe resistance
O/C	=	open or closed ended pipe pile
OP	=	open ended pipe pile
Overflow	=	indicates second bridge structure on project
ϕ’	=	drained friction angle
ϕIGM	=	cohesionless IGM
P	=	pipe pile
p	=	pile perimeter

p_a	=	atmospheric pressure
PDA	=	Pile Dynamic Analyzer
Perim.	=	pile perimeter
Pen.	=	pile embedment length
PSC	=	prestressed concrete pile
q_{max}	=	maximum end bearing stress
$q_{reduced}$	=	reduced end bearing stress
q_u	=	unconfined compressive strength
R*	=	SPT refusal
R	=	CAPWAP restrike calculation
RC	=	reinforced concrete pile
R_{CDOT}	=	CDOT calculated capacity
R_{MWSDOT}	=	WSDOT gates capacity calculated from measured energy transferred to the pile
R_{PWSDOT}	=	WSDOT gates capacity calculated with potential energy
RR	=	CAPWAP second restrike calculation
Running	=	actual pile length exceeds the anticipated design length
σ’	=	vertical effective stress
S	=	sandstone
Sh	=	shale
Shaft Capacity	=	portion of ultimate capacity derived from shaft frictional resistance
Si	=	siltstone
Soft Soil	=	depth of down-drag condition soil
SPT	=	Standard Penetration Test
Stiff.	=	cushion stiffness
TE	=	energy transmitted to the pile
Ult	=	ultimate, long term water table depth
WSDOT	=	Washington Department of Transportation

ABSTRACT

Pile foundations used to support bridges and other structures are designed and installed to sustain axial and lateral loads without failing in bearing capacity and without undergoing excessive movements. The axial load-carrying capacity of a driven pile is derived from friction or adhesion along the pile shaft and by compressive resistance at the pile tip. There are well-established analytical methods for evaluating pile capacity and for predicting pile driving characteristics for cohesive soil, cohesionless soil, and rock. However, past experience indicates these methods may not be reliable for piles driven into intermediate geomaterials (IGMs), which often exhibit a wide array of properties with characteristics ranging from stiff or hard soil to soft weathered rock. Methods to determine the axial capacity, driving resistance, and long-term resistance of piles driven into intermediate geomaterials are not well established.

Nine projects, in which piles were driven into IGMs, from the Montana Department of Transportation were analyzed. Each project contained information from CAPWAP dynamic analyses, construction records, and design reports. The purpose of any analyses, of the nine projects, was to better predict the behavior of piles in IGMs. IGMs were divided into two broad types, cohesive and cohesionless. The computer program DRIVEN is often used to predict the axial capacities of piles; however, in IGMs the design method is unreliable. Attempts were made to determine trends within the available data. Normalized resistances for shaft and toe capacities did yield slight correlations of shaft resistance to pile length in IGMs. Iterative solutions using DRIVEN to match the CAPWAP ultimate capacity did not provide meaningful trends or correlations. Slight modification of MDT's original DRIVEN inputs was required in most cases to match the CAPWAP ultimate capacity. Because no meaningful trends were found from analysis, other capacity calculation methods were used to determine other methods that accurately predict pile capacity within IGMs. The Washington Department of Transportation Gates formula is the most accurate method of those attempted. More research is required for further analysis of piles in IGMs.

CHAPTER 1

INTRODUCTION

Pile foundations are designed and installed to sustain axial and lateral loads without bearing capacity failure or excessive settlements. Axial resistance is developed from a combination of friction or adhesion along the pile shaft and compression resistance at the pile toe.

Bridge foundations within the state of Montana are often founded on driven piles, due to their high axial and lateral capacity and resistance to settlement. Geotechnical engineers use the computer programs DRIVEN and GRLWEAP to determine the axial capacity of these piles. The computer program DRIVEN is used to calculate the ultimate axial static capacity of a pile based on soil strength characteristics (Mathias and Cribbs 1998). The computer program GRLWEAP is used to help select the pile driving hammer and system, and to predict the response of the pile during driving (GRLWEAP 2005). These computer programs were developed for use as design and analysis tools to predict pile behavior in soil.

The axial capacity of some bridge foundations necessitates driving piles into materials that are classified within the continuum bracketed by soil and rock. In recent technical literature, these materials have been classified using the term intermediate geomaterials (IGMs). In the past, other names have been used for IGMs, including: formation materials, indurated soils, soft rocks, weak rocks, and hard soils.

Experiences during construction indicate that piles driven into IGMs do not always behave as predicted. Piles driven into IGMs stop short of their design elevation

(premature refusal) or require driving to greater depth (known as running) to achieve the required capacity. IGMs do not behave predictably, even with the advanced computer programs available to predict axial capacity and driving behavior. Pile Dynamic Analyzer (PDA), a capacity analysis method conducted in the field, on these projects have displayed higher or lower than predicted capacities due to refusal and running, respectively. Construction costs for foundations can be greatly increased due to unpredictable capacity and drivability behavior in IGMs.

Because the behavior of piles founded in IGMs is not well known, Montana Department of Transportation (MDT) often recommends evaluating the post-driving axial capacity in the field by conducting a PDA. Other capacity analyses include static load tests and CAPWAP analyses. Static load tests involve driving reaction piles and complex monitoring systems; consequently, this type of testing, while accurate, is relatively expensive and is not commonly used by MDT. PDAs are conducted during pile driving (or restrike) by attaching accelerometers and strain gages to the pile. The pulses of stress that travel down the length of the pile and reflect upward are monitored and are used to determine the ultimate capacity using stress-wave theory, signal matching techniques and the computer program CAPWAP can be used to further refine the analyses.

The purpose of this study was to determine if an improved method of analysis could be employed to evaluate piles driven into IGMs using data obtained from Montana Department of Transportation (MDT) construction projects. This involves evaluating the accuracy of current design methods, assessing existing trends within the provided data, and determining the accuracy of other existing capacity prediction methods.

Another purpose of this study is to determine relationships between the DRIVEN and GRLWEAP program inputs, construction observations, and CAPWAP capacities from the PDA analyses. The goal is to be able to better predict the behavior of piles driven into IGMs with respect to axial capacity and depth of embedment. The information needed to meet these research objectives includes:

- DRIVEN reports,
- CAPWAP analyses,
- actual end-of-driving blow counts,
- GRLWEAP results, and
- capacities calculated using different predictive methods.

CHAPTER 2

OVERVIEW OF INTERMEDIATE GEOMATERIALS

Intermediate geomaterials (IGMs) reside at the center of a continuum between soil and rock (Johnston and Novello 1993). Thus, principles from both soil and rock mechanics apply to IGMs in terms of material behavior and design methodology. The analysis and design of piles within IGMs must include a geologic component (focused on method of formation) and a geotechnical component (focused on the engineering response) (Papageorgiou 1993). Gannon et al. (1999) accurately describes IGMs in the following quote:

> *"Weak rocks are either intrinsically weak (they have undergone a limited amount of gravitational compaction and cementation), or they are products of the disintegration of previously stronger rocks in a process of retrogression from being fully lithified and becoming weak through degradation, weathering and alteration."*

IGM formation processes fit into two basic categories: 1) soil has been strengthened, or 2) rock formations have been weakened to the level of IGM strength. Regardless of the formation process, IGM engineering properties vary with the geologic and geotechnical components of the IGM. Within the scope of this investigation, there are two overriding types of IGMs, cohesive and cohesionless. Cohesive IGMs include IGMs with an intrinsic component bonding; for example, siltstone, claystone, mudstone, sandstone, argillaceous, and arenaceous materials. Cohesionless IGMs include materials without an intrinsic particulate bonding, which primarily includes very dense granular materials.

Definition of IGMs

Because of their variability, the behavior of IGMs is far from predictable. Wide ranges of material behavior have resulted in a multitude of disparate definitions in the literature, all based on material strength. The most common laboratory test used to define an IGM is the laboratory unconfined compression (uniaxial) test. The most common field test, in-situ standard penetration test (SPT), has also been used to define IGMs. Table 1 summarizes definitions of IGMs from multiple sources using the unconfined compression value or the SPT N-value.

Table 1. Definition of IGMs by Author

Author (Year)	Type of IGM	Definition
Clarke and Smith (1993)	All	Unconfined Compression < 5MPa
International Society of Rock Mechanics (de Freitas 1993)	All	Unconfined Compression 5-25 MPa
Geological Society of London (de Freitas 1993)	All	Unconfined Compression 1.25-5 MPa
Finno and Budyn (2000)	All	Unconfined Compression 0.5-5 MPa SPT N-values >50 Blows/ 0.3 m
Marinos (1997)	All	Undrained Cohesion > 0.3 MPa Unconfined Compression > 2 MPa
Johnston (1989)	All	Unconfined Compression >0.5 MPa
Gannon et al. (1999)	All	Unconfined Compression >0.6 MPa
Akai (1997)	All	Unconfined Compression 1-10 MPa
O'Neill et al (1995)	All	Unconfined Compression 0.5-5 MPa
Mayne and Harris (1993)	Cohesionless	SPT N-values > 50 blows/ 0.3 m
de Freitas (1993)	Arenaceous*	Unconfined Compression 1-25 MPa
Dobereiner and de Freitas (1986)	Sandstone	Saturated Unconfined Compression from 0.5-20 MPa

*Arenaceous – sand based sedimentary rock

The definition of IGMs using the SPT method is generally recognized as an SPT N-value of greater than 50 blows per 0.3 meters (Mayne and Harris 1993, Finno and Budyn 1993). However, there is no consensus regarding a limit based on the unconfined compression strength. The lower limit in the literature ranges from 0.5 to 5 MPa, with the upper limit ranging from 5 to 25 MPa. The wide range of published definitions is indicative of the variability of IGM geotechnical engineering properties.

Behavior of IGMs

"IGM is heterogeneous, with many inhomogeneities, particularly over horizontal and vertical distances comparable to the length, breadth, and separation of pile sockets," (Gannon et al. 1999). The variation in material strength over small distances emphasizes the need for geological and geotechnical considerations when evaluating IGM properties (Krauter 1993). Geological considerations include the formation method, jointing, fissuring and strength of the formation mass. Geotechnical considerations include the type of bonding between the particulates, and any frictional components.

Geological components of IGMs are specifically related to the behavior of the formation mass. A rock formation can be weak due to the geometry of its joints and fissures or the material itself can be weak. As in rock, if the constituent rock is strong and the jointing geometry causes weakness, the formation will be weak. However, if the constituent rock is weak then the overall formation will also be weak. IGMs exhibit the same properties: the material itself may be weak or the jointing characteristics may cause weakness. There are two property types to be analyzed when discussing IGMs, 1) the

formation mass properties, which include joints and fissures, and 2) constituent material properties, which focus on the material specifically. Constituent material properties are typically determined from tests on samples from boreholes. These types of samples are useful for examining material properties, but do not give a good indication of jointing and fissuring. Either the formation mass properties or the IGM constituent material control the weakness and behavior (Hsu and Nelson 1993, Akai 1993).

Some soil mechanics principles apply in IGMs. It has been observed that the maximum pore water pressure within mudstone triaxial testing occurs at the peak strength of the material (Wu, Marsden and Hudson 1993). Because the effective stresses at failure occur when the pore water pressure is the highest, this provides evidence towards effective stress principles applying within mudstone (Johnston 1989). Extrapolating this idea to mudstone behavior, if effective stress principles apply, than Mohr-Columb failure conditions may be valid as well (Wu, Marsden and Hudson 1993).

Within mudstone, the pore and sample volume changes coincided, showing that the material matrix is incompressible, but still influenced by pore water pressure (Wu, Marsden and Hudson 1993). Because the matrix of the material cannot consolidate further, the compression characteristics of the material relate to the coefficient of volume compressibility, a measure of the compressibility of the material matrix, and not the coefficient of consolidation, the measure of the compression of the particles within the material (Haberfield and Johnston 1993). While permeability characteristics in soil are often based on the coefficient of consolidation, in mudstone, this does not provide an accurate measure of the movement of pore water.

Analyses of the geologic components of a material must also include the stress states of the in-situ material as they are directly related to geologic processes. The stress history of mudstone affects the deformation and strength properties; for example, the mechanical behavior of IGMs changes from ductile to brittle with the increase in confining pressure (Wu et al. 1993, Atkinson et al. 1993, Akai 1993). Along with the stress history of IGMs, other geologic processes can affect IGM engineering behavior. The extent of IGM weathering can drastically change the elastic moduli of mudstone (Reeves, Hilary and Screaton 1993).

Geotechnical components of IGMs include the types of bonding between the particles within the IGM specifically chemical bonding. For example, caliche is formed through the evaporation of pore water. As the pore water evaporates, dissolved salts are deposited on particles of sand and silt. Over time, the salts form bonds between particles and a very strong formation is created with high apparent shear strength (Yilmazer 1993). The particle compression that occurs during lithification or diagenesis forms chemical bonds between the particles of the material.

Types of bonding can also be affected by external sources, including fresh water. For example, most cohesive IGMs degrade with exposure to water (Spink and Norbury 1993). The component bonding of cohesive IGMs is often due to lithification, which is the slow compression of the material matrix pressing the pore water from the pore space. When exposed to fresh water, an increase in water content along with the released overburden pressure from sample removal causes the bonding to decrease and consequently a reversal of the lithification process. Argillaceous IGMs, like mudstone

and shale, are particularly prone to degradation. Observed strength losses of greater than 60% in shale and 40% in mudstone are not uncommon (Spink and Norbury 1993). Arenaceous material can also lose strength when exposed to water (de Freitas 1993).

Cohesive IGMs often contain clay particles, which can influence the bonding chemical reactions. Clay content of the in-situ material can also affect the behavior when exposed to water. In one case, low clay content mudstone exhibited a collapsible behavior and high clay content caused expansive behavior (El-Sohby, Mazen and Aboushook 1993). In another case, expansive behavior in a very dense clay IGM deposit displayed swelling pressures greater than the overburden stresses within the lithology (Brouillette, Olson and Lai 1998).

Cohesionless IGMs, by definition, have no intrinsic bonding. Thus, geotechnical analysis methods are typically applied to determine the frictional characteristics of the particulates. Dense sandy gravels are the most common type of cohesionless IGMs in Montana. These dense sandy gravels undergo significant dilation before failure, creating high friction angles. Dilation is the volume increase that occurs when load is applied and mass expands as particles move around each other in order to induct failure in the material.

Causes of Weakness

The shear strength of IGMs is less than intact rock, but greater than soil. This relative weakness in IGMs is due to the processes by which IGMs are formed. Either the strengthening processes were interrupted or the disintegration process reduced the

strength into the realm of IGMs (Gannon et al. 1999). The strengthening process includes deposition followed by lithification, diagenesis or cementation. The weakening processes are controlled by weathering. These processes are shown within Figure 1.

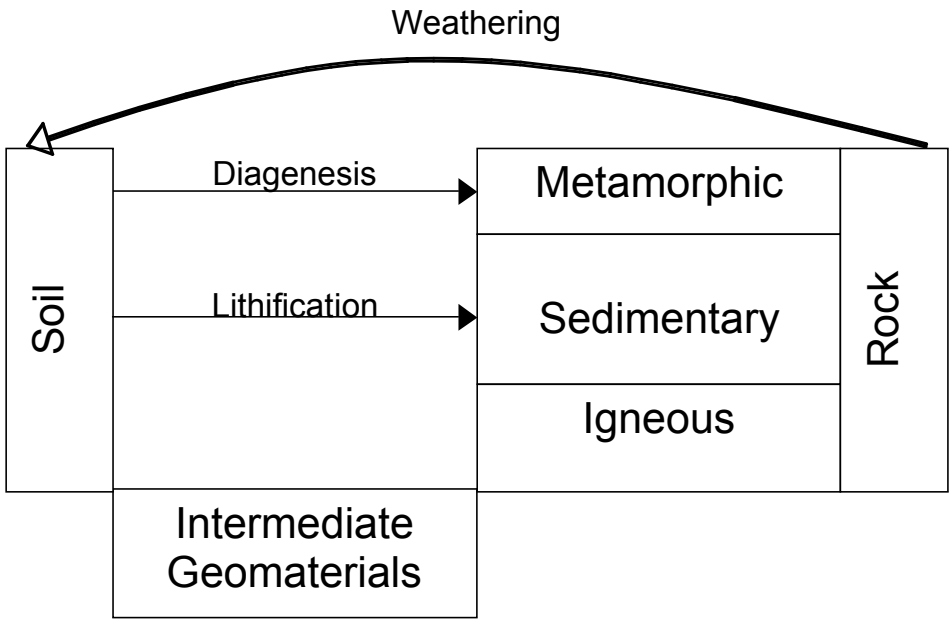

Figure 1. IGM formation processes.

Strengthening processes form sedimentary and metamorphic IGMs. Lithification is a formation process for sedimentary rock, in which the material is compressed causing pore water to slowly be pressed from the pores of the IGM allowing bonding to form between the original particulates. Diagenesis is a metamorphic process, in which there is a physical, chemical or biological change in the sediment causing bonding to form. Intrinsic weaknesses can form during these processes, which include: loose texture (poor bonding), the presence of cavities, and poor cementation (Tanimoto 1982, Oliveira 1993). Cavities within the matrix of an IGM can severely reduce the strength and stiffness

properties, due to the lack of load transfer through void regions. Cementation is the process of bonding particles with salts left behind as pore water evaporates. The loose texture and poor cementation bonding between the particles within the IGM matrix are due to incomplete strengthening processes.

Weathering is the process of strength reduction in rock masses. It affects strength in two forms, mechanical and chemical (Clayton and Serratrice 1993). Mechanical weathering includes a reduction in overburden stress, thermal changes, techonisation, and freeze thaw effects. Joints and fissures are formed through all mechanical weathering processes. Reductions in overburden stress cause fracturing due to the release of pressure in the vertical direction. Techonisation is the process of forming joints and fissures due to earthquake stresses and movements. Dissolution, hydrolysis, oxidation and carbonation form the processes of chemical weathering, which damage the component bonding of the material. For example, carbonation causes the formation of carbonic acid, a common ingredient in acid rain, which dissolves limestone formations. The engineering properties of IGMs vary greatly with the extent of material weathering (Cripps and Taylor 1981).

IGM Properties Summary

IGMs vary widely and many authors have tried to definitively determine the properties and behaviors. Cohesive IGMs are defined by uniaxial compression test strengths between 0.5 MPa and 25 MPa (Johnston 1989). SPT-N values of greater than 50 blows per 0.3 meters define cohesionless IGMs (Mayne and Harris 1993).

IGMs often exhibit heterogeneities that vary over distances, which are comparable to the length, breadth and separation of pile sockets (Gannon et al. 1999). Abrupt changes in subsurface conditions emphasize the value of both geological and geotechnical considerations when conducting a site evaluation where IGMs are suspected.

The geologic factors of IGMs influence the behavior of the material in two ways: the intrinsic IGM material strength and the overall formation behavior. The intrinsic IGM material strength is the strength of the bonded geomaterial, excluding the impacts of jointing and fissuring. Joint and fissure impacts on properties and strengths, are included within the overall formation behavior.

Geotechnical considerations include an evaluation of bonding forces that contribute to IGM strength. The bonding between the particulate material comprising IGMs will often degrade in water; for example, shale and mudstone observed a 60% and 40% loss in strength, respectively. The clay content also affects the expansive or collapsible behavior of IGMs.

The causes of relative weakness in IGMs are either the weakening of a stronger rock formation or the strengthening of a soil deposit. Lithification, diagenesis, and cementation strengthen formations by creating chemical bonding between the particles. Because the bonding processes are not complete, intrinsic weaknesses within the formation exist, including: loose texture, cavities, and poor cementation. The cavities within a formation reduce the surface areas for load transfer, thus increasing the stress in those regions.

IGMs in Montana

IGMs typically encountered in Montana include both cohesive and cohesionless. Cohesive IGMs in Montana are often shale, claystone, siltstone and sandstone, while cohesionless IGMs observed within the projects studied are exclusively dense sandy gravels often containing high quantities of silt. A location map of the projects studied along with the IGM type is shown in Figure 2.

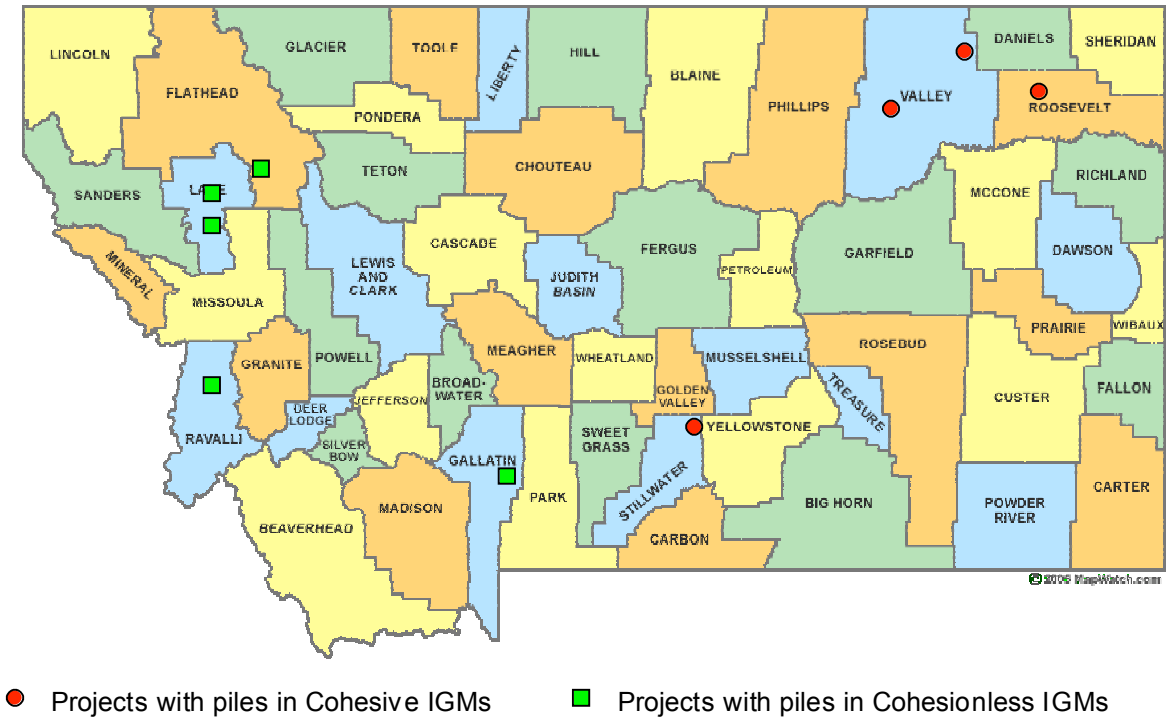

Figure 2. Map of project locations and IGM types in Montana.

In all cases evaluated in which piles were driven into cohesive IGMs, the pile refused before reaching the design depth. In these instances, the CAPWAP calculated capacity at this higher elevation was similar or greater than the required capacity at the

design elevation. Projects in which piles were driven into cohesionless IGMs observed running behavior. These piles required extended driving to greater depths than predicted. In these cases, the CAPWAP predicted capacity was either similar or lower than the required design capacity, even at this greater depth.

Sampling and Testing Methods

Laboratory testing methods cannot fully correct for disturbances that occur when IGM samples are collected using either soil or rock sampling methods. Research conducted by de Freitas (1993) recognized that larger differences in strength are apparent between laboratory and field-testing as the strength of the IGM decreases. Current sampling methods cannot be used to collect reasonably undisturbed samples of IGMs, which is one cause of the discrepancy between laboratory and in-situ testing methods. This can cause mistaken classification of geomaterials. For example, an IGM on the lower boundary of strength may be mis-classified as a dense soil, if the sampling process excessively disturbs the sample. Gannon et al. (1999) writes:

> "*Early recognition of the presence of weak rock and the need for a piled foundation solution are essential for an effective site investigation to be planned and executed. For piling in weak rock the investigation involves three broad considerations: nature, properties and behavior."*

Most subgrade investigations rarely investigate IGMs as an independent material; investigations include the soil and the bedrock materials but not the material in between. IGM sampling is complicated, because soil-sampling methods do not work well and rock-sampling methods do not yield good samples for lab testing (Oliveira 1993).

Sampling

The most common methods for sampling IGMs include the standard penetration test (SPT) and rock coring; however, neither of these methods result in undisturbed samples. Therefore, attention must be paid to the investigation methods used to sample the IGM, in order to accurately interpret the testing behavior of the material.

SPT should not be the primary sampling method. IGMs can damage the SPT sampler, yielding skewed SPT N-values with severely disturbed samples (Thompson and Leach 1989). Rock coring does work adequately within IGMs. IGMs typically have very poor rock quality designation and core recoveries can vary from 10 to 80% depending on the IGM strength. Drilling fluid can impact the observed strength properties of the IGM, as noticed with the impact of fresh water on mudstone and shale.

Large blocks of geomaterial taken intact from the subsurface are known as block samples. Cripps and Taylor (1981) determined that block sampling can yield reliable laboratory testing results. They also concluded that the specimen orientation significantly affects the observed strength of the material (Cripps and Taylor 1981).

Solutions to the difficult sampling process will require more research and further ingenuity. New sampling methods can be developed to collect undisturbed samples or samples with less disturbance (Akai 1993, Reddy and Sastri 1993). Other options for IGM investigation include overlapping the soil and rock sampling techniques to provide a more accurate picture of the IGM (Gannon et al. 1999). Also, the generation of a model that contains all relevant site information can provide a more accurate pile capacity prediction. This model should include the following information:

- geology,
- overburden,
- geometry,
- groundwater conditions,
- properties of the rock, and
- the predicted behavior of the system.

This model can be useful in design and the generation of a sampling program (Gannon et al. 1999).

In-Situ Testing of IGMs

In-situ tests address the problems of IGM sampling (Gannon et al. 1999). Testing IGMs in their in-situ state of stress is preferable to analyzing the material in a laboratory, due to sampling issues and formation disturbance during sampling. Common in-situ tests include plate load tests, pressuremeter tests, SPT and rock coring. While these methods improve the predicted behavior, more methods are needed specifically for IGMs (Atalla 1993).

The main purpose of the plate load test is to evaluate the stiffness properties of large volumes of geotechnical materials that contain defects, such as joints and fissures (Johnston 1995, Campos et al. 1993). However, the test is expensive, difficult and the properties of the material can change with the required test site preparations (Clarke and Smith 1993).

The pressuremeter test is also used on IGMs and can be more accurate than laboratory testing of samples (Akai 1993). This test provides the strength and stiffness

properties of the formation (Haberfield and Johnston 1993). Pressuremeter testing can be conducted in two ways; either the pressuremeter apparatus is placed in an existing borehole or a special self-boring pressuremeter is used. The self-boring pressuremeter is recommended, because it can drill into a formation while minimizing changes to in-situ stresses or properties (Clarke and Smith 1993).

Because IGMs are known to exhibit different properties in the horizontal and vertical directions due to in-situ stresses, pressuremeter testing can yield different results in the horizontal and vertical directions. The length of the pressuremeter device, compared to the geometry of joints and fissures within the formation, allows for the measurement of jointing and fissuring impacts on strength, if the length of the pressuremeter is significantly long. Nevels and Laguros (1993) recommend applying pressuremeter testing only when deformation controls the design of structures founded on IGMs. Others designers are reluctant to use the test, stating that it needs more research (Findlay and Brooks 1995).

The amount of energy required to collect a sample of material can be correlated to the strength of the material. For example, SPT and penetration rate of rock coring can be correlated to the strength of the material. The penetration rate of rock coring can be used to determine in-situ stresses of a formation. Sorensen et al. (1993) found a significant inverse correlation between rate of penetration (rock coring) and the horizontal stress in the formation; the slower the penetration rate the higher the stress within the formation. The correlations between the SPT N-value and the friction angle of soils are well documented, but extrapolating this idea for IGMs yields very different results.

Thompson and Leach (1989) found a linear correlation between SPT N-values and a ratio of shear modulus to shear strain modulus (geological moduli). There is also a good correlation between SPT N-values and pressuremeter parameters calculated from measurements near the center of the pressuremeter probe (Nevels and Laguros 1993). Other than the limited successes with SPT correlation within IGMs, the SPT does not provide a reliable measure of IGM strength (Tomlinson 1977).

Laboratory Testing of IGMs

Currently available testing equipment often cannot measure the stiffness of IGMs over the range of interest (Atkinson et al. 1993). Available triaxial equipment may not have the loading capacity to test IGM samples or the displacement measurement sensitivity to determine the stiffness and strength properties of IGMs. However, triaxial and unconfined compression testing is used most often with IGMs. Unconfined compression testing provides only a strength measurement.

Triaxial testing provides consolidation and strength properties of the sample. Often rapid initial consolidation has been noticed during triaxial testing due to the draining of pore water from microfissures in the IGM structure (Brouillette et al. 1993). These weak horizontal planes and microfissures within the IGM control the failure plane of the sample, unlike the typical failure plane in soil (Brouillette et al. 1993). In IGMs, the triaxial behavior depends on the confining pressure. At high confinement, IGMs exhibit rock-like behavior and at low confinement, soil-like behavior (Cripps and Taylor 1981).

Unconfined compression testing is a form of triaxial testing in which the cell or confining pressure is zero gage or atmosphere. Analysis of unconfined compression testing must include information in the following areas:

- the test is most widely used in rock,
- sample preparation is very important,
- increased moisture content or saturation can negatively affect the strength, and
- strength can also vary with the sample orientation (Dobereiner and de Freitas 1986, Akai 1993).

Some authors have also conducted oedometer testing on IGM samples. Akai (1993) observed that oedometer results can overestimate the settlement by factors of 10 to 30.

Summary of Sampling and Testing Methods

Many sampling and testing methods have been used to evaluate IGMs. Soil and rock sampling methods have been used, yet neither yield satisfactory results (Clarke and Smith 1993). In-situ testing methods are recommended, but their accuracy in IGMs is disputed. Even laboratory testing of IGMs has not yielded the accuracy usually expected from soil sample analysis.

No currently avaiable sampling methods provide reasonably undisturbed samples in IGM deposits. The weaker the IGM, the more disturbed the sample and the more inaccurate the result of subsequent laboratory testing (Thompson and Leach 1989). The common sampling methods, SPT and rock core, often have very poor sample recovery

(de Freitas 1993). For the most part, new methods need to be created to decrease the amount of sample disturbance and lower the testing cost (Reddy and Sastri 1993).

Of the in-situ testing methods, the self-boring pressuremeter is the recommended test for use in IGMs, due to its limited changes to the in-situ formation stresses (Clarke and Smith 1993). Strength and stiffness properties of the formation can be accurately determined with the pressuremeter test (Haberfield and Johnston 1993).

Triaxial and unconfined compression laboratory testing is often used to obtain IGM properties. The unconfined compression test is most often used due to the wide loading range usually available. The resulting material strength from unconfined compression testing decreases with increased moisture content or saturation of the material (Dobereiner and de Freitas 1986). Changes in the failure mode of IGMs due to the triaxial tests' confining pressure observed that the higher the confining pressure, the more brittle the failure (Cripps and Taylor 1981).

CHAPTER 3

BACKGROUND OF ANALYTICAL METHODS

Pile foundations are commonly used for bridges and buildings when the soil cannot support the applied loads without excessive settlement, or the nature of loading cannot adequately be supported on shallow foundations. Most bridges require deep foundations due to the combination of loads and moments, and the potential for scour. Pile foundations, used to support the bridge structure, are the main focus of this project.

Pile axial capacity consists of a sum of shaft resistance (skin friction) and end bearing (tip resistance). Static axial capacities can be calculated using DRIVEN, and the drivability of a pile can be determined using the computer program GRLWEAP. This is a common approach used by the Geotechnical Section of Montana Department of Transportation (MDT). In some cases, lateral loads may control pile length; usually calculated using the computer program L-PILE. However, axial loading most often controls the design of piles extending into IGMs. This capacity can be evaluated or tested using the Pile Dynamic Analyzer (PDA) and the Case Pile Wave Analysis Program (CAPWAP).

Computer programs used in pile design fall within two categories predictive and capacity analysis. Descriptions and uses of each program are provided within Figure 3. Program accuracy increases from left to right and downward within the figure. Further analysis of each program is shown within the following discussion.

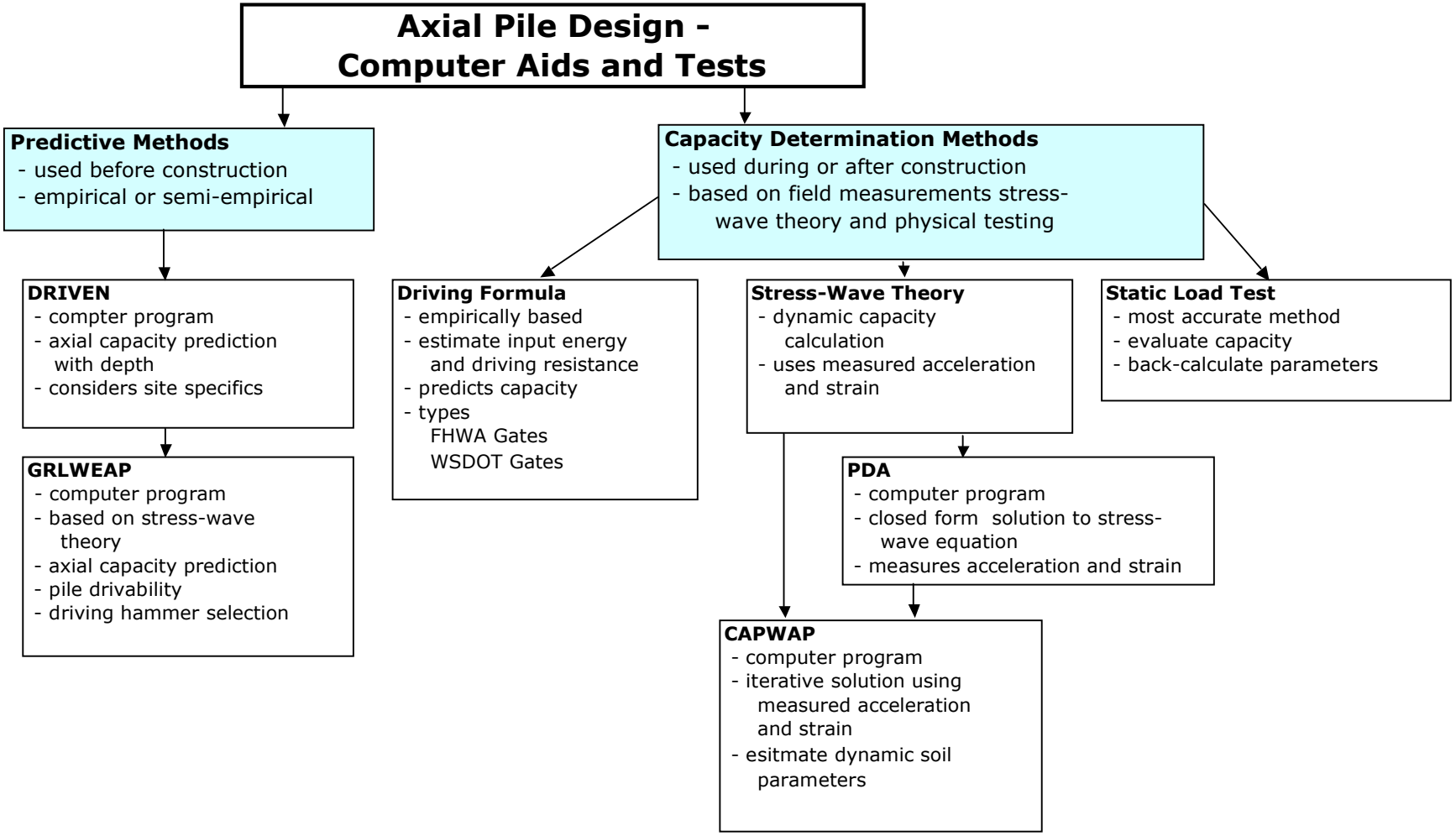

Figure 3. Flow chart of computer programs and capacity analysis methods.

DRIVEN

DRIVEN is a computer program created by the Federal Highway Administration (FHWA) to calculate the static axial capacity of a pile. This program automates the axial design process and allows the user to enter soil strength parameters within the lithology, site conditions, pile type and pile size in order to calculate capacity.

For each layer of the lithology, soil strength parameters are entered for either cohesive or cohesionless soils. Inputs for cohesive soil include undrained shear strength (c_u) or a user defined adhesion (c_a). Adhesion is an empirically derived factor that relates undrained shear strength to frictional resistance per unit area. The relationships between adhesion and undrained shear strength are derived from Tomlinson as cited in (Mathias and Cribbs 1998). The input of undrained cohesion is most often used within cohesive IGMs. Cohesionless soil inputs include SPT N-values or internal soil friction angles, for both side friction and end bearing. MDT typically used friction angles to input cohesionless IGMs. The Nordlund method is used to determine the capacity of piles in cohesionless layers (Mathias and Cribbs 1998).

Common pile types and parameters are programmed into DRIVEN. Multiple analyses can be conducted to determine the most economical pile type for a project. DRIVEN will automatically choose a "plugged" analysis with restrike and ultimate capacity calculations in both geomaterial types. Driving skin friction calculations and end bearing calculations are considered plugged after the depth driven is thirty times the diameter of the pile, for cohesionless soils (Mathias and Cribbs 1998).

Other factors needed to make an accurate calculation in DRIVEN are potential scour and down-drag conditions. Scour includes either local scour around each pile or pile group, and channel scour. Some soil lithologies include soils that induce down-drag conditions. DRIVEN addresses down-drag conditions by calculating the uplift pressures for the depth input and including this within the shaft capacity calculation.

After all the inputs are completed, DRIVEN calculates the end-bearing and shaft capacities verses depth for the long term, restrike and driving capacities. Outputs are presented in both graphical and tabular form. Thus, the required depth can be determined based on the required design capacity.

Based on time since driving, some assumptions about scour and pore water pressure are made in each calculation type. Driving capacity calculations include the assumption that no dissipation in excess pore water has occurred. Within restrike capacity calculations, DRIVEN methods assume the dissipation of excess pore water pressure but do not take scour into account. Ultimate capacity calculations take all factors into account to determine capacity.

The use of the Tomlinson method, within DRIVEN, has exhibited inconsistencies. Specifically, when the DRIVEN predicted capacity is compared to either static load test or CAPWAP capacities. Problems relate to the predicted bearing capacities of gravels with rounded particles, and limitations within built in methods for cohesive or materials.

Idaho Transportation Department (ITD) compared CAPWAP results to predicted capacities calculated by DRIVEN. In rounded riverbed gravels, DRIVEN capacity calculations from either SPT N-value inputs or friction angle inputs were compared.

Capacities from SPT N-value inputs were "significantly overestimated" due to an assumption within DRIVEN that friction angle of angular and rounded deposits are the same (Burgert and Buu 2007).

The Tomlinson α method is used to calculate the shaft capacity of piles in cohesive soils. The shaft capacity is calculated by summing the product of the pile perimeter, the depth of the cohesive layer and the adhesion. The adhesion is estimated from the Tomlinson α method by the following equation:

$$c_a = \alpha\, c_u \qquad (1)$$

where, α is an empirical adhesion factor. The value of α is determined from correlating α and a ratio of the undrained shear strength to the vertical in-situ effective stress at the center of the layer (Das 2005). DRIVEN, however, does not calculate an α value; adhesion is directly correlated to undrained shear strength. Also, the correlation does not extend beyond 150 kPa undrained shear strength, creating a limiting adhesion. For example, assume the unconfined compression strength is 200 kPa at a depth of 10 meters with soil unit weight of 22 kN/m^3 and a deep water table. Hand calculations using Tomlinson's charts directly are compared to DRIVEN calculations are as follows.

Direct Tomlinson solution proceeds as follows:

- The effective vertical stress at 10 meters is 220 kPa.
- The c_u/σ' ratio is 0.909.
- From Figure 11.24 (Das 2005), α is 0.52.
- c_a, from the hand calculation is 104 kPa.

Using this information and Figure 7-3 within the DRIVEN Users Manual, the DRIVEN c_a is 40 kPa (Mathias and Cribbs 1998). As shown, if DRIVEN used the standard Tomlinson's charts, the adhesion factor used to calculate the unit skin friction (f_s) could significantly increase in value, even with a limiting value of α. The difference within the calculated values of f_s is the primary reason for reduced shaft resistance predictions in DRIVEN with cohesive IGMs. This limitation of its design methods often needs to be considered only in the scope of IGM analyses. It is only significant for materials with high values of c_u, such as cohesive IGMs and very hard clay deposits.

Stress-Wave Theory

Many empirical formulas have been developed to relate the end of driving blow count to the static ultimate capacity of the pile. However, because the methods used to evaluate the energy transferred are crude, the solutions are approximate at best. The wave equation, first introduced by Smith (1960), uses waves of stress created during the pile driving process to determine the ultimate dynamic capacity of the pile.

The wave equation is used to track the movement of stress waves along a pile. A stress wave occurs when a force, like the blow of a hammer, impacts an object. The stress from the impact moves in a wave along the pile length. If the pile is bearing against a stiff or hard surface, like compacted soil, the initial impact wave will rebound, either in whole or in part. Comparison of the initial wave to the rebound wave provides a measure of the energy removed from the wave by the movement of soil along the shaft and toe of the pile.

In order to complete this calculation, a model was created to enable computer computation. The hammer impact is the initial energy within the system. That energy flows through the hammer cushion, which is modeled as a spring, transfers only a percentage of the overall energy to the pile. The coefficient of restitution is the percentage of the energy transferred to the cushion. The remaining energy continues through the helmet, modeled as a weight, and into the pile. The energy is transmitted thru the pile as a stress wave. The pile is represented as a series of weights and springs, each spring has stiffness equal to the Young's modulus of the steel. The relative displacement of each weight is used to model the movement of the wave along the system.

During driving, the energy loss properties of soil are modeled by quake and damping parameters. Quake is the amount of displacement a pile must undergo before the soil yields. A recommended value for both shaft and end quake of IGMs is 2.5mm. Quake is modeled using a spring. Energy is removed from the system until the quake displacement is reached within the spring. Damping represents the amount of energy that is removed from the system due to the movement of the soil along the shaft and at the toe of the pile. Modeled as a dashpot, energy is removed from the calculation a percentage of the pile velocity. This model is used within the calculations conducted by GRLWEAP and CAPWAP.

GRLWEAP

GRLWEAP is an iterative solution to the wave equation in which multiple combinations of inputs allow calculation of pile drivability, blow count versus resistance charts, and stresses within the pile during driving. GRLWEAP also calculates the ultimate capacity of a pile using the α and β methods with inputs from a file created within DRIVEN, or manually if a DRIVEN analysis was not conducted.

GRLWEAP inputs include hammer, pile and soil parameters. Common hammer systems are available in a database based on hammer and pile type. Hammer system parameters include ram weight, helmet weight, cushion thickness, cushion coefficient of restitution, cushion stiffness, cushion area, and cushion elastic modulus. These parameters can also be directly input within the graphical user interface. Inputs pile information includes pile type, elastic modulus, length, embedment length, cross-sectional area, perimeter and toe area. The geometric pile parameters can be calculated by GRLWEAP; however, when using this calculation method, the toe area is always assumed plugged.

Soil strength values can be input using either SPT N-values or DRIVEN input files. The DRIVEN input file is most commonly used. This file inputs the pile used in design, the soil profile and the predicted pile resistance with respect to depth. The inputs of the driving system and energy parameters must still be entered before an analysis can be run.

In order to determine which of the geomaterial parameters had the greatest affect on the capacity, a parametric study was conducted using a DRIVEN input file, and

hammer and pile parameters form a bent on MDT project 2144, Bent 1. The analysis type used within GRLWEAP is called the *Bearing Capacity – Proportional Shaft Resistance* calculation, which is useful for determining internal stresses for hammer selection. The pile analyzed on this project is a 508 mm closed ended pipe, embedded 5.19 meters into a cohesive (shale) IGM. More information on this project is available in Chapter 5, Appendix A and Appendix B. The shaft and toe quake and damping values were increased independently. The percentage change in the final blow count at the CAPWAP ultimate capacity of the pile was compared to the percent change in the isolated parameter shown in Table 2. The higher the ratio of input and output variation, the greater the parameter impacts the overall calculation. The damping parameters had a considerably greater affect, when compared to quake. Specifically, the toe damping has the greatest affect on the final blow count when compared to shaft damping.

Existing stresses within the pile during driving also affects the blow count calculations. As a stress wave travels within a pile, the stress may not completely dissipate due to mobilized frictional forces along the pile perimeter. These stresses are known as residual stresses and can greatly affect the calculations (Rausche et al. 2004). Residual stresses within a pile increase the apparent pile length, which causes higher skin friction and lower tip capacity (Briaud and Tucker 1984). Methods are available to perform residual stress analyses. This analysis type can provide more accurate results; however, the analysis methods require more extensive calculations and need to be refined before they can be used universally. Within a standard GRLWEAP analysis, one hammer blow is used to perform the calculation. However, residual stress analyses

require multiple hammer blows to properly include residual stresses in a drivability analysis because residual stresses develop over time, increasing with each blow (Briaud and Tucker 1984). This analysis approach is not widely used and needs further research to determine its field accuracy. Due to the stiffness of IGMs, residual stresses are thought to develop within the pile during driving.

Table 2. Parametric Study of GRLWEAP Quake and Damping Parameters

Quake		**Damping**		**Blow**	**%**		
Shaft	**Toe**	**Shaft**	**Toe**	**Count**	**Parameter**	**% BC**	**Ratio: % BC Change/**
(mm)	(mm)	(s/m)	(s/m)	(blow/.3m)	**Change**	**Change**	**%Parameter Change**
2.5	2.5	0.65	0.5	87.4			
3	2.5	0.65	0.5	87.6	20.00%	0.23%	1.14%
3.5	2.5	0.65	0.5	87.7	40.00%	0.34%	0.86%
4	2.5	0.65	0.5	87.9	60.00%	0.57%	0.95%
4.5	2.5	0.65	0.5	88	80.00%	0.69%	0.86%
5	2.5	0.65	0.5	88.2	100.00%	0.92%	0.92%
2.5	3	0.65	0.5	89	20.00%	1.83%	9.15%
2.5	3.5	0.65	0.5	90.8	40.00%	3.89%	9.73%
2.5	4	0.65	0.5	92.6	60.00%	5.95%	9.92%
2.5	4.5	0.65	0.5	94.5	80.00%	8.12%	10.15%
2.5	5	0.65	0.5	96.7	100.00%	10.64%	10.64%
2.5	2.5	0.7	0.5	89.1	7.69%	1.95%	25.29%
2.5	2.5	0.8	0.5	92.6	23.08%	5.95%	25.78%
2.5	2.5	0.9	0.5	96	38.46%	9.84%	25.58%
2.5	2.5	1	0.5	99.5	53.85%	13.84%	25.71%
2.5	2.5	1.1	0.5	102	69.23%	16.70%	24.13%
2.5	2.5	1.2	0.5	105.5	84.62%	20.71%	24.47%
2.5	2.5	1.3	0.5	109.1	100.00%	24.83%	24.83%
2.5	2.5	0.65	0.6	94.3	20.00%	7.89%	39.47%
2.5	2.5	0.65	0.7	100.2	40.00%	14.65%	36.61%
2.5	2.5	0.65	0.8	106.7	60.00%	22.08%	36.80%
2.5	2.5	0.65	0.9	113.2	80.00%	29.52%	36.90%
2.5	2.5	0.65	1	119.5	100.00%	36.73%	36.73%

Note: Analysis was performed on MDT Project CN 2144, Bent 1, using Bearing Capacity – Proportion Shaft Resistance in GRLWEAP

CAPWAP

CAPWAP is a computer program used to analyze data collected during pile installation to determine the ultimate resistance of the pile from stress wave calculations. There are two parts to a dynamic capacity analysis: a Pile Dynamic Analyzer (PDA) and a CAPWAP analysis. PDA is a closed form solution to the wave equation that uses data from accelerometers and strain gages attached to the pile to provide an approximate prediction of the dynamic capacity. CAPWAP uses an iterative solution to the wave equation that varies the quake and damping parameters of the lithology to more accurately determine the capacity. However, this adjustment is not entirely automated. Certified CAPWAP operators determine the parameter to adjust in the wave match, using guidelines provided by Pile Dynamic Inc., the developers of CAPWAP.

The primary advantages of CAPWAP and PDA analyses include:

- reduction or elimination of static load tests,
- immediate assessment of internal stresses,
- indication of potential installation problems (if a test pile is used), and
- improved understanding of subsurface conditions and their effect on pile capacities (Baker 1984).

To ensure the accuracy of CAPWAP a database of CAPWAP capacities and static load test capacities has been compiled and compared by Likins and Rausche (2004). The author expanded this database through literature review. The field data displayed a significant correlation. "CAPWAP is about as reliable for determining the ultimate capacity as a static load test definition of failure," (Likins and Rausche 2004). A

comparison of static load test capacity and CAPWAP capacity is provided in Figure 4, which IGM and soil materials. A table of the references and values used in this figure is provided in Appendix C. Further analyses in this study are compared to CAPWAP capacities; thus, the determination of the test accuracy was required.

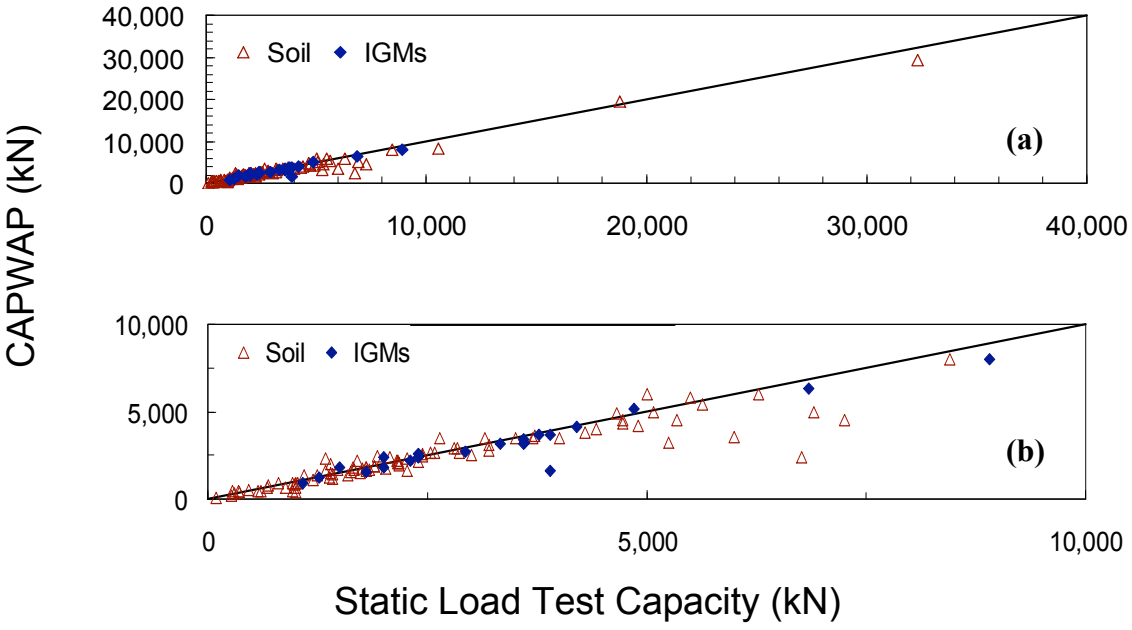

Figure 4. A comparison of static load test and CAPWAP capacities from the literature. (a) A plot of all data. (b) Data points at lower capacities.

The data shown in Figure 4 provides a significant correlation between CAPWAP and static load testing. The literature provided 115 static load and CAPWAP capacity comparisons. Of those, 21 were within cohesive and cohesionless IGMs. The IGMs analyzed, from literature review, did not show significantly large variation between static and CAPWAP capacities, with one exception. Shown in Figure 4(b), this outlier was considerably under predicted by CAPWAP.

Other the past decade, analyses have become routine and well-accepted in practice. CAPWAP is an effective method to estimate capacity, ensuring a reasonable factor of safety. However, some inherent inaccuracies exist in the approach as a result of the operator and within varied parameters. In some cases, varied parameters in the calculation are adjusted too high. High case damping is one of these problems, this material property that is due to mineralogical or depositional characteristics causing an overestimation of the ultimate pile capacity (Thompson and Goble 1988).

Other Design Methods

The current design approach for IGMs in Montana uses DRIVEN to calculate the ultimate capacity profile with depth, L-PILE to determine lateral capacity and deflections, and GRLWEAP to determine the appropriate hammer system for the pile and soil conditions. Some designers apply both soil and rock mechanics principles to analyze IGMs resulting in very conservative results (Johnston 1995, Johnston 1989). Another design method, by Reese et al. (2005), assumes a high quality sampling method for the method to be valid. High quality sampling assumes a rock recovery of greater than 50%. Due to the highly conservative nature of some design methods and the required rock recovery these methods are not often used within IGMs.

All of the current design methods are empirical or semi-empirical. Empirical methods rely only on observation of pile behavior. Semi-empirical methods can be more accurate; however, are difficult to formulate and to use. As they rely on both theoretical

and empirical information. Specifically, difficulty in its use is due to the significant material variation and complicated behaviors.

In IGM pile design, few methods apply directly. However, the methods by Gannon et al. (1999) and Colorado Department of Transportation (2006) are formulated specifically for IGMs and are presented in detail below.

Gannon et al. (1999) presents design methods specifically drilled shafts within cohesive and cohesionless IGMs. The cohesive design method is essentially the β method for soils, in which side resistance is calculated using the adhesion parameter calculated in the following equation:

$$c_a = \sigma' K_o \tan(\phi') \qquad (2)$$

where, σ' is the vertical effective stress at the center of a layer, K_o is the coefficient of earth pressure at rest and ϕ' is the drained friction angle of the geomaterial. K_o and ϕ' can be calculated using testing or from the following equations:

$$K_o = [1 - \sin(\phi')]\left[\frac{0.2N_{60}}{\sigma' / p_a}\right] \qquad (3)$$

$$\phi' = \tan^{-1}\left\{\left(\frac{N_{60}}{12.2 + 20.3(\sigma' / p_a)}\right)^{0.34}\right\} \qquad (4)$$

where, p_a is atmospheric pressure and N_{60} is the adjusted SPT N-value. The adhesion is then multiplied by the perimeter of the pile and the depth of the layer to determine the side resistance for a specific layer within the lithology. The summation of the soil and IGM layer resistances provides the shaft resistance. Again, this method is only valid for

IGM layers in drilled shafts. Other methods are required for calculating shaft resistance in the overlying soil layers.

The end bearing calculation is calculated from the following equation:

$$q_{\max} = 0.59\left[N_{60}\left(\frac{p_a}{\sigma'}\right)\right]^{0.8}\sigma' \qquad (5)$$

where, q_{max} is the maximum toe resistance. However, q_{max} needs to be reduced for shaft diameters (B_b) ranging from 1.27 to 1.9 meters, by the following equation:

$$q_{reduced} = \frac{1.27 q_{\max}}{B_b} \qquad (6)$$

where, $q_{reduced}$ is the reduced toe resistance.

The Gannon et al. (1999) method may apply within IGMs; however, to the authors knowledge it has never been applied. Comparing back calculated c_a or f_s values for IGM layers on completed projects with the predicted values from this method will determine the applicability of the Gannon et al. (1999) method to driven piles within IGMs.

The Colorado Department of Transportation (CDOT) design method treats cohesive IGMs as hard rock, when designing driven piles. Consequently, the design of piles within these materials relies primarily on the end-bearing capacity, which is assumed to be a function of the structural capacity. The allowable axial capacity of the pile is assumed to be the allowable structural capacity as calculated by AASHTO publication (FHWA-HI-97-013). The allowable structural capacity of the pile is then multiplied by a factor of safety to determine the ultimate capacity of the pile. For example, the allowable design stress for a steel pile is $0.25f_y$, where f_y is the yield stress

of the steel. The depth of driving is based on past experience within the region, or piles are driven to virtual refusal. Virtual refusal is defined as 2.5 cm or less of penetration for the final 10 blows (CDOT 2005).

The CODT method does not allow the prediction of pile embedment in areas with little past experience. Piles can be driven to virtual refusal but this provides no indication of the required pile length at the site.

Accurate predictive methods are incredibly valuable. They can predict the pile embedment and the corresponding capacity at that depth. However, within IGMs certain predictive methods may not be reliable. For this reason, capacity determination methods should be used on piles supported on IGMs. Two factors need to be considered when determining which method is used to determine capacity: the amount of uncertainty within the material properties or the design method and the economics of construction. The more unknowns within the design, the more accurate the capacity determination method needs to be. More accurate testing can be uneconomical on some design projects.

CHAPTER 4

DEEP FOUNDATION DESIGN EXPERIENCE IN IGMS

Most foundation research on IGMs has been for drilled shafts; however, some information is available on driven pile foundations in IGMs. Most of the studies reviewed in the literature analyze IGM properties, including strength and stiffness, in an attempt to determine more accurate design methods. Many factors control the capacity of the foundation and are input into an accurate design method; namely, geomaterial strength and frictional properties (Abu-Hejleh et al. 2005).

Drilled shafts and driven piles differ primarily due to their installation method and loading capacity. Drilled shafts are made from augured holes that are then filled with concrete and rebar, which can provide higher capacities when compared to a single driven pile. Driven piles are pounded into the subsurface by a hammer that imparts enough energy to resist the continually increasing resistance from shaft and end-bearing.

Foundations in IGMs are sensitive to the installation methods, as pile driving can alter the properties of the surrounding material, which can affect the foundation capacity (Tomlinson 1977).

Drilled Shafts

The ultimate capacity of any foundation on IGMs should be determined using calculation methods that include IGM strengths after the material is altered by the installation processes. As a result of material weakening during installation, the designer must decide the most accurate IGM properties for use in foundation analysis. The region

effected by weakening and the design method accuracy, for either the shaft friction or the end bearing, has been studied independently to determine the effects of weakening for different IGM types.

Shaft resistance of piles in IGMs is comparatively higher than the resistance when piles are founded in soil or hard rock (Seidel and Haberfield 1995). The side resistance of drilled shafts in IGMs is influenced by strength, socket roughness, rock mass fracturing and wall socket smear (Hooley et al. 1993, Johnston et al. 1993). Socket roughness and wall socket smear have the largest affect on capacity.

There are three classifications of socket roughness: rough, smooth and smeared. In most design methods, a socket is only considered rough if artificial methods are used to increase the roughness of the socket, creating a mechanical interlock between the geomaterial and the concrete at the edge of the shaft (Reese et al. 2005). Smooth sockets have no artificial roughness and have not been affected by sidewall smear. The smear zone is created due to exposure of the socket wall to drilling fluid or fresh water (Hassan and O'Neill 1997, Hassan et al. 1997). The depth of the smear zone is affected by the permeability of the IGM and the exposure time. Smeared sockets are assumed to exhibit the same behavior as smooth sockets, even if mechanical roughening of the socket is used, due to the unknown depth of the smear zone (Hassan and O'Neill 1997). The failure modes for each type of socket wall are distinctive; rough sockets and smooth sockets fail through settlement and interface slip, respectively (Hassan and O'Neill 1997).

In order to maintain conservative designs and depending on the IGM type, some designers, unsure of the material or the failure method, ignore either end-bearing or skin resistance component of capacity. Ignoring the potential capacity, from either shaft resistance or end bearing, results in overly conservative designs (Finno and Budyn 1988). However, observations with the literature review revealed inconsistent recommendations as to which type of resistance to ignore cohesionless IGMs. Shaft resistances in cohesionless IGMs are also often ignored. However, a study in weathered diabase, a cohesionless IGM, the shaft resistance comprised 70 percent of the ultimate load (Webb 1977). Ignoring a portion of the capacity causes significant conservatism in drilled shaft design in IGMs.

Observations of design inputs have also been made within the literature. Designs in mudstone and claystone, cohesive IGMs, observed that effective stress parameters and, SPT and pressuremeter parameters provide better results, respectively (Schmidt and Rumpelt 1993, Abu-Hejleh 2005). Currently, the α method is most often used to design shaft resistance in IGMs. Observations within claystone, from static load tests, found a typical range of α from 0.15 to 0.45 (Johnston et al. 1993).

The required axial capacity of the foundation may not always control the design of the foundation. For example, in cohesive IGMs design may be governed by serviceability requirements, like settlement (Schmidt and Rumpelt 1993). When serviceability requirements control the design in IGMs, pressuremeter testing is recommended to more accurately estimate the settlement behavior (O'Neill et al. 1996).

Driven Piles

Piles in IGMs are particularly sensitive to installation methods (Tomlinson 1977). The pile must be strong enough to resist stresses during pile installation. However, the hammer must impart enough energy to drive the pile to the required design depth, countering the increasing shaft and end resistance with depth (Gerwick 2004). To counter the high driving resistance, Gerwick (2004) recommends the use of a hammer that is one size larger than determined from the GRLWEAP hammer selection results.

The process of pile driving can alter IGM properties and the alteration can be difficult to measure (Gannon et al. 1999). Changes in properties cause design inaccuracies. Due to the inaccuracy, Reeves et al. (1993) recommend dynamic testing of a pile at each bent or group to ensure the required capacity has been reached. All observations made by dynamic and static load testing are specific to the IGM and the site. These observations can be used to determine trends within IGM types.

Observations of piles in cohesionless IGMs, specifically glacial till, have found that these piles are primarily end bearing, for this reason displacement piles are recommended, as they increase the toe area (Gerwick 2004). Idaho Transportation Department's experience in cohesionless IGMs includes piles running when driven into dense rounded gravel deposits. CAPWAP analyses on these piles showed little increase in capacity even with further driving (Burgert and Buu 2007). The piles did not reach the required capacity at their design embedment.

CHAPTER 5

MONTANA DEPARTMENT OF TRANSPORTATION

PROJECT SUMMARIES

The evaluation of piles in IGMs was conducted in this study using data provided by the MDT Geotechnical Section. The data was obtained from bridge projects in which piles were driven into IGMs and dynamic analyses of pile capacity were conducted. The MDT information contained project specific data from nine bridge construction projects meeting the above criteria. The data sets for each project consisted of the following information:

- geotechnical design report,
- DRIVEN analyses,
- project plans,
- contractor hammer submittal,
- dynamic analysis reports, and
- pile driving logs.

The dynamic analyses conducted on each project included PDA and CAPWAP analyses. Pile and geomaterial summaries for each project, organized by MDT control number (CN), are shown in Table 3. Further specifics from each project are shown in Table 4, which provides detailed information, including:

- IGM strengths, in the form of unconfined compression strengths or SPT refusal information,
- details of pile embedment, and

- depth of the pile within the subsurface IGM

Further details pertaining to each project was available in the form of boring logs (and some subsurface profiles). Using the data furnished by MDT, the author-constructed subsurface profiles for each MDT project. Copies of these profiles are provided in Appendix B. These profiles graphically show subsurface materials, groundwater table, depths and locations of pile embedment, boring locations, and IGM strength measurements from unconfined compression or SPT testing.

Table 3. Projects with CAPWAP Analyses by Control Number

Project CN	Project Name	Project County	Primary IGM
Q744	Medicine Tree	Lake	Dense Gravel
1744	Vicinity of White Coyote	Lake	Dense Gravel
2144	Nashua Cr.	Valley	Shale
3417	West Fork of Poplar River	Roosevelt	Claystone, Siltstone, Sandstone
4226	Goat Cr.	Lake	Dense Gravel
4230	Bridger Cr.	Gallatin	Dense Gravel
4239	Big Muddy Cr.	Sheridan	Claystone
4244	Keyser Cr.	Stillwater	Dense Gravel

Six of the projects also included DRIVEN analyses for piles at each bent and a drivability study using GRLWEAP. Projects Q744, 1744 and 4226 were completed before DRIVEN was fully implemented by MDT; consequently, the author completed the DRIVEN analyses for these projects.

An additional project was available, but it had to be excluded form the analyses. The Swan River Project (4228) was excluded from the research analyses because of counter-intuitive CAPWAP results. The IGM on this project was dense silty gravel. A

610 mm diameter open pipe test pile was driven to the design depth and the next day a subcontractor conducted the PDA and CAPWAP analyses. The restrike CAPWAP capacity was considerably less than the design capacity. Multiple PDA analyses were conducted in the field during further driving. As the depth increased for the tested piles, the dynamic capacity decreased. For this reason, the project was excluded from the research.

A summary of the design and CAPWAP capacities of tested piles within the project scope are provided in Table 5. The actual (as built) and design (predicted) lengths of the piles are also shown in the table. Cohesive IGMs exhibit smaller depths of embedment compared to the design depth, known as early refusal. Thus, the capacity of piles in cohesive IGMs indicates that the predicted strength is too low. In cohesionless IGMs, the piles required driving to greater depths than planned. The sum of the excess pile required on all projects is approximately 100 meters or 24.3% of the total pile length required on all projects. The greater pile depths indicate an over prediction of the IGM strength in cohesionless IGMs.

On average, cohesive IGMs refused 0.33 meters early with a standard deviation of 2.82. While cohesionless IGM extended, on average, 4.73 meters further than design depth with a standard deviation of 6.56. However, there is considerable variability within each material type. For example, within the cohesive IGMs, one pile extended 8.61 meters further than the design depth and another refused 3.01 meters early. In Cohesionless IGMs, pile refusal varied from 2.75 meters early and extend 12.17 meters further than the design depth.

Table 4. Project Construction Summaries - IGM Strength

Project CN	IGM Type[1]	Pile Location[2]	Pile Type and Size[3]	Total Embedded Length (m)	Pile Length in IGM (m)	q_u[4] (kN)	SPT N-Value $(N_1)_{60}$[5]
Q744	ϕIGM	Bent 1	508mm OP	30.17	15.53	N/A	N_{ref}
		Bent 2	508mm OP	30.11	24.58	N/A	N_{ref}
1744	ϕIGM	Bent 1	H 360x108	21.01	13.71	N/A	N_{ref}
2144	cIGM	Bent 1	508mm CP	27.48	5.19	206 Sh	N/A
		Bent 3	508mm OP	27.58	1.68	83 Sh	N/A
		Overflow 1	508mm OP	25.77	4.77	223 Sh	N/A
3417	cIGM	Bent 1	406mm CP	12.79	9.74	294 C; 40,479 S	N/A
		Bent 2	762mm OP	14.36	8.46	197 C; 367 S	N/A
		Bent 3	762mm OP	14.62	8.52	449 C; 545 S	N/A
		Bent 4	406mm OP	12.80	5.79	579 C; 523 S	N/A
		Overflow 1	406mm OP	15.22	8.52	263 C; 2,808 S	N/A
		Overflow 2	610mm OP	13.62	9.92	328 S; 458 C; 868 C,S,Si	N/A
		Overflow 3	406mm OP	16.2	12.20	709 C; 19,390 S	N/A
4226	ϕIGM	Bent 1	406mm CP	9.3	0.51	N/A	N_{ref}
4230	ϕIGM	Bent 3	610mm OP	8.58	4.58	N/A	N_{ref}
		Bent 4	406mm OP	7.23	3.23	N/A	N_{ref}
4239	cIGM	Bent 1	H 310x125	33.04	4.08	N/A	N/A
		Bent 2	406mm CP	31.14	2.18	N/A	N/A
		Bent 4	H 310x125	41.24	12.28	N/A	N_{ref}
4244	cIGM	Bent 1	H 310x125	9.24	1.925	9,549 Sh; 9,797 S	N/A
		Bent 2	H 310x125	9.21	1.895	N/A	N_{ref}

1) cIGM = Cohesive IGM; ϕIGM = Cohesionless IGM; S = Sandstone; Si = Siltstone; C = Claystone; Sh = Shale
2) "Overflow" indicates a second overflow structure on the project. The number following Overflow is the bent number of this second structure.
3) OP = open-ended pipe pile, CP = closed-ended pipe pile.
4) "q_u" unconfined compression strength, are an average for the IGM at the Bent (abbreviations are below) Interbedded have more than one IGM classification.
5) "N_{ref}" indicates SPT refusal with greater than 50 blows/ 0.3m.

Table 5. Project Construction Summaries - Design vs. Actual Construction

Project CN	IGM Type[1]	Pile Location[2]	Pile Type and Size[3]	Design Axial Capacity (kN)	CAPWAP Measured Axial Capacity [4] (kN)	Design Pile Length (m)	Actual Pile Length (m)	Comments
Q744	ϕIGM	Bent 1	508mm OP	2300	1542, 2308*	18	30.17	Running[5]
		Bent 2	508mm OP	2300	956, 2140*,2152**	18	30.11	Running
1744	ϕIGM	Bent 1	H 360x108	1474	936, 1609*	14.2	21.02	Running
2144	cIGM	Bent 1	508mm CP	2720	2244	29.3	27.48	Early Refusal[6]
		Bent 3	508mm OP	2825	2388	28.9	27.58	Early Refusal
		Overflow 1	508mm OP	3150	2000, 3160*	26.2	25.77	Early Refusal
3417	cIGM	Bent 1	406mm CP	1810	1800	12.98	12.79	Early Refusal
		Bent 2	762mm OP	3870	3845, 4398*	14.74	14.36	Early Refusal
		Bent 3	762mm OP	3870	3850	14.74	14.62	Early Refusal
		Bent 4	406mm OP	1670	2074	12.97	12.80	Early Refusal
		Overflow 1	406mm OP	1790	2125	16.3	15.22	Early Refusal
		Overflow 2	610mm OP	2870	3074, 4294*	15.83	13.62	Early Refusal
		Overflow 3	406mm OP	1560	2598	17.03	16.2	Early Refusal
4226	ϕIGM	Bent 1	406mm CP	1950	1649	12.05	9.3	Early Refusal
4230	ϕIGM	Bent 3	610mm OP	2600	3200	8.58	8.58	
		Bent 4	406mm OP	2430	3195	7.23	7.23	
4239	cIGM	Bent 1	H 310x125	2025	2125	30.54	33.04	Running
		Bent 2	406mm CP	2205	2370	32.64	31.14	Early Refusal
		Bent 4	H 310x125	2025	2202	32.64	41.24	Running
4244	cIGM	Bent 1	H 310x125	2230	3500	12.22	9.24	Early Refusal
		Bent 2	H 310x125	2230	2550	12.22	9.21	Early Refusal

1) cIGM = Cohesive IGM, ϕIGM = Cohesionless IGM
2) "Overflow" indicates a second overflow structure on the project. The number following Overflow is the bent number of this second structure.
3) OP = open-ended pipe pile, CP = closed-ended pipe pile.
4) "*" indicates restrike capacity. "**" indicates a second restrike capacity.
5) Running indicates the pile required driving further than the design embedment in order to achieve the required capacity.
6) Early Refusal indicates that the pile could not be driven to the design embedment without probable structural damage.

Piles driven at very high blow counts (small set) into stiff materials are prone to structural damage, from excessively high stresses. Utilizing the information presented within the CAPWAP analysis reports, the maximum driving stresses for each project were compiled and compared with the allowable driving stresses from AASHTO 1996. Relatively high pile driving stresses occurred in all the projects analyzed, as shown in Table 6. The higher stressed piles (i.e., piles that experienced stresses in excess of 90% of the allowable driving stress) were driven into both cohesive and cohesionless IGMs; there were no discernable trends based on IGM type. Of the higher stressed piles, 30% exceeded the allowable driving stress recommended by AASHTO. The piles were all steel pipe piles driven (open or closed ended).

Table 6. Driving Stresses within Piles

CN	Bent[2]	IGM Type	Pile Size and Type[3]	f_y[1,4] (MPa)	Allowable Driving Stresses (MPa)	Maximum Compressive Stresses (MPa)	% of Allowable Driving Stress
3417	O1	CH	P406	310	279	286.2	102.6%
3417	O3	CH	P406	310	279	282.9	101.4%
4239	2	CL	P406	241	216.9	219.9	101.4%
3417	1	CH	P406	310	279	276.5	99.1%
Q744	1R	CL	P508	241*	216.9	207	95.4%
3417	4	CH	P406	310	279	261.8	93.8%
Q744	2RR	CL	P508	241*	216.9	201.2	92.8%
Q744	2R	CL	P508	241*	216.9	200.4	92.4%
Q744	2	CL	P508	241*	216.9	198.1	91.3%
2144	O1R	CH	P508	310	279	251.6	90.2%

Notes:

1) f_y is the yield stress of the steel.
2) "R" indicates values from a CAPWAP restrike analysis.
   "RR" indicates values from a second CAPWAP restrike analysis.
3) "P" indicates pipe pile; the number following is the pile diameter in millimeters.
4) "*" indicates that the steel grade was not known, f_y is assumed to be the lower of the reported grades in the CAPWAP report.

CHAPTER 6

ANALYSIS OF PROJECT DATA

Deep foundations are relatively expensive and can constitute a significant percentage of the overall cost on bridge projects. Uncertainties in subsurface conditions can result in higher construction costs due to higher factors of safety in design, higher construction bids, and higher frequency of contractor claims. The natural variability of IGMs exacerbates uncertainties in deep foundation design and may ultimately increases the construction costs. This study was undertaken to find a reliable relationship between pile resistance and IGM properties.

For the analyses conducted in this study, IGMs were divided into two broad categories, cohesive and cohesionless. Cohesive IGMs have an intrinsic bonding or cohesion within their structure; for example, claystone, sandstone and siltstone. Cohesionless IGMs are very dense materials, often sandy gravels, which do not contain any bonding between the particulates.

Data analyzed in this study were compiled from information provided by MDT, as described in the previous chapter. Information from each of the nine projects was collected and compiled, including initial drive and restrike data from CAPWAP reports, DRIVEN analyses, and GRLWEAP analyses. CAPWAP information was obtained from CAPWAP reports completed for each project. Unless noted otherwise, DRIVEN inputs for each bent were obtained from the DRIVEN reports provided by MDT. GRLWEAP analyses were conducted by the author for each project bent using hammer and cushion information submitted by the contractor. Remaining information was determined using

engineering judgment, based on the soil profiles and foundation reports. A spreadsheet containing all of the above information was compiled and is provided in Appendix B.

The methodology behind this research is iterative. Evaluations were conducted by creating numerous parameter comparisons to search for trends or useful relationships within the available information. The variability of IGM materials provided an interesting challenge because of the unpredictable response of the material to pile driving, and because of the many variables involved with pile driving and pile resistance. The analytical comparison was divided into the following three categories or steps:

1) evaluate the accuracy of current design procedures,
2) investigate possible correlations between project data and predictive methods, and
3) determine the accuracy of other capacity prediction methods.

The following sections describe the evaluations and comparisons in terms of these three steps.

Evaluate Accuracy of Current Design Methods

The first step within the analysis was to determine the accuracy of the current design methods used by the MDT Geotechnical Section. Comparison of DRIVEN calculated static capacities that were used by MDT to design the pile to the measured dynamic capacity from CAPWAP. The DRIVEN capacities used in this comparison were created using parameters determined from the DRIVEN reports provided by MDT, or if none were available, the author created input files based on the geotechnical project

report. The depth used to determine the capacity was obtained directly from the CAPWAP report. End-of-driving depths were used for the capacity calculations on all projects. If a restrike CAPWAP analysis was conducted, the embedment depth at the end of restrike was used to determine the restrike capacity. Linear interpolation was used to determine capacity at intermediary depths.

A comparison of the ultimate capacities is shown in Figure 5. Shaft and toe capacity comparisons are provided in Figure 6 and Figure 7, respectively. The y-axis of these plots represents the DRIVEN capacity calculated using the MDT original inputs, from initial drive and restrike. The x-axis represents the measured dynamic capacity from the CAPWAP analyses. The diagonal (45°) line of each plot can be used to visually asses the accuracy of DRIVEN predictions.

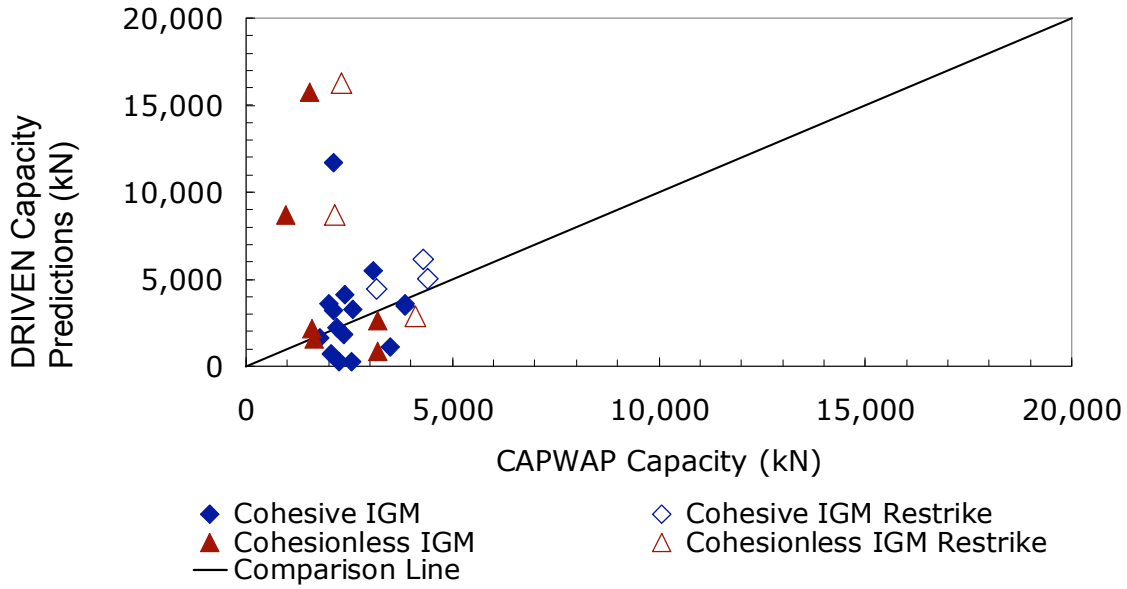

Figure 5. Comparison of MDT capacity predictions to measured CAPWAP capacity.

The ultimate capacity comparison shown in Figure 5 clearly demonstrates the inherent variability of pile capacity in IGMs. Most of the projects had considerable variation between the predicted capacities calculated with DRIVEN and the measured CAPWAP capacity. Five of the six restrike analyses were over predicted using DRIVEN.

To refine the analyses, the data was further dissected into shaft and toe resistances. Figure 6 shows a trend in which DRIVEN under predicted the shaft resistance in cohesive IGMs in 12 out of 20 (60%) and cohesionless IGMs in 4 of 8 (50%) projects, respectively.

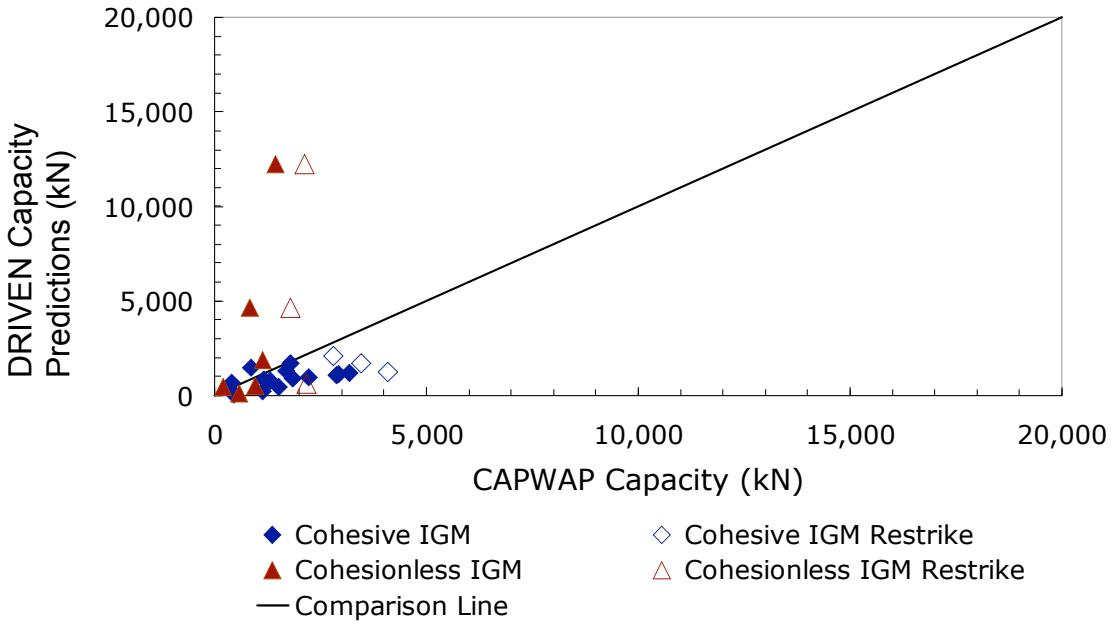

Figure 6. Comparison of MDT original shaft capacity inputs to CAPWAP shaft capacity.

The comparison in Figure 7, shows the variability of predicted toe capacity. A trend was observed in which the predicted toe capacity of cohesionless IGMs were under

predicted for 4 of 8 (50%) projects. For cohesive IGMs, 6 of 20 (30%) CAPWAP analyses observe an under prediction of toe capacity.

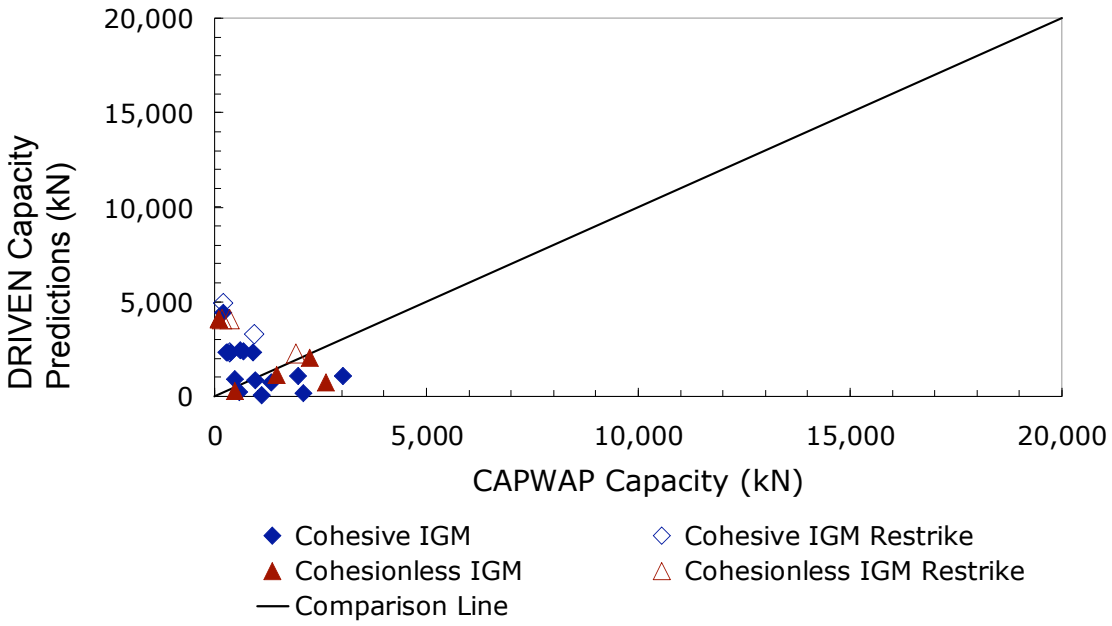

Figure 7. Comparison of MDT original toe capacity to CAPWAP toe capacity.

One limitation within DRIVEN is the correlation between undrained cohesion and adhesion. The Tomlinson α method determines adhesion by multiplying the undrained shear strength of the geomaterial by an adhesion factor, α. Within DRIVEN, the adhesion factor is correlated directly to the undrained shear strength of the material. That is, the adhesion factor does not take into account material-type, pile embedment depth, or pile size, as in the original Tomlinson (1979) method. Consequently, the engineer could more accurately determine the shaft capacity by calculating the adhesion value through other means and manually inputting this adhesion into DRIVEN, for the cohesive IGM layer. This could improve accuracy of the toe capacity calculation. DRIVEN often over

predicts the pile capacity in cohesionless IGMs. Thus, friction angles of cohesionless IGMs need to be reduced in order to more accurately model the in-situ pile capacity using DRIVEN.

Investigate Possible Correlations

From the comparisons between the DRIVEN analyses used in design and CAPWAP capacities, a conclusion was reached that further analyses of both shaft and toe capacity were required in order to more carefully examine the data for potential trends or correlations. This was the second step of the analysis process, in which two comparisons were used: 1) normalized capacity comparisons and 2) iterative solutions. The normalized capacity comparisons included the CAPWAP resistances divided by either the perimeter of the pile or the plugged area of the pile. The iterative solutions were developed by varying soil strength parameters in DRIVEN for the IGM layers until the DRIVEN capacity output matched the CAPWAP capacities.

Normalized Capacity Comparisons

Normalized capacity comparisons allow a more accurate comparison of data between projects by isolating material properties form measured values. The pile perimeter, the pile toe area, and the length of the pile within the IGM were used to normalize the CAPWAP shaft and toe capacities. The normalized shaft resistance, N_{shaft}, was defined using the following equation:

$$N_{shaft} = \frac{CAPWAP_{shaft}}{p} \qquad (7)$$

where, p is the perimeter of the pile and $CAPWAP_{shaft}$ is the measured CAPWAP shaft resistance. The normalized toe resistance, N_t, was determined using the following equation:

$$N_t = \frac{CAPWAP_{toe}}{A} \quad (8)$$

where, A is the plugged area of the pile and $CAPWAP_{toe}$ is the measured toe resistance. The plugged area is the full toe area of the pile; a box area for H-piles and the entire circular area for pipe piles.

N_{shaft} was compared to the length of the pile within the IGM, as shown in Figure 8. There is a slight visual trend within the figure; a stready linear increase to 1,500 kN/m that becomes horizontal at approximately 7 meters and decreases beyond this point. The CAPWAP shaft capacity included within this calculation is the total shaft capacity of the pile; unfortunately, this also includes the shaft resistance from the soil layers above the IGMs. It is theorized that the correlation could be improved if the soil and IGM shaft resistances were separated from the total CAPWAP shaft resistance. However, there is no measured value of the shaft capacity within the project information provided by MDT. Predicted values of the shaft capacity involve a high degree of uncertainty and are thus too unreliable to use as a refinement specifically within this analysis. Using boring logs and engineering judgment, the elevation of the top of the IGM layer can be determined. If a CAPWAP analysis is conducted at this determined elevation, the shaft resistance from just the soil layers could be removed from the ultimate capacity allowing a better correlation of the normalized resistance.

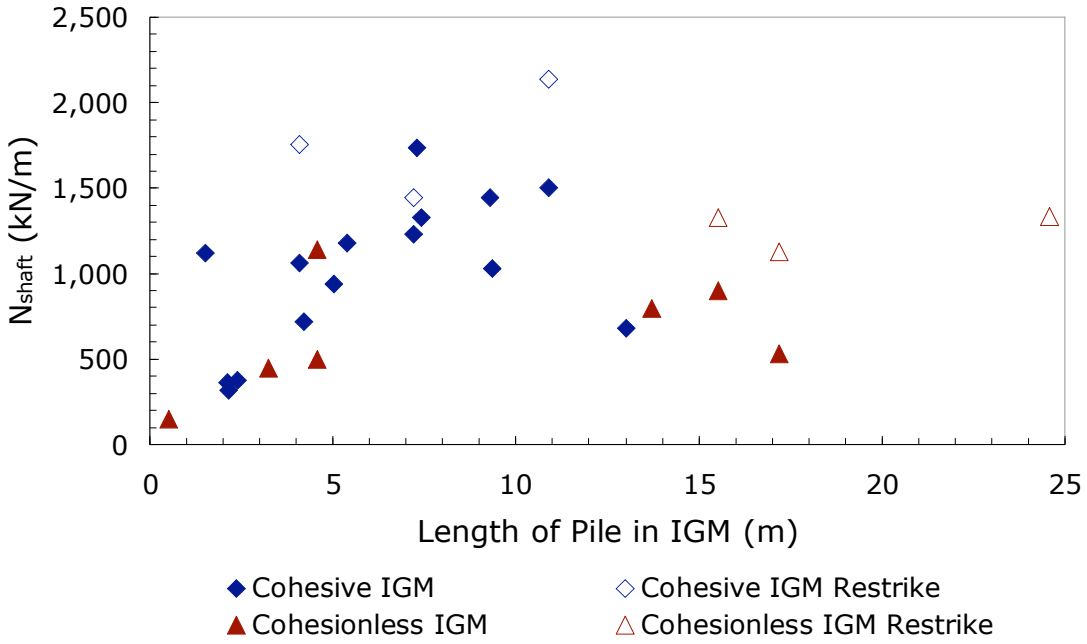

Figure 8. Normalized shaft resistance compared to pile length in IGM.

It is in the nature of IGMs to vary with geology, location and depth. For this reason, the normalized shaft resistance comparison was also analyzed by project. As shown in Figure 9, the data points tend to cluster by project. The most varied projects are those with cohesionless IGMs, specifically project numbers 4239 and Q744. The projects with piles in cohesive IGMs show trends of well-defined clusters, as for project numbers 2144, 3417 and 4244.

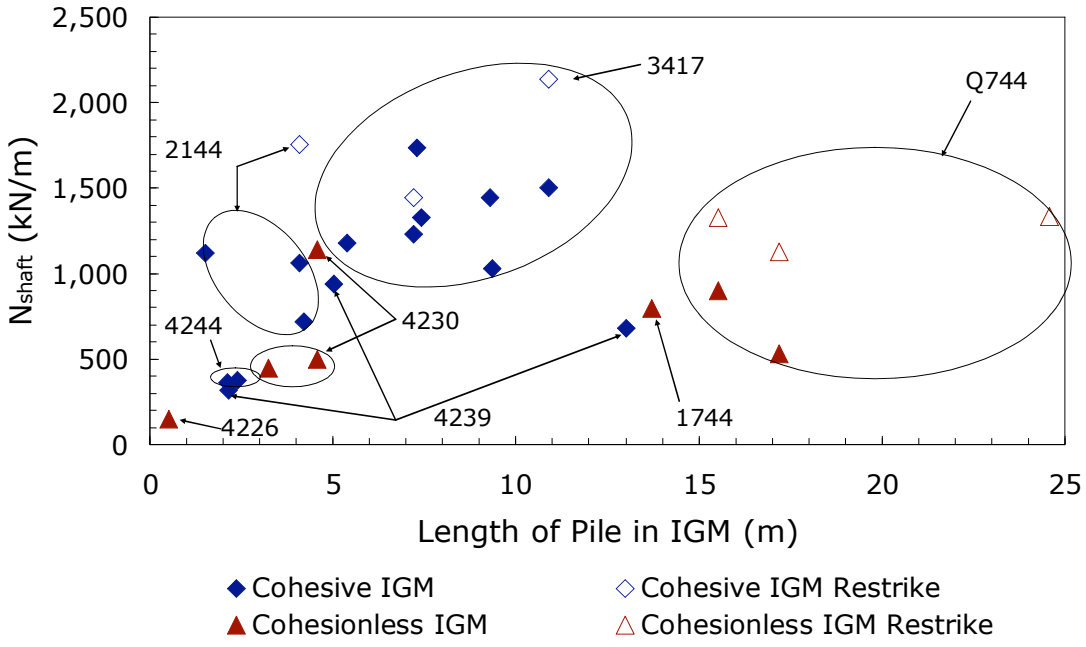

Note: Four digit numbers are MDT project control numbers.

Figure 9. Normalized shaft resistance compared to pile length in IGM by project.

The normalized toe capacity compared with unconfined compression strength and with pile length in IGMs is shown in Figure 10 and Figure 11, respectively. The comparison of toe capacity with unconfined compression strength parameters indicates large data scatter and no apparent trends. Intuitively, an increase in toe capacity would be expected as the unconfined compression strength of the IGM increases; however, this was not the case for the data evaluated.

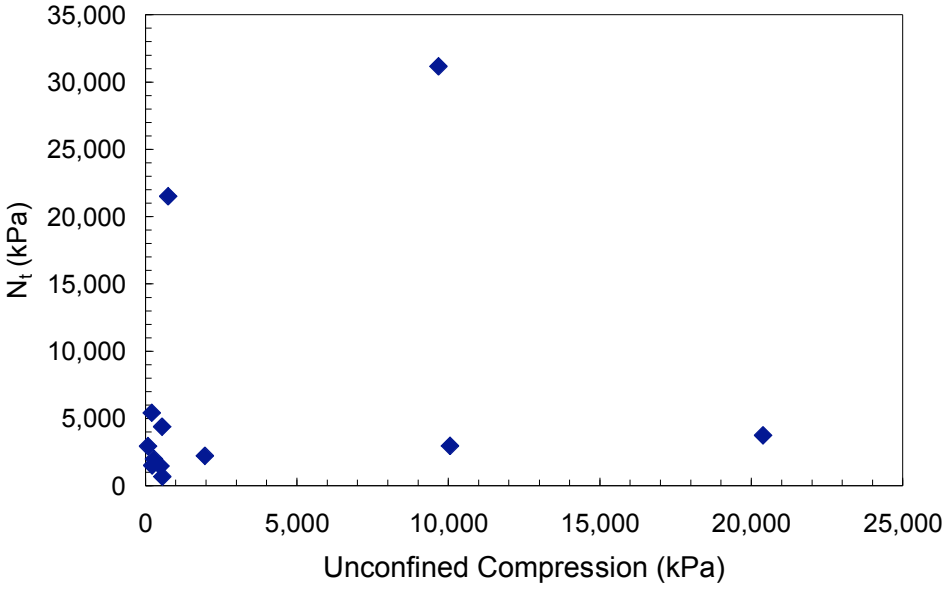

Figure 10. Comparison of normalized toe resistance with unconfined compression strength of cohesive IGMs.

Figure 11 shows a slight correlation of decreasing toe capacity with the length of the pile in IGMs. However, the post installation material properties of the IGM are not accurately known because the pile driving process can significantly alter the material. Due to the unknowns from pile installation and geologic trends in which the IGM strength increases with depth, the correlation is limited in its usefulness.

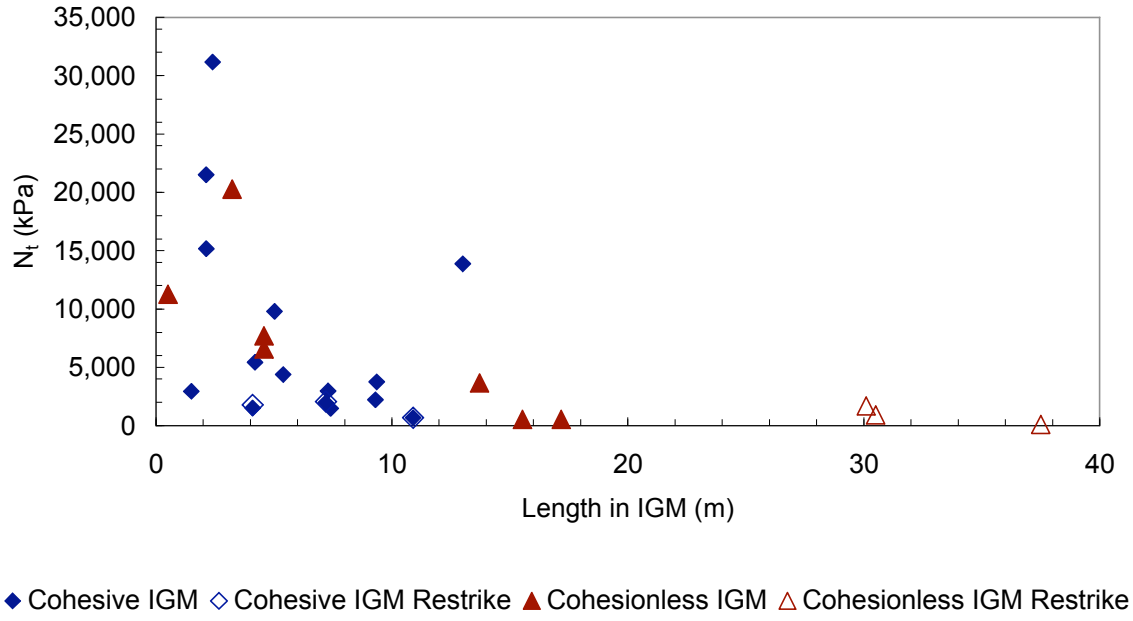

Figure 11. Comparison of normalized toe resistance with length of pile in IGM.

Interative Solutions

Iterative solutions were created by varying inputs in DRIVEN until the DRIVEN predicted capacity matches the CAPWAP ultimate resistance and shaft resistance. The following equation was used to vary the inputs in each IGM layer:

$$Input_{new} = M \times MDT_{input} \qquad (9)$$

where, M is the varied multiplier and MDT_{input} is the original input used in the MDT report. MDT_{input} includes only strength parameters for IGM layers, undrained cohesion in cohesive IGMs and ϕ' in cohesionless IGMs. M was varied until $Input_{new}$ resulted in a capacity that matched the measured CAPWAP capacity at the final constructed field depth, to within ± 1.0%. This process was used to match the ultimate capacity of both

initial drive and restrike CAPWAP analyses. These solutions are known as CAPWAP match solutions.

This process has been used to predict the shaft resistance in the IGM layer(s), known as Q_{slayer}. The normalized shaft resistance within the IGM layer, N_{slayer}, is defined by the following equation:

$$N_{slayer} = \frac{Q_{slayer}}{p} \qquad (10)$$

where, Q_{slayer} is the shaft resistance within the IGM layer derived from the CAPWAP match solutions and p is the perimeter of the pile. Figure 12 and Figure 13 show comparisons of N_{slayer} to the unconfined compression strength and the pile length in IGMs, respectively.

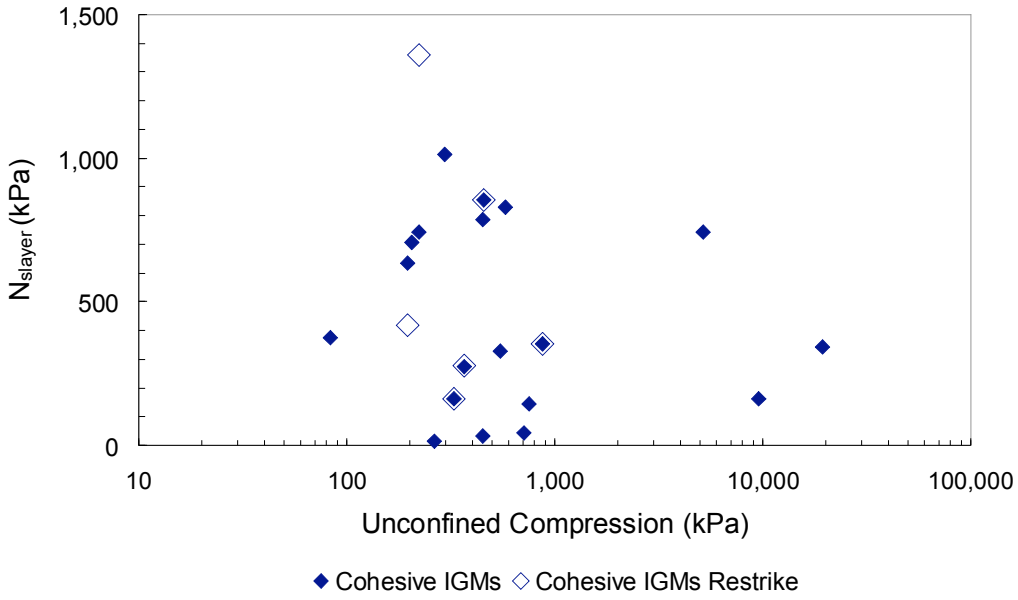

Figure 12. Comparison of normalized shaft resistance compared to unconfined compression strength.

The logarithmic scale on the x-axis was used in order to better view the data. No trends are apparent within Figure 12. This implies that the shaft resistance does not depend on the strength of the material. A trend that is opposite of the expected response, with increasing strength comes decreasing shaft resistance. Trends were not observed within Figure 13. The expected behavior is increased N_{slayer} with increased length in IGM, however no trend of this type were observed.

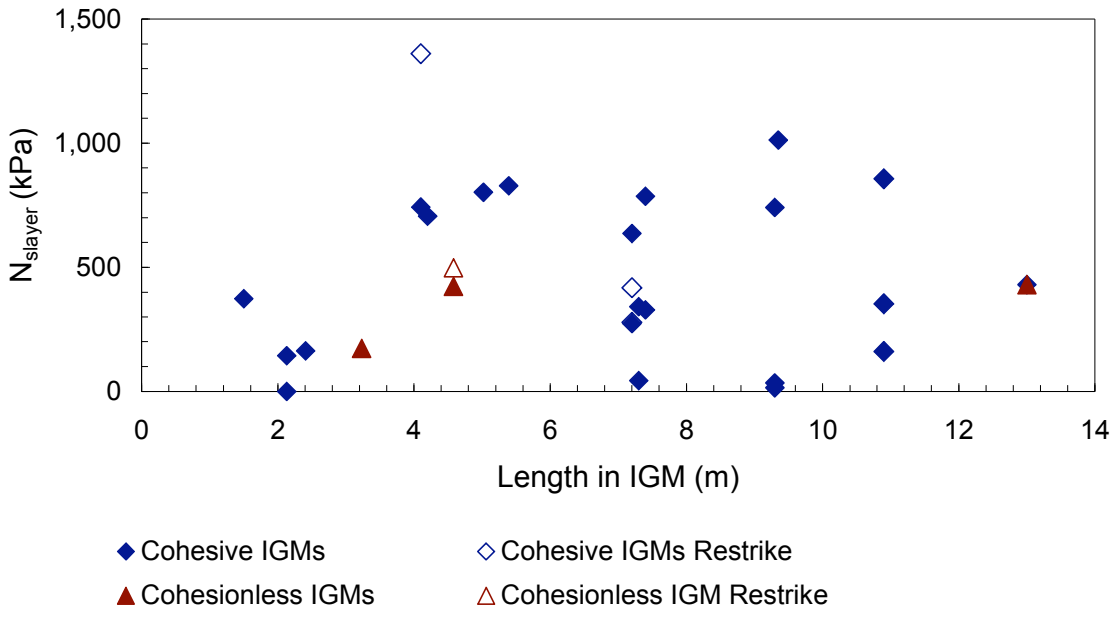

Figure 13. Comparison of normalized shaft resistance compared to length of the pile in IGMs.

The data was further examined by comparing the M required to match the CAPWAP ultimate capacity between IGM types. Some IGM strength inputs could not be altered to match the ultimate CAPWAP capacity, as the adjusted input exceeded reasonable values. The following M value comparisons include 19 of the 28 CAPWAP analyses. Projects in which matches could not be achieved in cohesionless IGMs within

friction angles of 50° or less were excluded. Most of the projects did not need considerable variation in order to match the CAPWAP capacity. Figure 14 shows the number of M values (y-axis) within a certain range (x-axis). Seventy percent of the M values were required to be within the range of 0.9 and 1.1.

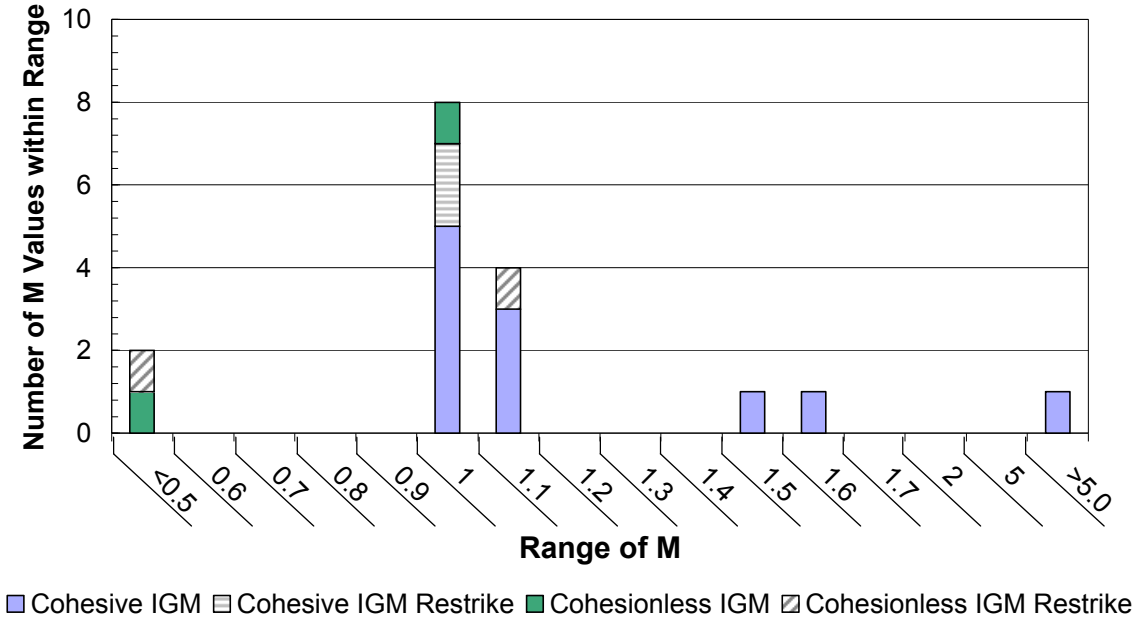

Figure 14. Number of M values between the given ranges.

It was theorized that M might correlate with either the length in IGMs, or the CAPWAP capacity. A comparison was then made with the length of the pile in IGMs and the CAPWAP capacity. These are shown in Figure 15 and Figure 16, respectively. The M value was placed on a logarithmic scale allowing the points to be more accurately distinguished. The cluster of M values near 1.0 is apparent within these comparisons. This would seem to indicate that only slight changes to input parameters are required to reach filed capacities. However, there was no apparent trend within the data for either

figure. Consequently, it is concluded that the M values do not depend on the pile length in IGMs or the measured CAPWAP capacity.

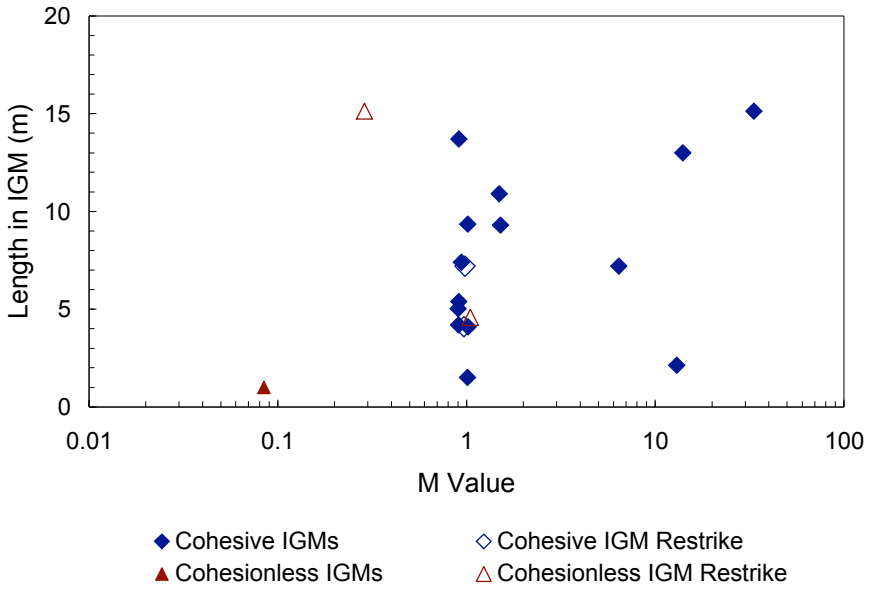

Figure 15. Comparison of M required for a CAPWAP capacity match to the pile length in IGMs.

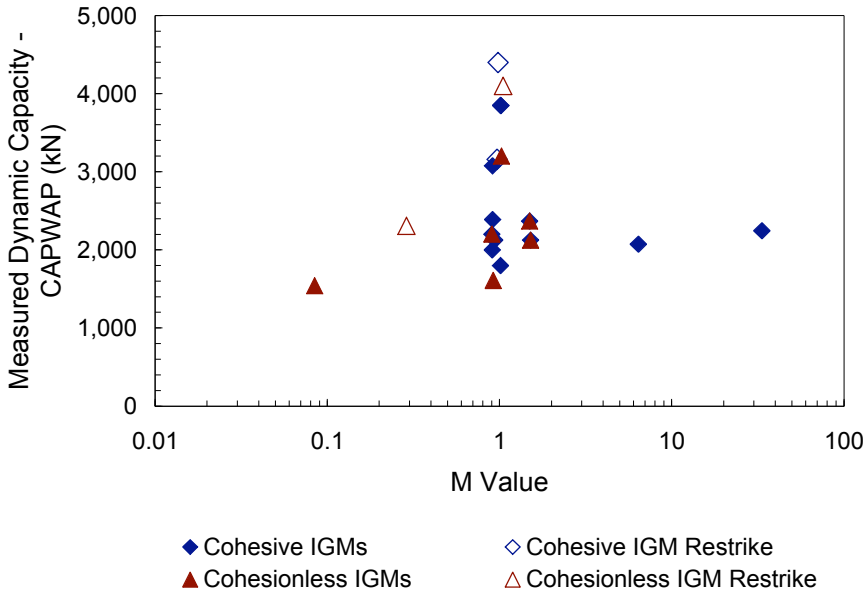

Figure 16. Comparison of M required for a CAPWAP capacity match to the measured CAPWAP capacity.

The iterative solutions include numerous unknowns, including:

- material properties,
- inaccuracies within analytical procedures (DRIVEN), and
- unknowns in subsurface information.

However, no other method was available to accurately remove the shaft resistance from the overlying soil region from the overall shaft capacity. These plots were used to predict the normalized resistance comparisons if the shaft resistance from overlying soil could be removed. There is a slight increasing trend within Figure 13; however, using CAPWAP to remove the soil shaft resistance from the total capacity would be more accurate. More research is required to determine adhesion coefficients from CAPWAP testing. The adhesion values from further research should also be compared to the type of IGM and, in cohesive IGMs, the type of chemical bonding intrinsic to the material.

Accuracy of Other Capacity Prediction Methods

The comparisons evaluated using the provided project data for either normalized resistance or iterative solution analyses did not yield any useful trends that could improve the accuracy of capacity prediction in IGMs. For this reason, other prediction or capacity determination methods were also evaluated, including the WSDOT Gates formula and a method from the CDOT.

A new dynamic formula was recently incorporated in the WSDOT geotechnical manual. WSDOT updated the Gates Driving Formula in order to increase its accuracy based on an analysis of a large database of pile driving information (Allen 2007). The

database contained information from pile load tests, end-of-driving blow counts and beginning of restrike blow counts. Capacity information was the correlated by Allen (2007) with the potential energy imparted to the pile to create a revised version of the Gates Formula to increase its accuracy for driven piles in Washington. Using information provided in the MDT project CAPWAP reports, pile capacities were calculated using the WSDOT Gates formula based on the measured (R_1) and predicted (R_2) hammer energies.

Capacity 1 is the predicted energy equation. The predicted energy capacity is given by the following equation:

$$R_1 = 6.6 \times F_{eff} \times E^* \times \ln(10N_c) \qquad (11)$$

where, F_{eff} is the efficiency factor for specific hammer types, E* is the energy of the hammer in foot-pounds, and N_c is the pile penetration resistance in blows per inch. Hammers on all of the projects are open-ended diesel hammers on steel piles, F_{eff} is 0.47. E* in this case is potential energy of the hammer, or the stroke of the hammer multiplied by the ram weight. The penetration resistance, N_c, was evaluated from the CAPWAP reports provided by MDT

Capacity 2 is the measured energy equation. The capacity is calculated from measured energy by the following equation:

$$R_2 = 6.6 \times TE \times \ln(10N_c) \qquad (12)$$

where, TE is the energy transferred to the pile as determined from gauges attached to the pile during dynamic testing. TE values were directly input into the equation without any adjustment for hammer efficiency, because this value was measured from the pile during

driving. A comparison of the WSDOT Gates formulas utilizing measured and predicted energies compared to the CAPWAP capacity is provided in Figure 17.

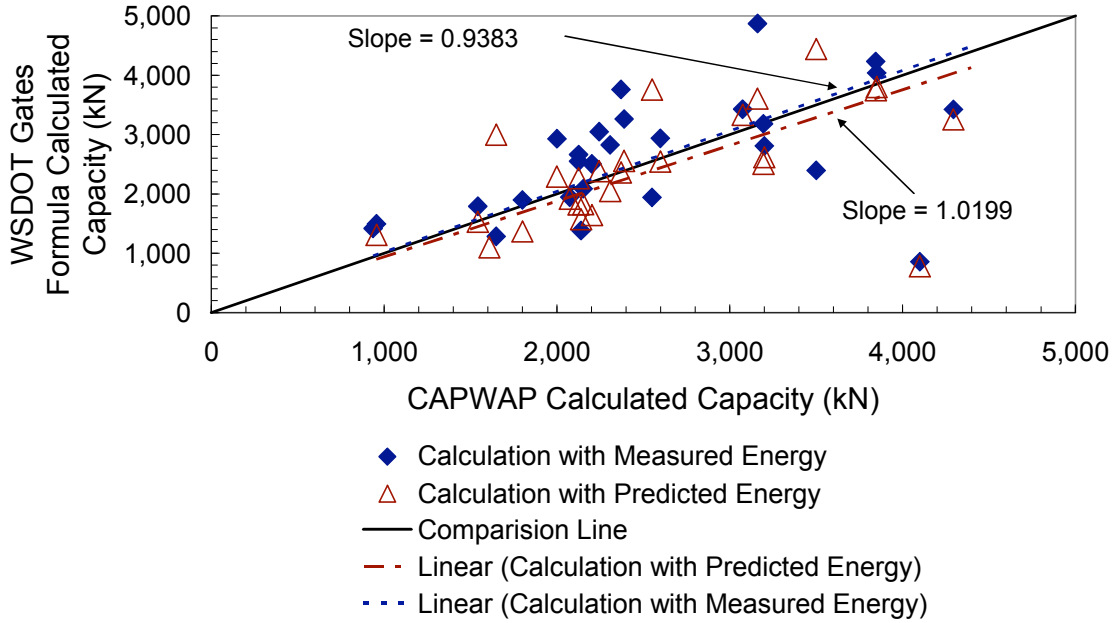

Figure 17. Comparison of the calculated WSDOT Gates capacities to the measured CAPWAP capacity.

While visually, the predicted energy appears to provide a better trend, the correlation is not as accurate when compared to the measured energy. The predicted energy equation may be more accurately correlated with its data (i.e., higher R^2 value); the slope of 0.9383 highlights the variation and inaccuracy of using this information. The measured energy provides more accuracy when compared to the comparison line (45°), this is apparent from the measured energy slope of 1.0199. However, the measured energy data does have more internal scatter (i.e., lower R^2 value).

CDOT uses a fraction of the structural strength of the pile to estimate the ultimate capacity of the pile in cohesive IGMs. The CDOT calculated capacity is calculated from the following equation:

$$R_3 = 0.25 \times f_y \times A_{open} \times FS \qquad (13)$$

where, f_y is the yield stress of the steel, A_{open} is the area of the pile, and FS is the factor of safety used in design (FS = 3). A_{open} is the cross sectional area of the pile. The CDOT capacity prediction method is further described in section Chapter 4.

A comparison of capacities calculated using the WSDOT Gates formula, the FHWA Gates formula, the CDOT method, DRIVEN, and GRLWEAP methods are shown in Figure 18 and Figure 19 for cohesive and cohesionless IGMs, respectively. The calculated capacities are compared to the measured CAPWAP capacities. DRIVEN and GRLWEAP are calculated with the original MDT inputs. Figure 18(a) shows all of the data, while Figure 18(b) shows more detail for the lower capacity values. The CDOT method and FHWA Gates formula consistently under predict the capacity by a considerable amount. DRIVEN and GRLWEAP predict each other very well; however, neither accurately matches the final CAPWAP capacity. The WSDOT Gates formula slightly over predicts the capacity in cohesive IGMs. However, overall the WSDOT Gates formula appears to predict measured CAPWAP capacity of the pile.

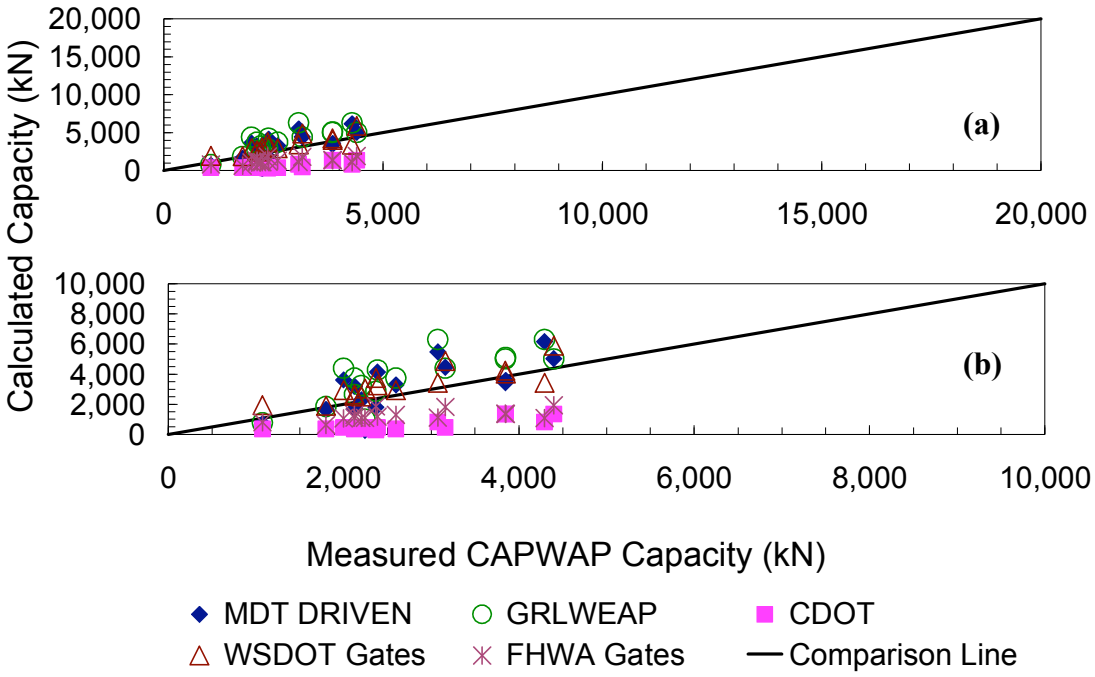

Figure 18. Comparison of all capacity calculations in cohesive IGMs. (a) All data at full scale. (b) Detail at lower capacities.

The analytical methods are somewhat more accurate in the cohesionless IGMs when compared to cohesive IGMs, shown in Figure 19. Again, Figure 19(a) displays all of the data, while Figure 19(b) shows more detail for lower capacity values. The DRIVEN and GRLWEAP correlations are similar to those in cohesive IGMs; that is, there is little correlation between them and the CAPWAP capacity. While the DRIVEN and GRLWEAP capacities are similar. The FHWA Gates formula is again conservative. As in cohesive IGMs, the WSDOT gates formula is best at predicting the measured CAPWAP capacity.

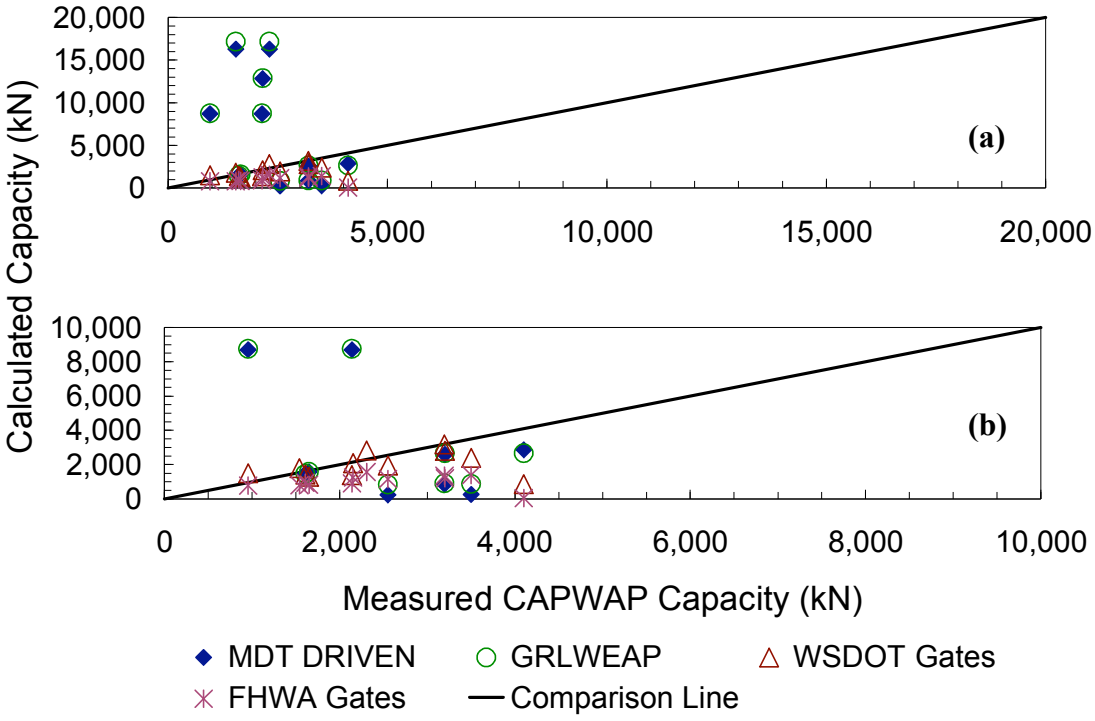

Figure 19. Comparison of all capacity calculations in cohesionless IGMs. (a) All available data. (b) Detail of points at lower capacities.

This data can also be observed by project bent. This information for cohesive and cohesionless IGMs is shown within Figure 20 and Figure 21, respectively. In cohesionless IGMs, DRIVEN analyses over predicted the capacity on two projects, Q744 and 1744, which comprise 60% of the CAPWAP tests within cohesionless IGMs. The WSDOT Gates formula consistently predicted more accurate capacities when compared to DRIVEN.

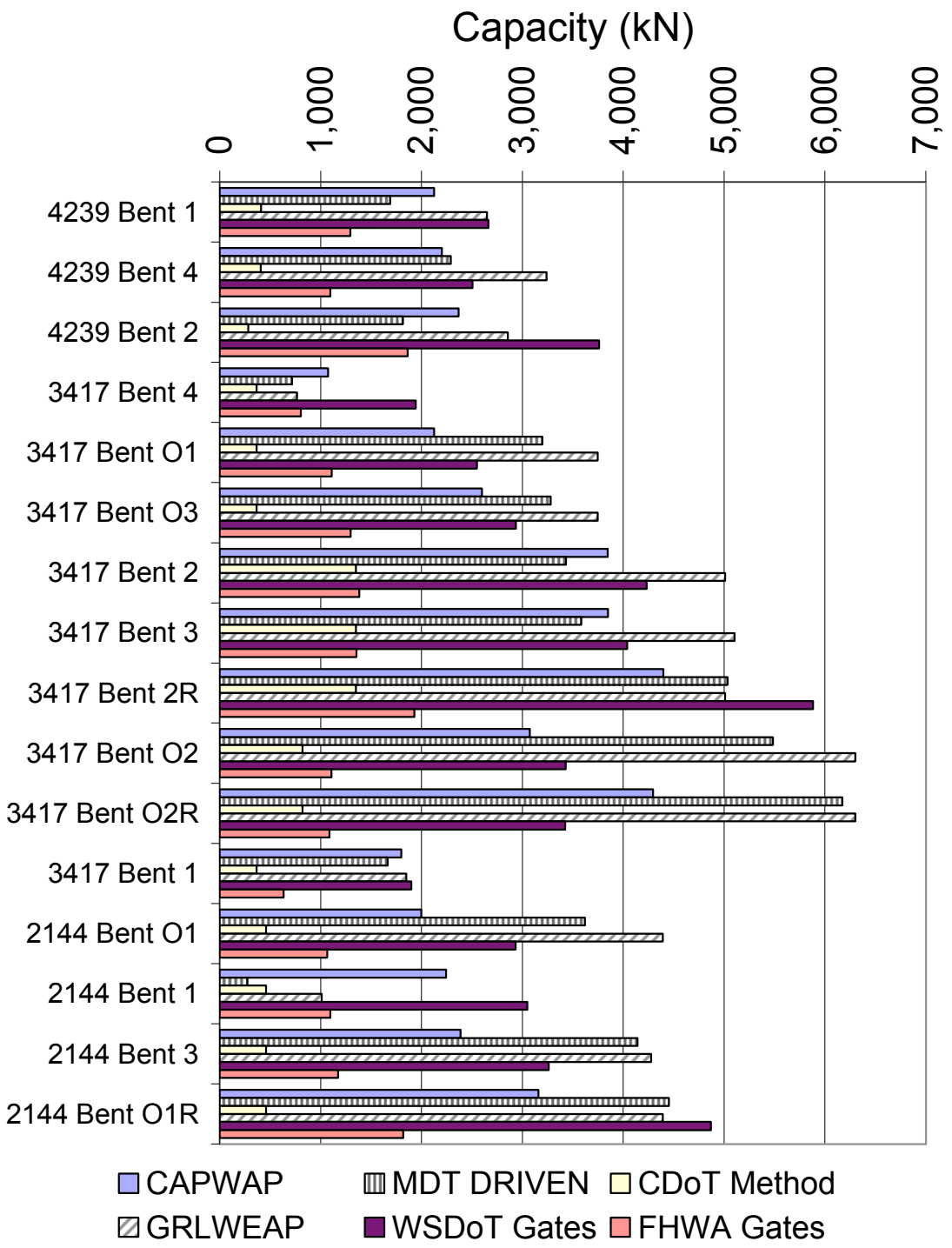

Figure 20. Comparison of capacity calculations in cohesive IGMs compared by project number and bent.

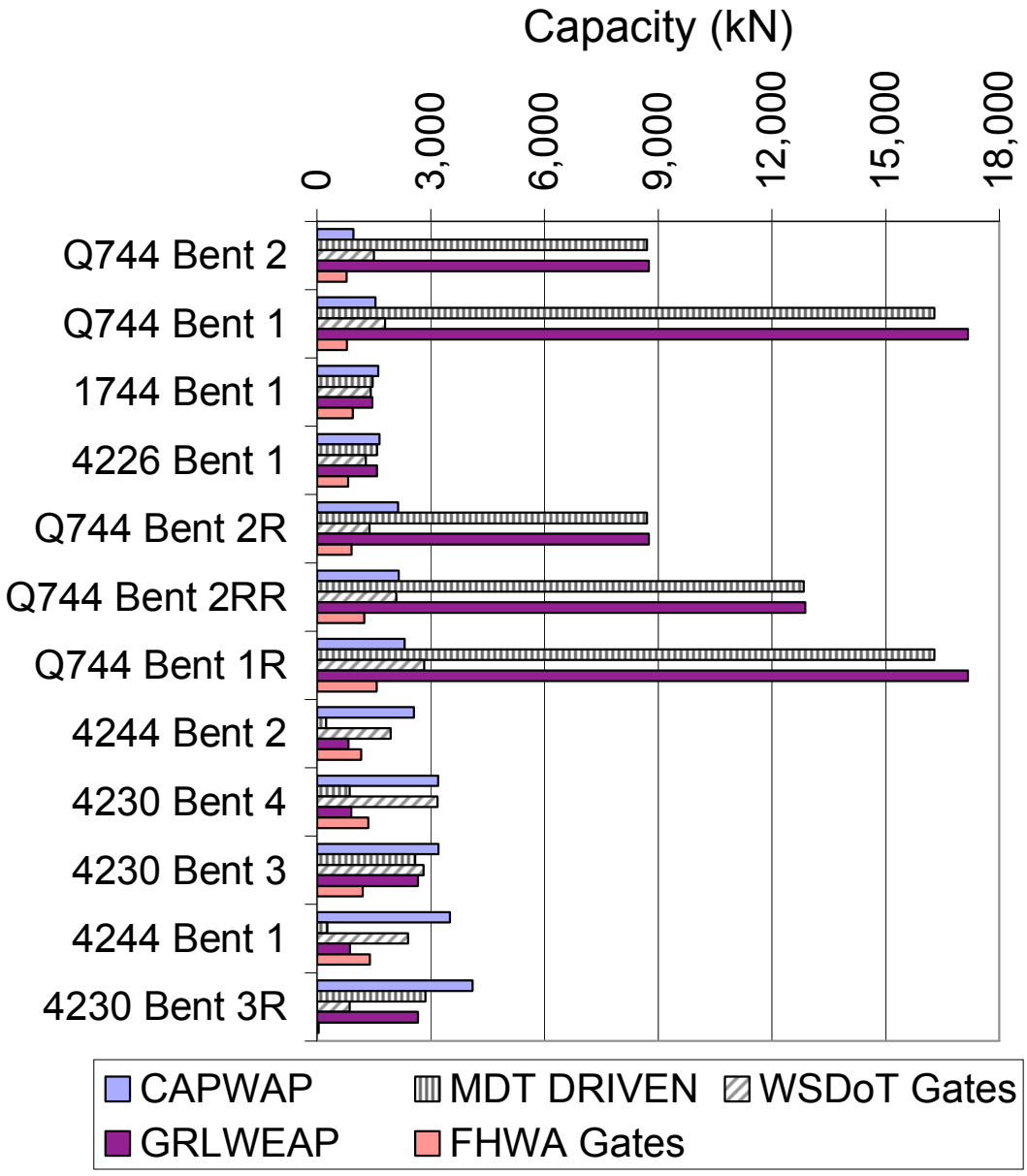

Figure 21. Comparison of capacity calculations in cohesionless IGMs compared by project bent.

Design methods include CDOT, DRIVEN and GRLWEAP. DRIVEN is still the best method for use in design. The CDOT method consistently under predicts the

ultimate capacity of the pile by a significant amount. Thus, this method is not recommended for use in design.

Field capacity checks include PDA, CAPWAP and WSDOT Gates formulas. While CAPWAP is by far the most accurate field analysis method, it is not practical for some projects. In these cases, the WSDOT Gates formula is recommended. It provides increased accuracy and decreased cost, from data easily measured in the field. Overall, the most accurate method of determining the capacity is through a static load test on the project. However, the expense of a static load test is not justified on some projects. In these cases CAPWAP analysis are the next option for accuracy and lower expense. However, field capacity checks cannot be used as a design tool. This type of analysis does not include any evaluation of the embedment length of the pile; it must be conducted during field driving.

Driving pile to the required capacity with no indication of the a predicted length is uneconomical. This is impractical and has the potential to increase the cost of the project. In order to create design methods that better predict the CAPWAP capacity, further research and analyses are required.

CHAPTER 7

CONCLUSIONS

Experience with pile foundations in IGMs indicates the predicted behavior frequently does not match the field pile response. Piles either refuse early or drive further than anticipated. Analyses of the projects provided by the MDT Geotechnical Section focused on the IGM material, pile design methods and design method accuracy for piles within IGMs.

The definitions of IGMs, material behaviors, sampling and testing methods, axial capacity design methods, and experiences with foundations founded in IGMs were compiled from a thorough literature review. Nine MDT projects were analyzed by the author to determine any trends to aid in design of piles in IGMs.

There are two different definitions for IGMs, based on type. Cohesive IGMs have an intrinsic bonding and include mudstone, claystone, siltstone and sandstone and are defined by unconfined compression test strengths between 0.5 to 25 MPa. Cohesionless IGMs do not have any apparent bonding between the particulates of the material. SPT N-values of greater than 50 blows per 0.3 meters define a cohesionless IGM.

The geological and geotechnical material behavior of IGMs should be considered when conducting foundation analyses. The geological component yields information regarding the strength of the material, the type of bonding and an indication of the heterogeneity expected within the formation. The geotechnical component yields information regarding frictional components, pore pressure characteristics and their affects on IGM strength and stiffness.

Sampling and testing concerns are the largest hurdle with IGMs. Accurate material properties cannot be determined unless quality samples are obtained from the field. However, rock coring and SPT sampling methods are not adequate to obtain quality samples of IGMs. In-situ methods, specifically the pressuremeter, can be used to determine accurate strength and stiffness parameters. However, these methods can be expensive and need to be performed correctly in order to yield adequate results.

Computerized analytical tools typically used for pile design include DRIVEN, GRLWEAP and CAPWAP. The programs have a long history of use and work well for piles driven into most types of soils. However, DRIVEN exhibits some problems within its calculation procedures when using large undrained cohesion values, which are common with IGMs. The undrained cohesion is multiplied by an α value to calculate the adhesion. DRIVEN directly correlates the unconfined compression strength to the adhesion without determining an alpha value. Because of this, there is a limiting value of adhesion after a c_u of 150 kPa. This limiting value of c_a can result in under prediction of shaft capacity in cohesive IGMs.

The software GRLWEAP is used to determine the drivability of piles and select driving hammers. The soil profile is input through a GRLWEAP input file created from DRIVEN. The soil profile is used in GRLWEAP to determine quake and Smith damping coefficients for the lithology. Because IGMs have specific inputs for quake and damping, GRLWEAP does not automatically input these values for IGM layers. These parameters must be input by the user. A study was used to determine the parameter that had the largest impact on the final predicted blow count of the pile. Through this study,

toe damping parameters were found to have the greatest impact. No further analysis was conducted within GRLWEAP, therefore the recommended quake and damping inputs should be used.

CAPWAP is a capacity determination tool that uses measured field data to accurately determine the dynamic capacity of pile foundations. Case studies in which a CAPWAP analysis and a static load test were conducted, on the same project, were compiled into a database. From this information, it was determined that the CAPWAP dynamic capacity is well correlated to the static load test capacity. Due to the high accuracy of the CAPWAP capacities when compared to static load tests, the CAPWAP capacity was used as a baseline comparison in this study.

Deep foundation experience with IGMs has been predominantly focused on drilled shafts. Based on documented experience in the literature, the installation method and its affect on the IGM material property was found to govern the drilled shaft capacity. Sometimes the designer determined that either the shaft or end bearing capacity of the drilled shaft should be ignored. However, different designers from around the country often chose to ignore different aspects of the drilled shaft capacity within the same type of IGM, causing juxtaposition in design methodology and very conservative final designs. Some of the same inconsistency was apparent within driven piles; however, information was not readily available. Most information on driven piles focused on their installation in stiff materials. As, driven piles in IGM often develop high driving resistances and are prone to damage in very dense materials.

Comparisons of data from nine projects provided by MDT were not conclusive enough to derive a more accurate capacity prediction method for future use. The WSDOT Gates driving formula shows promise as a good approach for checking capacity during pile installation, when dynamic testing is not economical. The CDOT method of capacity prediction, which is based on the structural capacity of the pile, significantly under predicts the CAPWAP capacity. Of the prediction methods, the software DRIVEN appears to be a reliable prediction tool. Due to problems within DRIVEN capacity prediction in cohesive IGMs, the designers should input a user defined adhesion value for a more accurate shaft resistance prediction whenever the undrained cohesion exceeds 150 kPa.

A slight trend was observed in the normalized shaft resistance plots of CAPWAP capacity compared to pile length in IGMs. If CAPWAP analyses could be conducted in the soil layers above the IGM layer to determine the shaft resistance from the overlying soil, this value could be removed from the overall shaft capacity. The adhesion could then be back calculated for the IGM from the shaft resistance within only the IGM.

Static load testing is the only method of precisely determining the axial capacity of deep foundations. Piles can be instrumented in order to determine the shaft resistance at points along the pile profile. Using this information, a more accurate adhesion value could be determined. There is no substitute for good quality data. Static load testing provides that information, if the test is well planned and documented. Detailed information from accurate subsurface profiles, in-situ pressuremeter testing, pile

construction records would be valuable for any further correlations of deep foundations within IGMs

IGMs are incredibly varied materials in which current geological and geotechnical knowledge provide engineers with a limited and incomplete understanding of their properties and behavior. To decrease uncertainties and thus construction costs, further research is necessary in the following areas:

- develop a sampling method for IGMs that allows the collection of undisturbed samples,
- determine correlations between in-situ testing and design methods,
- increase mechanistic understanding of end-bearing and shaft resistance,
- conduct fully instrumented pile static load tests to compare data from in-situ tests and design methods,
- isolate shaft capacities within IGMs, and
- formulate design methods specifically for piles within IGMs.

APPENDICES

APPENDIX A

MDT PROJECT SUBSURFACE PROFILES

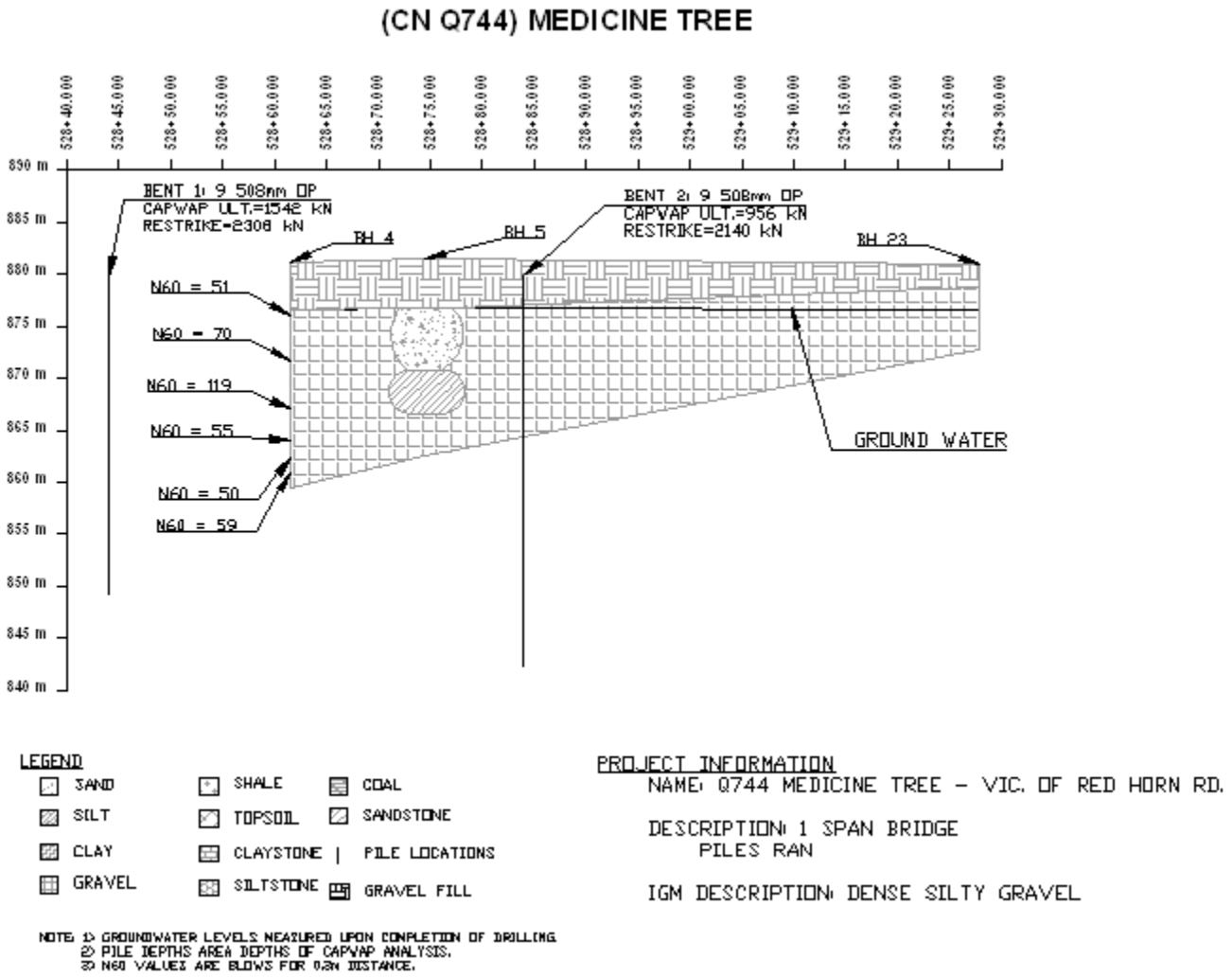

Figure 22. Soil profile for project Q744 – Medicine Tree.

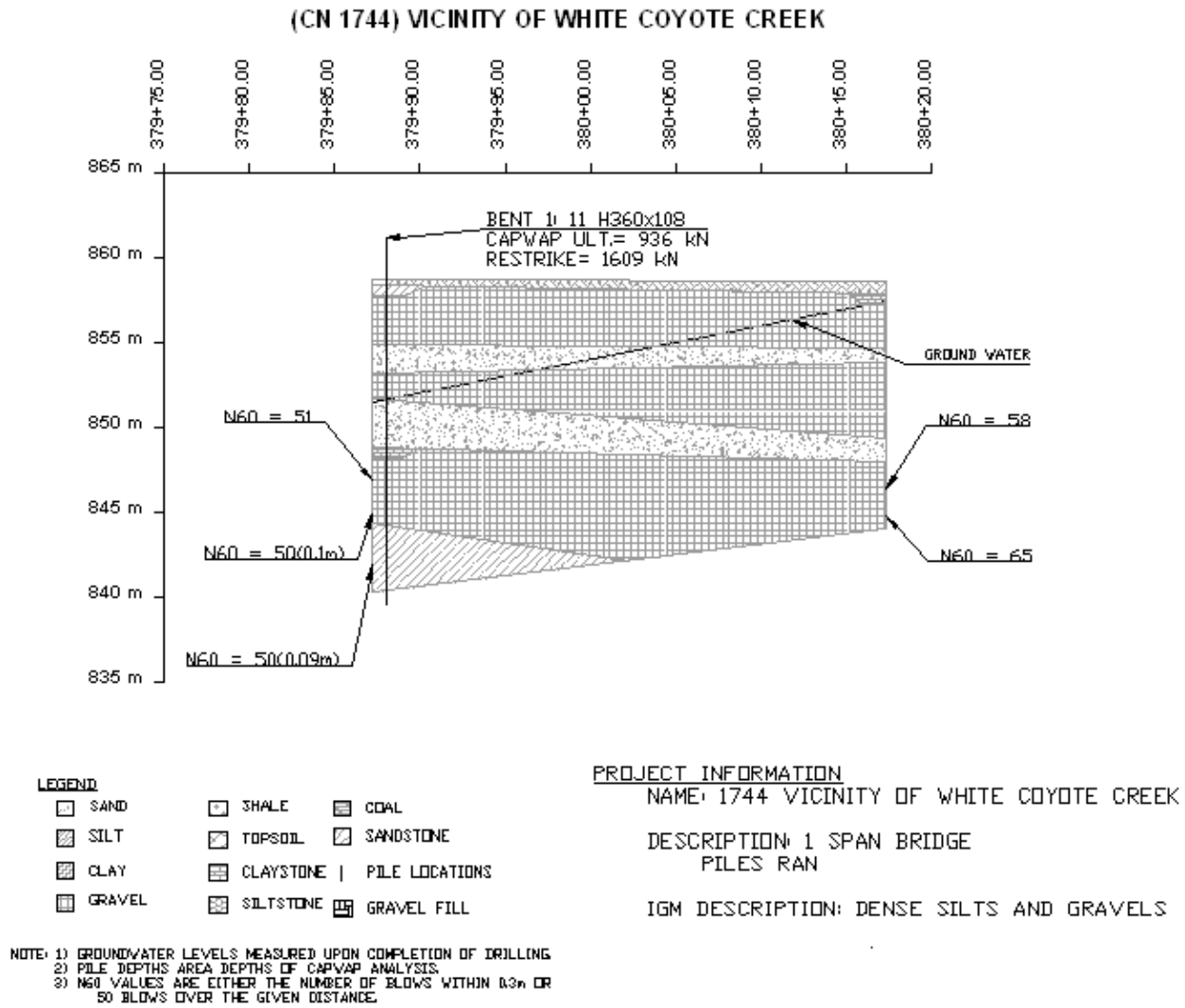

Figure 23. Soil profile for project 1744 (Vicinity of White Coyote Creek) main structure.

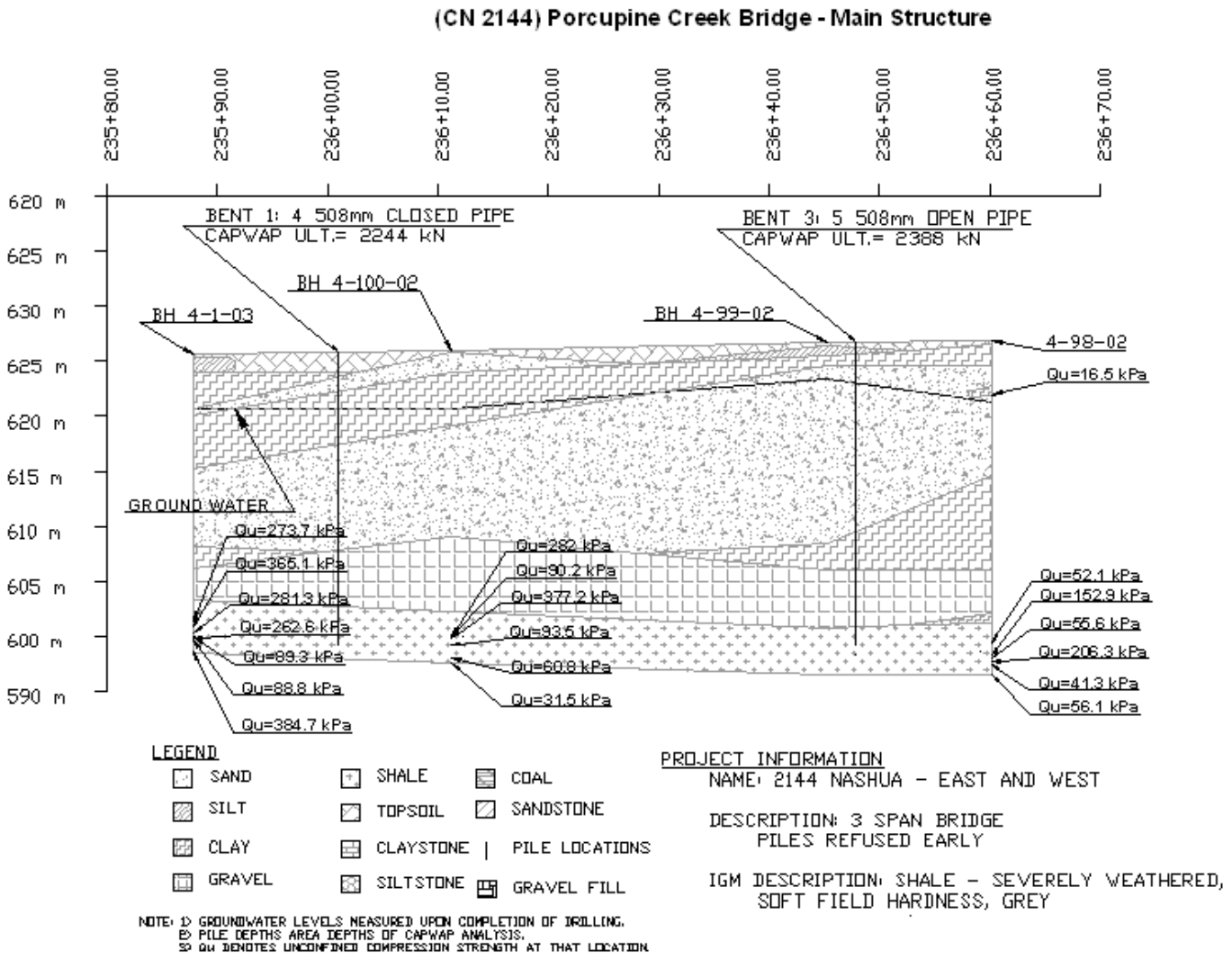

Figure 24. Soil profile for project 2144 (Nashua Creek) main structure.

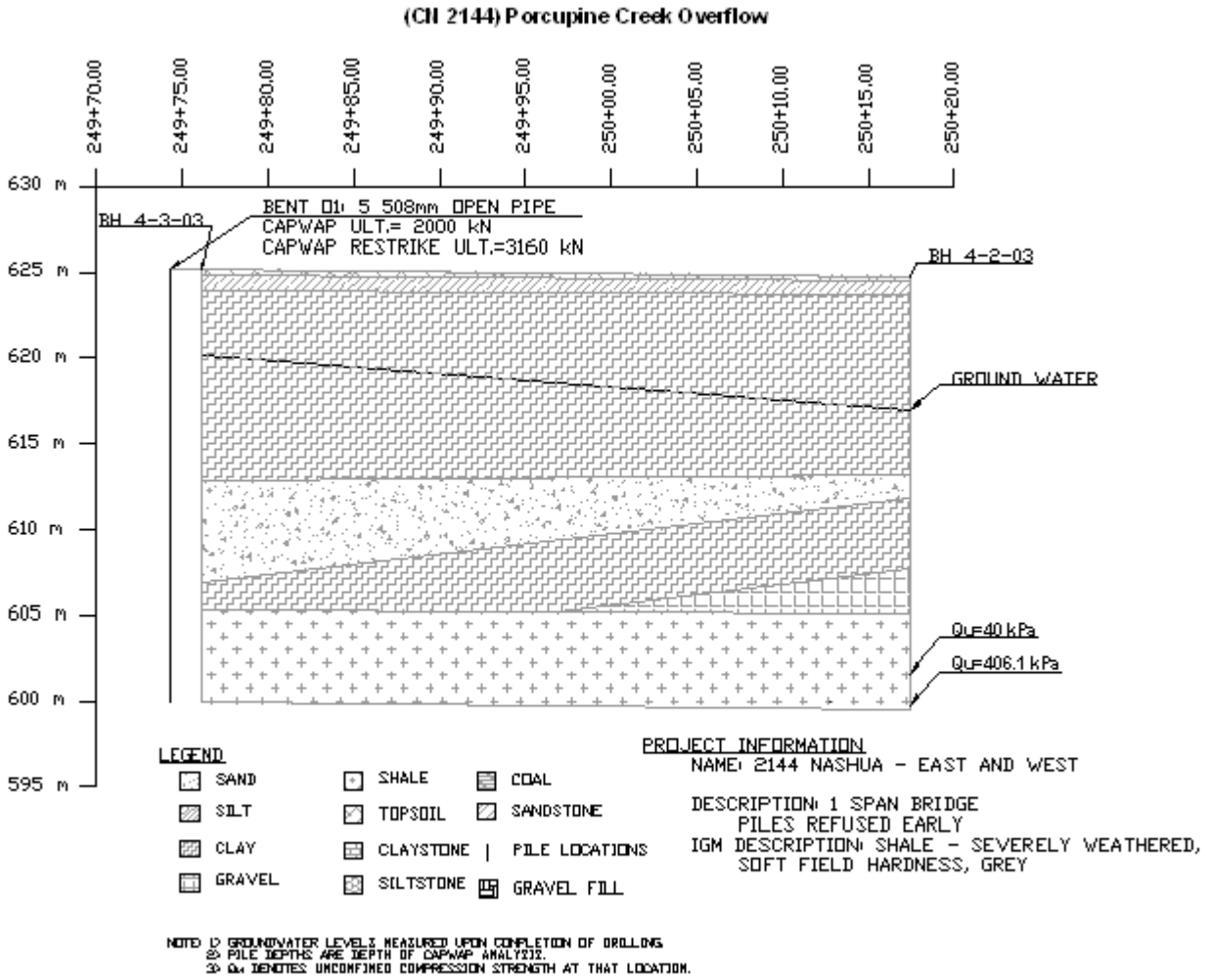

Figure 25. Soil profile for project 2144 (Nashua Creek) overflow structure.

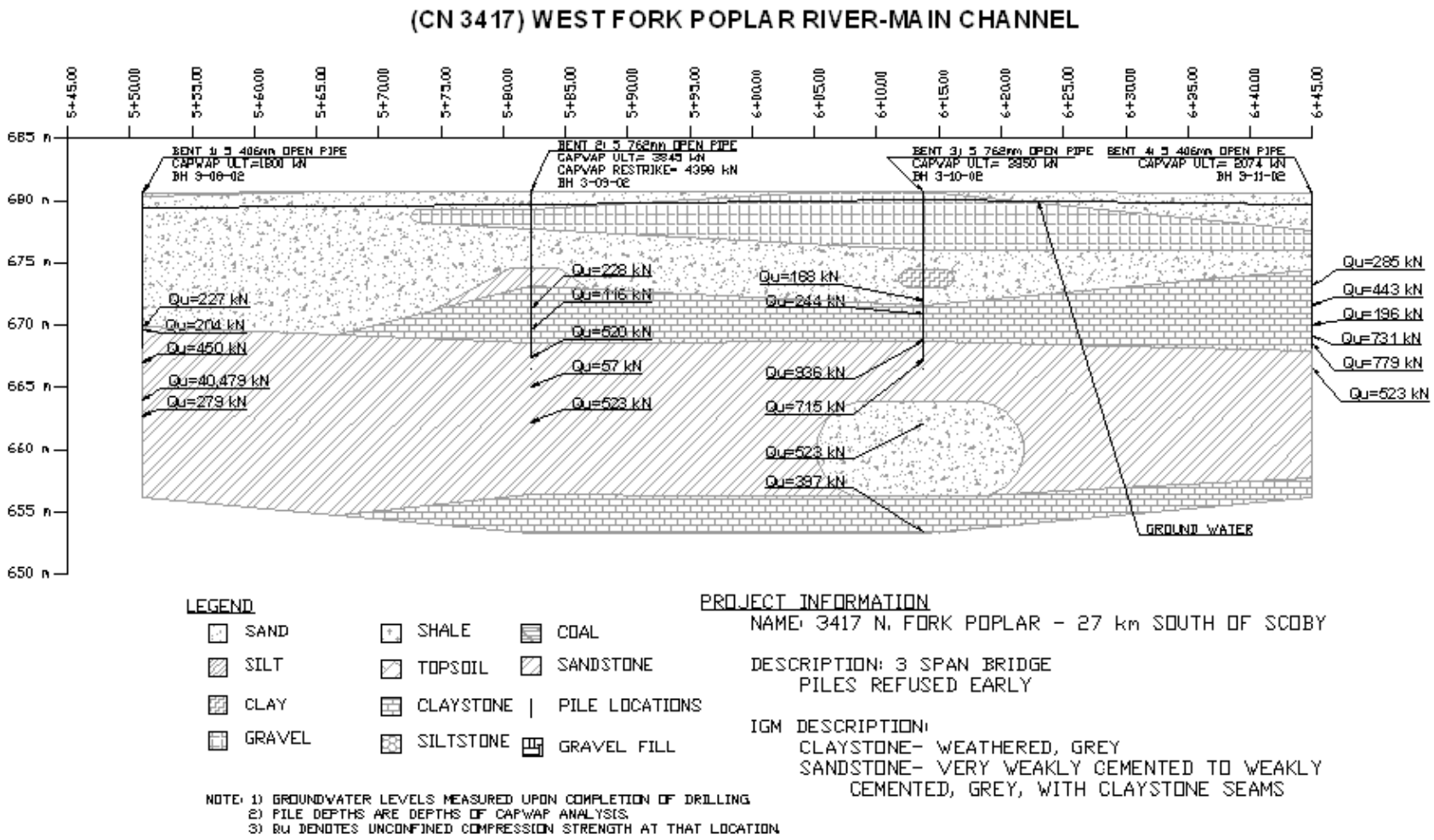

Figure 26. Soil profile for project 3417 (West Fork Poplar River) main structure.

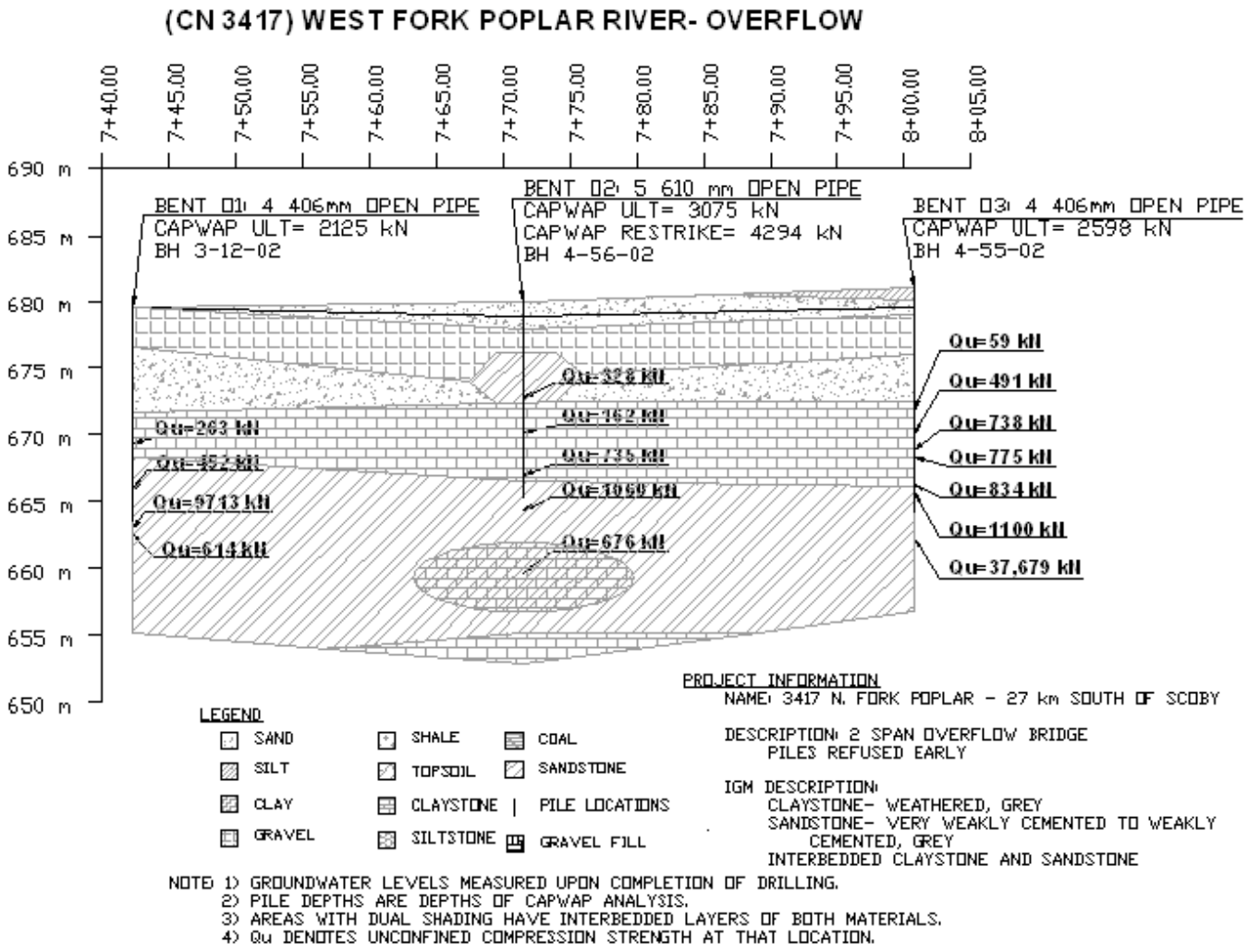

Figure 27. Soil profile for project 3417 (West Fork Poplar River) overflow structure.

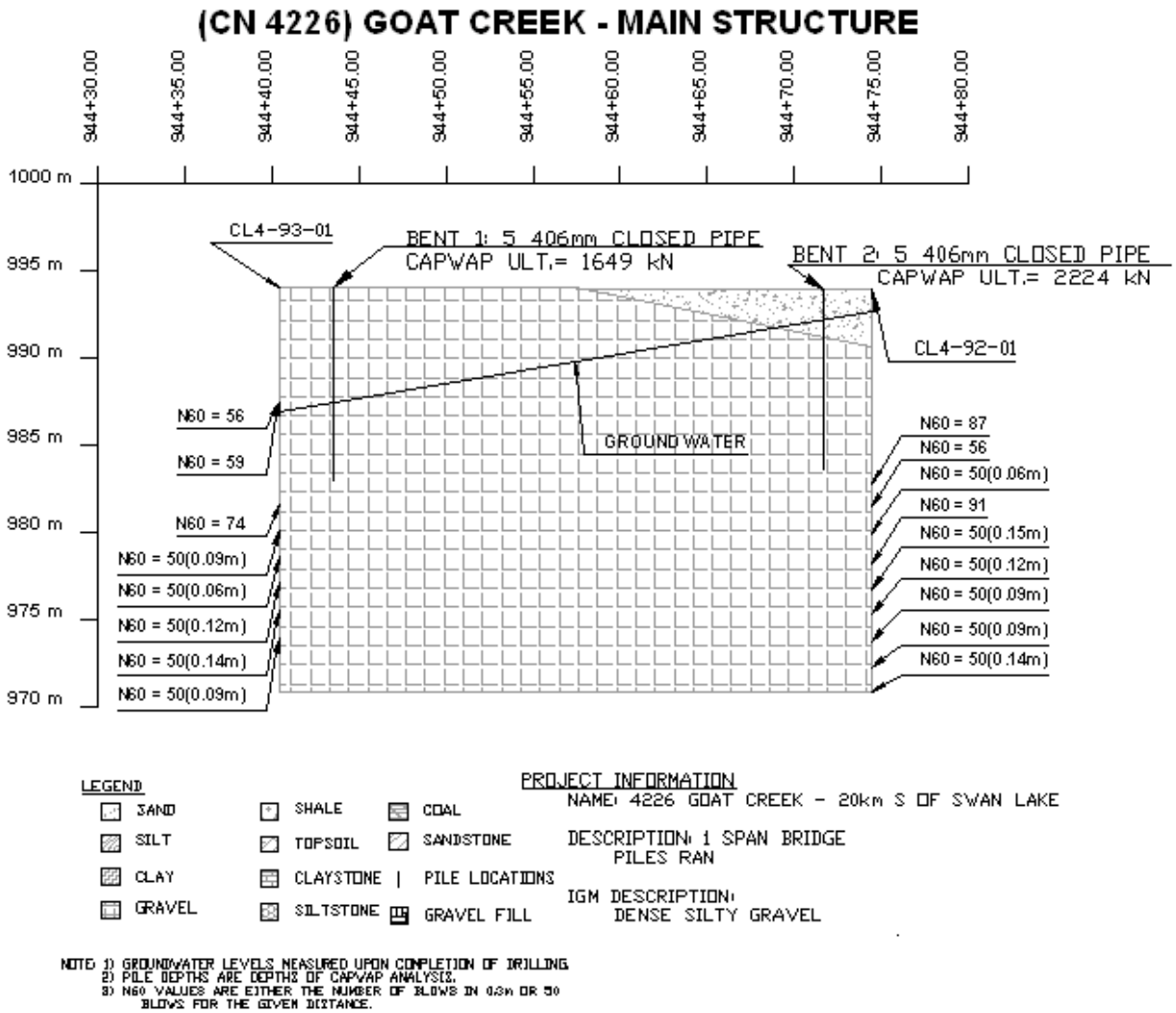

Figure 28. Soil profile for project 4226 (Goat Creek) main structure.

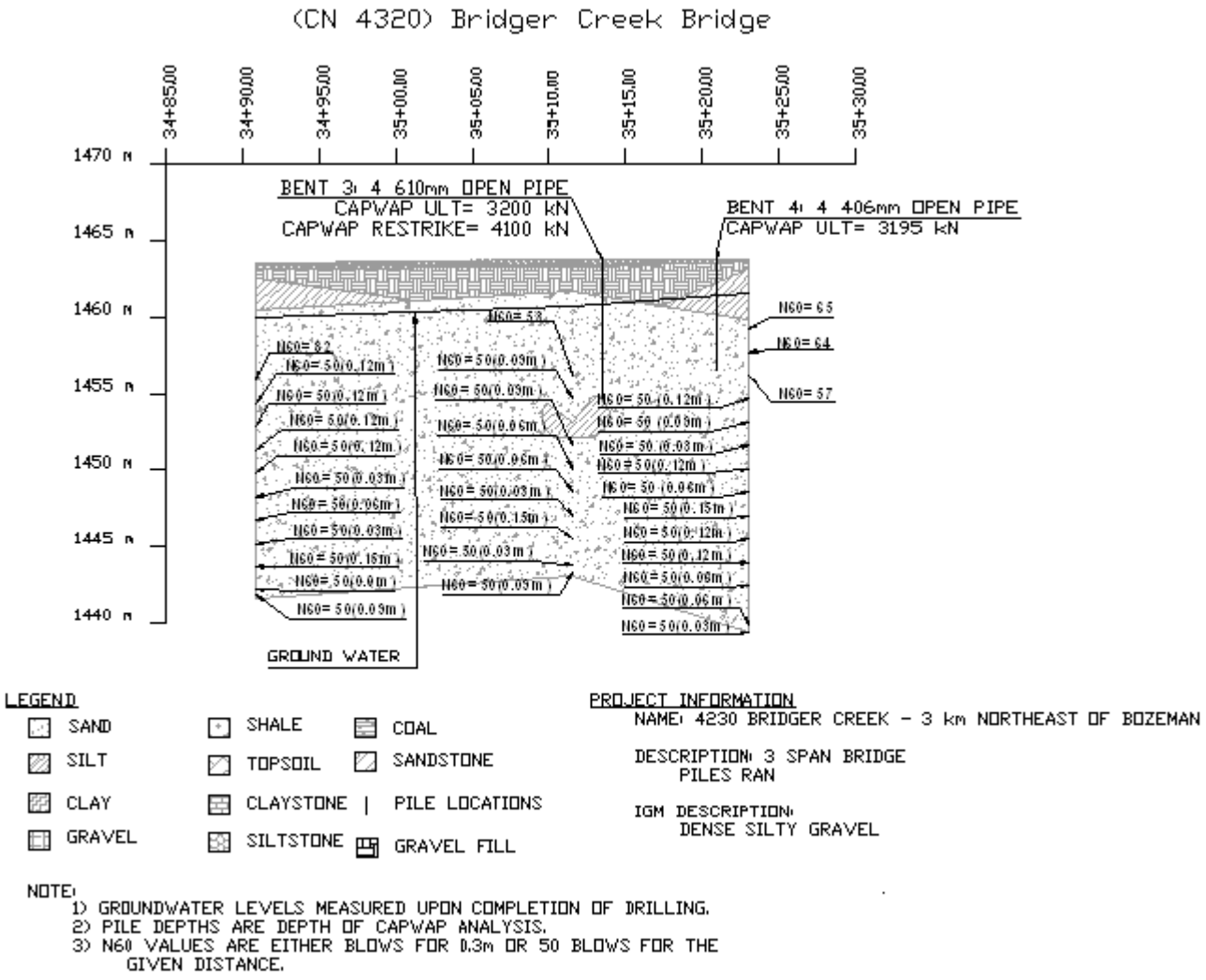

Figure 29. Soil profile for project 4230 (Bridger Creek) main structure.

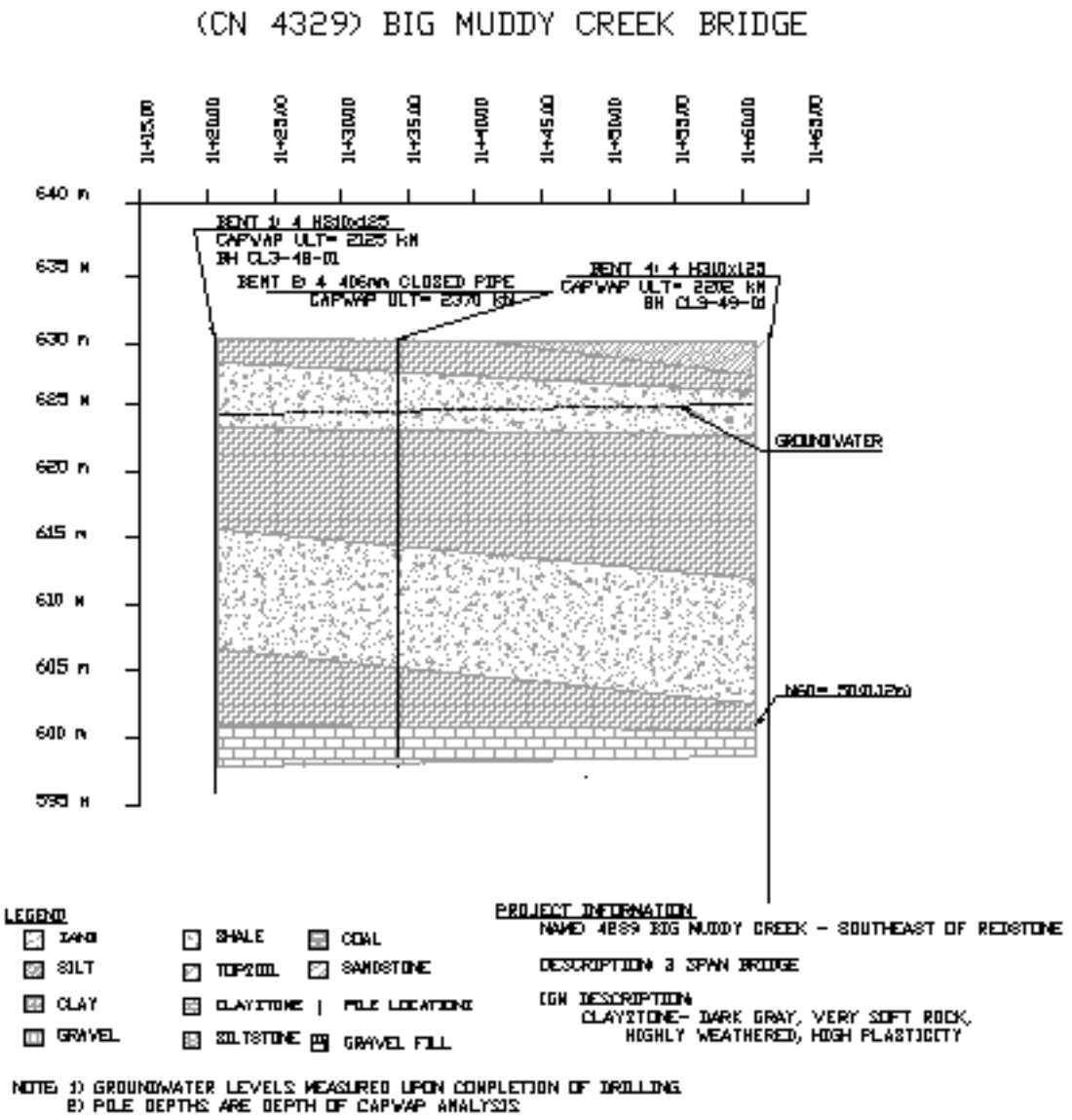

Figure 30. Soil profile for project 4239 (Big Muddy Creek) main structure.

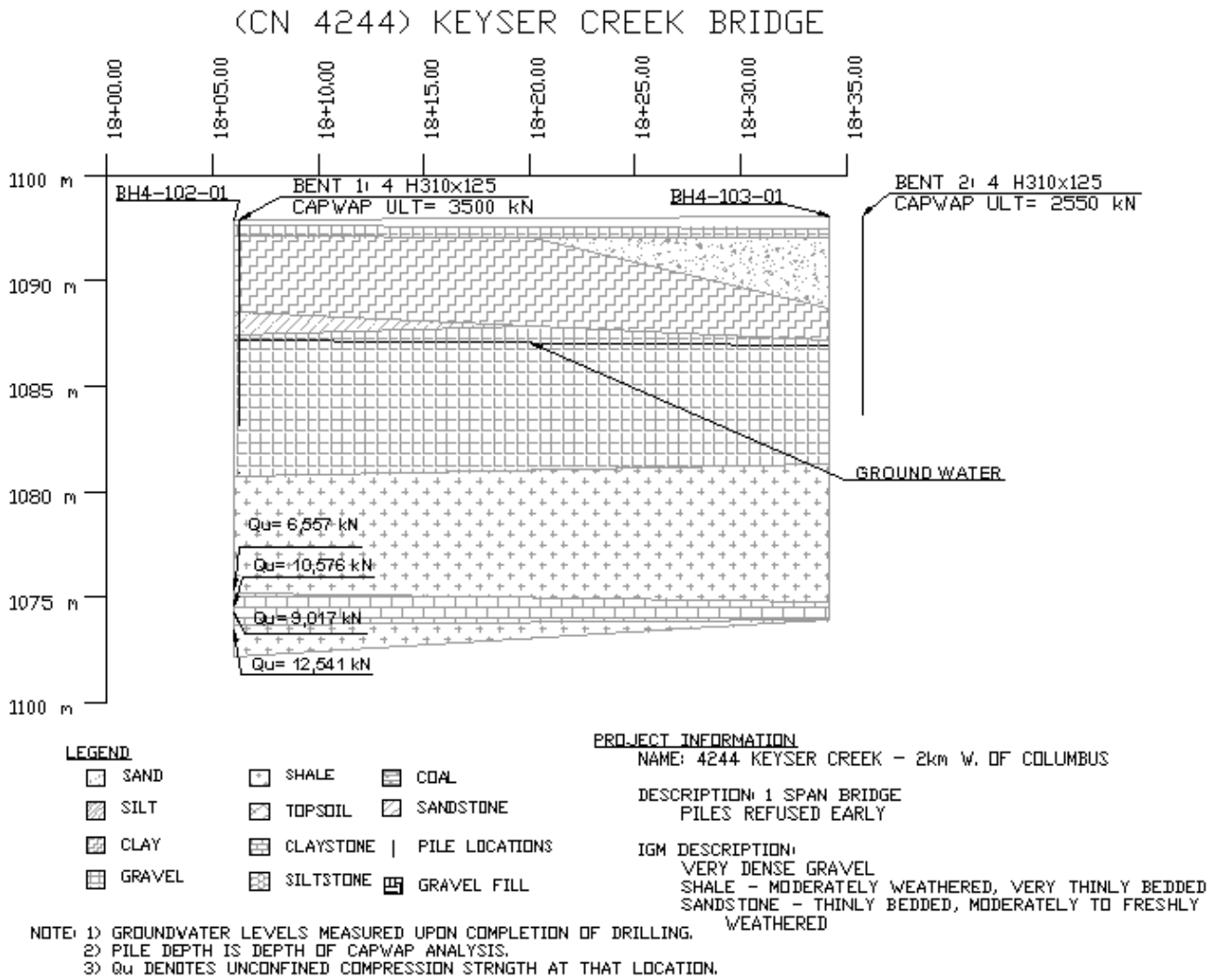

Figure 31. Soil profile for project 4244 (Keyser Creek) main structure.

APPENDIX B

COMPILED INFORMATION FROM MONTANA DEPARTMENT OF TRANSPORTATION FOR ALL ANALYZED PROJECTS

Table 7. CAPWAP capacities and depths of layers for DRIVEN analyses.

Project	Bent	IGM Type	CAPWAP Cap. (kN)	CAPWAP Shaft (kN)	CAPWAP Toe (kN)	Depth in IGM's (m)	Pile Pen. (m)	Layer Depth 1 (m)	2 (m)	3 (m)	4 (m)	5 (m)	6 (m)	7 (m)
Q744	1	CL	1542	1432	110	15.13	30.2	3.8	**7.3**	20				
	1R	CL	2308	2119.1	189	15.53	30.5	3.8	**7.3**	20				
	2	CL	956	845.9	110	17.51	30.1	3.8	**7.3**	20				
	2R	CL	2140	1794.4	345.6	17.51	30.1	3.8	**7.3**	20				
	2RR	CL	2152	2130.3	21.5	24.58	37.5	3.8	**7.3**	20				
1744	1	CL	1609.2	1140.3	468.9	13.71	21.01	0.9	3.8	5.5	9.8	10.5	**14.3**	20
2144	1	CH	2244	1143.7	1100.3	4.20	26.5	6.70	15.30	**22.30**	**27.70**	33.10		
	3	CH	2388	1791.1	596.9	1.50	27.4	18.30	20.70	**25.90**	30.00			
	O1	CH	2000	1694.4	305.6	4.10	25.1	12.50	18.50	**21.00**	30.00			
	O1R	CH	3160	2799.4	360.6	4.20	25.2	12.50	18.50	**21.00**	30.00			
3417	1	CH	1800	1315.1	484.9	9.35	12.4	**3.05**	16.15					
	2	CH	3845	2940.7	904.3	7.20	13.3	**6.10**	**12.19**	27.43				
	2R	CH	4398	3454.4	943.6	7.30	13.4	**6.10**	**12.19**	27.43				
	3	CH	3850	3176.7	673.3	7.40	13.5	**6.10**	**12.19**	27.43				
	4	CH	2074	1505.7	568.3	5.39	12.4	**7.01**	**13.11**	24.38				
	O1	CH	2125	1838.2	286.8	9.30	16	**6.70**	**10.20**	**13.60**	22.40			
	O2	CH	3075	2877	198	10.90	14.60	**3.70**	**7.50**	**13.40**	23.00			
	O2R	CH	4294	4094.8	199.2	10.90	14.60	**3.70**	**7.50**	**13.40**	23.00			
	O3	CH	2598	2212.7	385.3	7.30	16.80	4.00	**9.50**	**15.90**	23.00			
4226	1	CL	1649	191	1458.1	0.51	9.30	**3.30**	23.16					
4230	3	CL	3200	951.1	2248.9	4.58	8.58	**4.00**	20.00					
	3R	CL	4100	2179.7	1920.3	5.14	9.14	**4.00**	20.00					
	4	CL	3195	569	2626	3.23	7.23	**4.00**	16.00					
4239	1	CH	2125	1170.5	954.5	5.02	33.98	1.83	6.71	10.06	14.33	23.17	**28.96**	36.58
	2	CH	2370	406.6	1963.4	2.13	31.09	1.83	6.71	10.06	14.33	23.17	**28.96**	36.58
	4	CH	2202	851	1351	13.00	41.96	1.83	6.71	10.06	14.33	23.17	**28.96**	42.00
4244	1	CL	3500	465.1	3034.9	2.41	9.72	4.27	5.79	**7.32**	**12.19**	15.24		
	2	CL	2550	455.5	2094.5	2.13	9.44	4.27	5.79	**7.32**	**12.19**	15.24		

*Highlighted cells are IGM's

**Bolded text is start of IGM layer

Table 8. DRIVEN inputs for IGM material strength, groundwater, scour and driving strength loss.

Project	Bent	Qu by layer				Ground Water			Ult. Considerations			Driving Strength Loss						
		2 (kPa)	3 (kPa)	4 (kPa)	5 (kPa)	Drill. (m)	Dr./Res. (m)	Ult. (m)	Loc. Sc. (m)	LT Sc. (m)	Soft Soil (m)	1	2	3	4	5	6	7
Q744	1					3.7	3.7	3.7										
	1R					3.7	3.7	3.7										
	2					3.7	3.7	3.7										
	2R					3.7	3.7	3.7										
	2RR					3.7	3.7	3.7										
1744	1					1.1	1.1	1.1										
2144	1			206.20		0.00	0.00	0	0.00	0	15.3d							
	3			82.97		0.00	0.00	0	8.2	0	0							
	O1			223.1		0.00	0.00	0	0	0	6d							
	O1R			223.1		0.00	0.00	0	0	0	6d							
3417	1	293.7				1.22	1.22	0	0	0	0							
	2	197	366.7			1.52	1.52	0	2.377	3.749	0							
	2R	197	366.7			1.52	1.52	0	2.377	3.749	0							
	3	449.3	545			1.52	1.52	0	2.377	3.627	0							
	4	578.7	523			2.44	2.44	0	0	0	0							
	O1	263	452	5163.5		3.00	3.00	0	0	0	0							
	O2	328	457.5	868		1.50	1.50	0	1.97	0.03	0							
	O2R	328	457.5	868		1.50	1.50	0	1.97	0.03	0							
	O3		709	19390		2.40	2.40	0	0	0	0							
4226	1					3.66	3.66	0	0	0.53	0							
4230	3					3.00	0.00	0	0	0	0							
	3R					3.00	0.00	0	0	0	0							
	4					3.00	0.00	0	0	0	0							
4239	1					5.79	5.79	0	0	0	15.24d	30		30	30		30	10
	2					5.79	5.79	0	0	0	15.24d	30		30	30		30	10
	4					5.79	5.79	0	0	0	15.24d	30		30	30		30	10
4244	1			9549	9796.5	1.52	1.52	1.524	0	6.53	0		50					
	2			750		1.52	1.52	1.524	0	6.53	0		50					

Qu = Unconfined Compression Strength

Table 9. DRIVEN inputs for unit weight and strength inputs.

Project	Bent	Unit Weight							Original Inputs						
		1	2	3	4	5	6	7	1	2	3	4	5	6	7
Q744	1	22	20	21					30/30	122	40/40				
	1R	22	20	21					30/30	122	40/40				
	2	22	20	21					30/30	122	40/40				
	2R	22	20	21					30/30	122	40/40				
	2RR	22	20	21					30/30	122	40/40				
1744	1	14	17	16	16.5	16	18	18	93.6	38/38	36/36	37/37	543.94	40/40	606.25
2144	1	14	15	14	16	20	21		28/28	25	28/28	30	32/32	38/38	
	3	14	15	20	20				30/30	25	34/36	38/38			
	O1	14	15	20	20				50	28/28	50	36/38			
	O1R	14	15	20	20				50	28/28	50	36/38			
3417	1	125 pcf	130 pcf	150 psf					30/30	36/36	40000 psf				
	2	125 pcf	125 pcf	130 pcf					33/33	2100 psf	36/36				
	2R	125 pcf	125 pcf	130 pcf					33/33	2100 psf	36/36				
	3	125 pcf	125 pcf	130 pcf					33/33	2000 psf	36/36				
	4	120 pcf	130 pcf	130 pcf					30/30	4550 psf	36/36				
	O1	19	19.6	18	20				30/30	36/36	150	36/40			
	O2	19	18	18	20				30/30	34/36	200	36/34			
	O2R	19	18	18	20				30/30	34/36	200	36/34			
	O3	19	19.6	18	20				30/30	36/36	150	36/40			
4226	1	15	19						32/32	40/40					
4230	3	14	19						28/28	40/40					
	3R	14	19						28/28	40/40					
	4	14	19						28/28	40/40					
4239	1	120 pcf	110 pcf	122 pcf	124 pcf	115 pcf	127 pcf	145 pcf	2000 psf	28.1/28	500 psf	500 psf	28.1/28	4000 psf	20000 psf
	2	120 pcf	110 pcf	122 pcf	124 pcf	115 pcf	127 pcf	145 pcf	2001 psf	28.1/29	500 psf	500 psf	28.1/29	4000 psf	20000 psf
	4	120 pcf	110 pcf	122 pcf	124 pcf	115 pcf	127 pcf	145 pcf	2003 psf	28.1/31	500 psf	500 psf	28.1/31	4000 psf	20000 psf
4244	1	121.4 pcf	121.4 pcf	140 pcf	142.4 pcf	120 pcf			0/0	0	34/34	36/36	40000 psf		
	2	121.4 pcf	121.4 pcf	140 pcf	142.4 pcf	120 pcf			0/0	0	34/34	36/36	40000 psf		

Table 10. GRLWEAP input parameters and piles by project.

Project	Bent	Hammer	Cushion						Pile							
			Area (cm^2)	E (MPa)	Thick (mm)	COR	Stiff.	Helmet (kN)	Length (m)	Pen. (m)	Area (cm^2)	Toe Area (cm^2)	Perim. (m)	O/C	Size (mm)	Shell (mm)
Q744	1	I-42S	2568	1206	50.8	0.92	0	12.4489	32	30.17	100.07	100.07	1.6	O	508	12.7
	1R	I-42S	2568	1206	50.8	0.92	0	12.4489	32	30.5	100.07	100.07	1.6	O	508	12.7
	2	I-42S	2568	1206	50.8	0.92	0	12.4489	32.19	30.11	100.07	100.07	1.6	O	508	12.7
	2R	I-42S	2568	1206	50.8	0.92	0	12.4489	32.19	30.25	100.07	100.07	1.6	O	508	12.7
	2RR	I-42S	2568	1206	50.8	0.92	0	12.4489	32.19	37.49	100.07	100.07	1.6	O	508	12.7
1744	1	I-42S	2568	1206	50.8	0.92	0	9.7119	30.38	21.01	1283.66	138	1.434		360x108	
2144	1	D46-32	3168	1207	127	0.95	0	20.915	28.04	26.50	2026.83	100.07	1.5959	O	508	12.7
	3	D46-32	3168	1207	127	0.95	0	20.915	29.87	27.40	2026.83	100.07	1.5959	O	508	12.7
	O1	D46-31	3168	1207	127	0.95	0	20.915	26.6	25.10	2026.83	100.07	1.5959	O	508	12.7
	O1R	D46-32	3168	1207	127	0.95	0	20.915	26.6	25.20	2026.83	100.07	1.5959	O	508	12.7
3417	1	I-30	2565	1210	63.5	0.92	0	14.03	13.5	12.40	1294.62	79.73	1.2755	C	406	12.7
	2	I-80	3165	1210	63.5	0.92	0	20.36	15.24	13.30	4560.37	225.17	2.3939	O	762	19.05
	2R	I-80	3165	1210	63.5	0.92	0	20.36	15.24	13.40	4560.37	225.17	2.3939	O	762	19.05
	3	I-80	3165	1210	63.5	0.92	0	20.36	15.24	13.50	4560.37	225.17	2.3939	O	762	19.05
	4	I-30	2565	1210	63.5	0.92	0	14.03	13.5	12.40	1294.62	79.73	1.2755	O	406	12.7
	O1	I-30	2565	1210	63.5	0.92	0	14.03	17.8	16.00	1294.62	79.73	1.2755	O	406	12.7
	O2	I-80	3165	1210	63.5	0.92	0	20.36	15.85	14.60	2922.47	179.68	1.9164	O	610	19.05
	O2R	I-81	3165	1210	63.5	0.92	0	20.36	15.85	14.60	2922.47	179.68	1.9164	O	610	19.05
	O3	I-30	2565	1210	63.5	0.92	0	14.36	17.8	16.80	1294.62	79.73	1.2755	O	406	12.7
4226	1	I-42S	2568	1206	50.8	0.92	0	12.45	9.30	9.30	1294.62	79.73	1.2755	C	406	12.7
4230	3	D46-32	3168	1207	127	0.95	0	20.915	12.27	8.58	2922.47	180.15	1.9164	O	610	19.1
	3R	D46-32	3168	1207	127	0.95	0	20.915	12.27	9.14	2922.47	180.15	1.9164	O	610	19.1
	4	D46-32	3168	1207	127	0.95	0	20.915	10.1	7.23	1294.62	79.73	1.2755	O	406	12.7
4239	1	D25-32	1464.5	3654	50.8	0.8	0	8.452	50.52	33.98	973.44	159	1.248		310X125	
	2	D25-32	2677.41	3654.2	50.8	0.8	0	15.124	33.68	31.09	1294.62	79.73	1.2755	C	406	12.7
	4	D25-32	1464.5	3654	50.8	0.8	0	8.452	50.52	41.96	973.44	159	1.248		310X125	
4244	1	I-42S	2568	1206	50.8	0.92	0	9.7119	15.39	9.72	973.44	159	1.248		310X125	
	2	I-42S	2568	1206	50.8	0.92	0	9.7119	15.39	9.44	973.44	159	1.248		310X125	

Table 11. Final driving blow count and stroke along with quake and damping information from CAPWAP reports.

Project	Bent	Final BC (BL/.3m)	Stroke (m)	Damping		Quake	
				Shaft (sec/m)	Toe (sec/m)	Shaft (mm)	Toe (mm)
Q744	1	62	3.1	0.351	0.499	2.667	2.972
	1R	57	3.1	0.351	0.499	2.667	2.972
	2	54	2.7	0.279	0.299	2.54	2.54
	2R	118	2.5	0.279	0.299	2.54	2.54
	2RR	133	2.8	0.279	0.299	2.54	2.54
1744	1	59	2.6	0.15	0.49	2.54	5
2144	1	29	2.7	0.6	0.5	3.5	3
	3	31	2.7	0.6	0.4	2.5	2
	O1	29	2.5	0.65	0.4	2	2
	O1R	59	1.2	0.65	0.4	2	2
3417	1	19	2.9	0.45	0.25	1.5	11
	2	30	2.3	0.4	1.03	2.5	6.6
	2R	46	2.6	0.4	1.03	2.5	6.6
	3	33	2.3	0.4	1.03	2.5	6.6
	4	31	3.1	0.45	0.25	1.5	11
	O1	44	3.1	0.45	0.25	1.5	11
	O2	24	2.3	0.25	0.5	2.5	10
	O2R	50	2.3	0.25	0.5	2.5	10
	O3	56	3.2	0.45	0.25	1.5	11
4226	1	96	2.3				
4230	3	45	2.3	0.328	0.6	2.5	2.8
	3R	47	2.4	0.328	0.6	2.5	2.8
	4	53	2	0.328	0.6	2.5	2.5
4239	1	73	2.5	0.4	0.1	5	12
	2	150	2.6	0.861	0.128	1.75	13.36
	4	73	2.8	0.72	0.102	2.503	7
4244	1	148	3	0.65	0.5	2	1.5
	2	119	2.7	0.65	0.5	2	1.5

APPENDIX C

CAPWAP ANALYSIS AND STATIC LOAD TEST COMPARISON BASED ON LITERATURE REVIEW

Table 12. CAPWAP capacity (kN) and static load test results (kN) from the literature.

Background Data		Static Capacity		Dynamic	Reference	
Soil Type	Pile Type	Ultimate	Analysis Type	CAPWAP Ultimate	Author	Date
Soil	OP 610 mm	1344		2292	Rausche, Robinson and Likins	2004
Soil	PSC 610 mm x610 mm	3204		3097	Rausche, Robinson and Likins	2004
Soil	PSC 406 mm x406 mm	997		378	Rausche, Robinson and Likins	2004
Soil	PSC 406 mm x406 mm	961		481	Rausche, Robinson and Likins	2004
Soil	PSC 356 mm x356 mm	997		627	Rausche, Robinson and Likins	2004
Soil	PSC 406 mm x406 mm	2648		3453	Rausche, Robinson and Likins	2004
IGM - chalk	RC 275 mm x275 mm	1800		1560	Gravare and Hermansson	1980
IGM - Glacial Till	H 310x74	3605	Dav	3200	Thompson and Devata	1980
IGM - Glacial Till	CP 305 mm	2000	Dav	1780	Thompson and Devata	1980
IGM - Glacial Till	RC 305 mm	2310	Dav	2225	Thompson and Devata	1980
soil	H 310x74	1420	Dav	1160	Thompson and Devata	1980
soil	CP 305 mm	1335	Dav	1600	Thompson and Devata	1980
soil	H 310x74	2800	Dav	2890	Thompson and Devata	1980
soil	CP 305 mm	2450	Dav	2580	Thompson and Devata	1980
soil	Timber No 14	670	Dav	620	Thompson and Devata	1980
soil	RC 305 mm	1740	Dav	1510	Thompson and Devata	1980
IGM - Stiff Marl	CP 610 mm	3900	LPC	1610	Corte and Bustamante	1984
soil	PSC 900 mm to 1680 mm	3500		3500	Sanchez	1984
soil	PSC 900 mm to 1680 mm	5000		6000	Sanchez	1984
soil	RC 270 mm	460	Dav	535	Holm	1984
soil	RC 270 mm	300	Dav	310	Holm	1984
soil	RC 270 mm	1390	Dav	1210	Holm	1984
soil	RC 270 mm	990	Dav	820	Holm	1984
soil	RC 270 mm	690	Dav	750	Holm	1984
soil	CP 508 mm	360	Dav	361	Warrington	1988
soil	CP 508 mm	576	Dav	474	Warrington	1988
soil	CP 356 mm	344	Dav	477	Warrington	1988
soil	CP 508 mm	600	Dav	457	Warrington	1988
soil	CP 508 mm	280	Dav	436	Warrington	1988
soil	CP 90 mm	90		90	Nguyen, Berggren and Hansbo	1988
soil	CP 812 mm	5250	Dav	3200	Nguyen, Berggren and Hansbo	1988
soil	CP 298 mm	2170	Dav	2183	Cheng and Ahmad	1988
soil	CP 244 mm	1020	Dav	880	Cheng and Ahmad	1988
IGM-Till	CP 244 mm	2400	Dav	2375	Cheng and Ahmad	1988
soil	CP 244 mm	1630	Dav	1527	Cheng and Ahmad	1988
IGM-Shale	CP 324 mm	1080	Dav	921	Cheng and Ahmad	1988

Table 13. CAPWAP capacity (kN) and static load test results (kN) from the literature, continued.

Background Data		Static Capacity		Dynamic	Reference	
Soil Type	Pile Type	Ultimate	Analysis Type	CAPWAP Ultimate	Author	Date
IGM-Till	CP 324 mm	2935	Dav	2710	Cheng and Ahmad	1988
soil	PSC 400 mm	1420	Dav	1390	Thompson and Goble	1988
soil	PSC 610 mm	1760	Dav	1760	Thompson and Goble	1988
soil	PSC 500 mm	2180	Dav	1920	Thompson and Goble	1988
soil	PSC 500 mm	800	Dav	930	Thompson and Goble	1988
soil	CP 335 mm	2580	Dav	2670	Thompson and Goble	1988
soil	H 350 mm	3200	D/10	2777	Bustamante and Weber	1988
soil	H 350 mm	3700	D/10	3513	Bustamante and Weber	1988
soil	H 350 mm	5075	D/10	4966	Bustamante and Weber	1988
soil	H 350 mm	2020	D/10	1759	Bustamante and Weber	1988
soil	H 350 mm	2400	D/10	2107	Bustamante and Weber	1988
soil	H 350 mm	1800	D/10	1591	Bustamante and Weber	1988
soil	RC 280 mm	1600		1373	Chow et al.	1988
soil	H 350 mm	7250		4485	Huang	1988
IGM-Limestone	RC 355 mm	1270	BH	1200	Plesiotis	1988
IGM-Limestone	RC 450 mm	3333	BH	3166	Plesiotis	1988
IGM-Limestone	RC 450 mm	3777	BH	3666	Plesiotis	1988
IGM-Limestone	RC 450 mm	3900		3700	Seidel, Haustorfer and Plesiotis	1988
IGM-Limestone	RC 450 mm	4200		4118	Seidel, Haustorfer and Plesiotis	1988
IGM-Limestone	RC 450 mm	3600		3416	Seidel, Haustorfer and Plesiotis	1988
IGM-Limestone	PSC 600 mm	6840	Dav	6301	Seidel, Haustorfer and Plesiotis	1988
soil	PSC 600 mm	5341	Dav	4533	Yao et al.	1988
soil	PSC 600 mm	4724	Dav	4340	Yao et al.	1988
soil	CP 245 mm	1810		1807	Yao et al.	1988
soil	RC 250 mm	1250		1335	Fellenius	1988
IGM-Chalk	CP 762 mm	4850		5170	Skov and Denver	1988
soil	RC 300 mm	880		640	Skov and Denver	1988
soil	RC 350 mm	2450		2450	Skov and Denver	1988
soil	PSC 350 mm	2180		2050	Holloway and Romig	1988
soil	PSC 600 mm	2270	Max	2310	Likins et al.	1992
soil	PSC 450 mm	1666	Max	1702	Likins et al.	1992
soil	PSC 450 mm	2540		2668	Likins et al.	1992
soil	PSC 600 mm	2869		2615	Likins et al.	1992
soil	PSC 600 mm	3724		3617	Likins et al.	1992
soil	PSC 900 mm	4900		4210	Likins et al.	1992
soil	PSC 900 mm	6905		4994	Likins et al.	1992

Table 14. CAPWAP capacity (kN) and static load test results (kN) from the literature, continued.

Background Data		Static Capacity		Dynamic	Reference	
Soil Type	Pile Type	Ultimate	Analysis Type	CAPWAP Ultimate	Author	Date
soil	PSC 510 mm	6000	Dav	3580	Riker and Fellenius	1992
soil	PSC 600 mm	4300		3830	Seidel and Klingberg	1992
soil	PSC 600 mm	4420		4000	Seidel and Klingberg	1992
soil	Sheet Pile	1100		1344	Hartung, Meier and Rodatz	1992
soil	OP 2000 mm	32340		29400	Shioi, Yoshida, Meta and Homma	1992
soil	CP 244 mm	2070		2390	Fellenius, Edde and Beriault	1992
IGM-Marl	H 350 mm	2400	D/10	2600	Bustamante, Gianeselli and Schreiner	1992
IGM-Marl	H 350 mm	2000	D/10	2400	Bustamante, Gianeselli and Schreiner	1992
soil	RC 350 mm	4000		3486	Chapman and Wagstaff	1992
IGM-Phyllite	RC 350 mm	3600		3160	Seidel, Anderson and Morrison	1992
soil	OP 610 mm	4658.9		4922.5	Wakiya et al.	1992
soil	OP 610 mm	6762		2382.4	Wakiya et al.	1992
soil	PSC 1370 mm	1935		2450	Svinkin	2000
soil	PSC 1370 mm	2840		2880	Svinkin	2000
soil	PSC 1370 mm	3160		3480	Svinkin	2000
soil	PSC 610 mm	1841	Dav	1672	Svinkin and Skov	2000
soil	PSC 762 mm	2273	Dav	1601	Svinkin and Skov	2000
soil	H 310 mm	1400	Dav	1512	Svinkin and Skov	2000
soil	H 310 mm	1400	Dav	2002	Svinkin and Skov	2000
soil	OP 1200 mm	5500		5800	Seidel and Kalinowski	2000
soil	OP 1200 mm	18800		19400	Seidel and Kalinowski	2001
soil	OP 800 mm	4725		4530	Matsumoto et al.	2002
soil	Pipe	2165		2040	Matsumoto et al.	2002
soil	Rail	1200	D/10	1110	Lima	2000
IGM-Desnse Sand	Screw 850 mm	1500		1809	Cannon	2000
soil	CFA 600 mm	1700		2200	Cannon	2000
soil	OP 400 mm	2150	D/10	2200	Shibata et al.	2000
soil	OP 400 mm	3000	D/10	2500	Shibata et al.	2000
soil	PSC 300 mm	1900		1863	Zheng, Zheng and Chen	2000
soil	PSC 300 mm	1900		1881	Zheng, Zheng and Chen	2000
soil	PSC 300 mm	1980		2188	Zheng, Zheng and Chen	2000
soil	PSC 400 mm	2160		2051	Zheng, Zheng and Chen	2000
soil	OP 910 mm	10567		8303	Zhou Guoran and Wu Jiaduo	2000
soil	PSC 600 mm	8453		8001	Zhou Guoran and Wu Jiaduo	2000
soil	PSC 800 mm	5636		5448	Zhou Guoran and Wu Jiaduo	2000

Table 15. CAPWAP capacity (kN) and static load test results (kN) from the literature, continued.

Background Data		Static Capacity		Dynamic	Reference	
Soil Type	Pile Type	Ultimate	Analysis Type	CAPWAP Ultimate	Author	Date
soil	PSC 180 mm	262		216	Albuquerque and Carvalho	2000
soil	CFA 350 mm	1006	VV	877	Kormann et al.	2000
soil	CFA 350 mm	1473	VV	1700	Kormann et al.	2000
soil	CFA-D 450 mm	1800		1797	Klingberg and Mackenzie	2000
soil	PSC 350 mm	1657		1779	Holeyman et al.	2000
soil	PSC 350 mm	965		919	Holeyman et al.	2000

REFERENCES CITED

AASHTO (1996). "Standard Specifications for Highway Bridges." American Association of State Highway and Transportation Officials; Washington, D.C., 16th Edition.

Abu-Hejleh, N. M., M. W. O'Neill, D. Hanneman, and W. J. Attwooll. (2005). "Improvement of the Geotechnical Axial Design Methodology for Colorado's Drilled Shafts Socketed in Weak Rocks." *Journal of the Transportation Research Board*: Number 1936: pp. 100-107.

Akai, K. (1997). "Testing Methods for Indurated Soils and Soft Rocks- Interim Report."*Geotechnical Engineering of Hard Soils-Soft Rocks*: Proceedings of an International Symposium for ISSMFE, IAEG and ISRM in Athens, Greece, September 1993, 1707-1737. A. A. Balkema.

Albuquerque, P. J. R., and D. de Carvalho (2000). "Dynamic Load Test and Elastic Rebound Analysis for Estimation of the Bearing Capacity of Piles in Residual Soil." Proceedings of the 6th International Conference on the Application of Stress-Wave Theory to Piles: Sao Paulo, Brazil; 667-681.

Allen, T. (2007). "Development of New Pile-Driving Formula and Its Calibration for Load and Resistance Factor Design." *Transportation Research Record*: Journal of the Transportation Research Board. No. 2004; 20-27.

Atalla, M. (1993). "Description, Classification and testing of Calcareous Rock Similar Soils." *Geotechnical Engineering of Hard Soils-Soft Rocks*: Proceedings of an International Symposium for ISSMFE, IAEG and ISRM in Athens, Greece, September 1993, 21-27. A. A. Balkema.

Atkinson, J. H., M. R. Coop, S. E. Stallebrass and G. Viggiani. (1993). "Measurement on Stiffness of Soils and Weak Rocks in Laboratory Tests." *The Engineering Geology of Weak Rock*: Proceedings of the 26th Annual Conference of the Engineering Group Geological Society in Leeds, UK, September 1990, 21-28. A. A. Balkema.

Baker, V. A., N. A. Thomsen, C. R. Nardi, and M. J. Talbot. (1984). "Pile Foundation Design Using Pile Driving Analyzer." *Analysis and Design of Pile Foundations.* Eds. Joseph Ray Meyer. New York: American Society of Civil Engineers. 119-137.

Briaud, J. and L. M. Tucker. (1984). "Residual Stresses in Piles and the Wave Equation." *Analysis and Design of Pile Foundations.* Eds. Joseph Ray Meyer. New York: American Society of Civil Engineers. 119-137.

Brouillette, R. P., R. E. Olsen and J. R. Lai. (1993). "Stress-Strain characteristics of Eagle Ford Shale." *Geotechnical Engineering of Hard Soils-Soft Rocks*: Proceedings of an International Symposium for ISSMFE, IAEG and ISRM in Athens, Greece, September 1993, 397-404. A. A. Balkema.

Burgert, C and Buu, T. (2007). "Correlation of Computer Program DRIVEN with ITD Pile Case Histories." 33rd Northwest Geotechnical Workshop in Couer D' Alene, Idaho, September 2007; Presentation Slides.

Bustamante, M., L. Gianeselli and C. Schreiner (1992). "Comparative Study on the Load Bearing Capacity of Driven Steel H-Piles in a Layered Marl." Proceedings of the 4th International Conference on the Application of Stress-Wave Theory to Piles: the Hague, Netherlands; 531-536.

Bustamante, M., and H. Weber (1988). "Dynamic and Static Measurements of Steel H-Pile Capacities." Proceedings of the 3rd International Conference on the Application of Stress-Wave Theory to Piles: Vancouver, British Columbia, Canada; 579-590.

Campos,J. O., A. B. Paraguassu, L. Dobereiner, L. Soares and E. B. Frazao. (1993). "The Geotechnical Behavior of Brazilian Sedimentary Rocks." *Geotechnical Engineering of Hard Soils-Soft Rocks*: Proceedings of an International Symposium for ISSMFE, IAEG and ISRM in Athens, Greece, September 1993, 69-84. A. A. Balkema.

Cannon, J. G. (2000). "The Application of High Strain Dynamic Pile Testing to Screwed Steel Piles." Proceedings of the 6th International Conference on the Application of Stress-Wave Theory to Piles: Sao Paulo, Brazil; 393-398.

Cannon, J. G. (2000). "Case-Study on the Application of High Strain Dynamic Pile Testing to Non-Uniform Bored Piles." Proceedings of the 6th International Conference on the Application of Stress-Wave Theory to Piles: Sao Paulo, Brazil; 399-402.

Chapman, G. A. and J. P. Wagstaff (1992). "Predictions of Pile Performance Using Dynamic Testing." Proceedings of the 4th International Conference on the Application of Stress-Wave Theory to Piles: The Hague, Netherlands; 537-543.

Cheng, S. S. M., and S. A. Ahmad (1988). "Dynamic Testing versus Static load Test: Five Case Histories." Proceedings of the 3rd International Conference on the Application of Stress-Wave Theory to Piles: Vancouver, British Columbia, Canada; 477-489.

Chow, Y. K., K. Y, Wong, G. P. Karuanaratne, and S. L. Lee. (1988). "Estimation of Pile Capacity from Stress-Wave Measurements." Proceedings of the 3rd International

Conference on the Application of Stress Wave theory to Piles: Vancouver, British Columbia, Canada; 626-634.

Clarke, B. G. and A. Smith (1993). "Self-Boring Pressuremeter Tests in Weak Rocks." *The Engineering Geology of Weak Rock*: Proceedings of the 26th Annual Conference of the Engineering Group Geological Society in Leeds, UK, September 1990; 233-241.

Clayton, C. R. I., and J. F. Serratrice. (1997). "General Report Session 2: The Mechanical Properties and Behavior of Hard Soils and Soft Rocks." *Geotechnical Engineering of Hard Soils-Soft Rocks*: Proceedings of an International Symposium for ISSMFE, IAEG and ISRM in Athens, Greece, September 1993, 1839-1878. A. A. Balkema.

CDOT (2005). "Colorado Department of Transportation Standard Specifications: Road and Bridge Construction."

Colorado Department of Transportation (2006). "Draft CDOT Driven Steel Piles State-of the Practice: Geotechnical Investigation and Recommendation Perspective." Internal Report Colorado Department of Transportation.

Corte, J. F., and M. Bustamante (1984). "Experimental Evaluation of the Determination of Pile Bearing Capacity from Dynamic Tests." Proceedings of the 2nd International Conference on the Application of Stress-Wave Theory to Piles: Stockholm, Sweden; 17-24.

Cripps, J. C, and R. K. Taylor. (1981). "The Engineering Properties of Mudrocks." *The Quarterly Journal of Engineering Geology*. Volume 14: pp. 325-346.

Das, B. M. (2005). Principles of Foundation Engineering. 5th Edition.

de Freitas, H. (1993). "Introduction to Session 1.2: Weak Arenaceous Rock." *The Engineering Geology of Weak Rock*: Proceedings of the 26th Annual Conference of the Engineering Group Geological Society in Leeds, UK, September 1990, 115-123.

Dobereiner, L. and M. H. de Freitas. (1986). "Geotechnical Properties of Weak Sandstones." *Geotechnique*. Volume 36 (March 1986), Issue 1: pp.79-94.

El-Sohboy, M. A., S. O. Mazen and M. I. Aboushook. (1993). "Geotechnical Aspects on Behavior of Weakly Cemented and Over-consolidated Soil Formations." *Geotechnical Engineering of Hard Soils-Soft Rocks*: Proceedings of an International Symposium for ISSMFE, IAEG and ISRM in Athens, Greece, September 1993, 91-104. A. A. Balkema.

Fellenius B. H. (1988). "Variation of CAPWAP Results as a Function of the Operator." Proceedings of the 3rd International Conference on the Application of Stress Wave Theory to Piles: Vancouver, British Columbia, Canada; 814-825.

Fellenius, B. H., R. D. Edde and L. L. Beriault. (1992). "Dynamic and Static Testing for Pile Capacity in a Fine-Grained Soil." Proceedings of the 4th International Conference on the Application of Stress-Wave Theory to Piles: The Hague, Netherlands; 401-408.

Findlay, J. D. and N. J. Brooks. (1995). "Requirements for Deep Foundation Execution in Weak Rocks." *The Interplay Between Geotechnical Engineering and Engineering Geology*: Proceedings of the 11th European Conference on Soil Mechanics and Foundation Engineering in Copenhagen, Germany, May 1995, pp. 1-10.

Finno, R. J., and E. R. Budyn. (1988). "Panel Report: Design Parameters for Drilled Shafts in Intermediate Geomaterials." *The Geotechnics of Hard Soils-Soft Rocks* Proceedings of the 2nd International Symposium on Hard Soils, Soft Rocks in Naples, Italy, October 1988, 35-40. A. A. Balkema.

Gannon, L. A., G. G. T. Masterton, W. A. Wallace, and D. Muir Wood. (1999). Piled Foundations in Weak Rock. London: Ciria.

Gerwick, B. C. (2004). "Pile Installation in Difficult Soils" *Journal of Geotechnical and Geoenvironmental Engineering*. Volume 130, Issue 5: pp.454-460.

Gravare, C. J. and I. Hermansson (1980). "Practical Experiences of Stress-wave Measurements." Proceedings of the 1st International Conference on the Application of Stress-Wave Theory to Piles: The Hague, Netherlands; 99-120.

GRLWEAP 2005, Pile Dynamics Incompany. Computer software.

Harberfield, C. M. and I. W. Johnston. (1993). "Factors Influencing the Interpretation of Pressuremeter Tests in Soft Rock." *Geotechnical Engineering of Hard Soils-Soft* in Athens, Greece, September 1993, 91-104. A. A. Balkema.

Hartung, M., K. Meier and W. Rodatz (1992). "Dynamic Pile Test on Sheet Piles." Proceedings of the 4th International conference on the Application of Stress-Wave Theory to Piles: The Hague, Netherlands; 259-264.

Hassan, K. M., M.W O'Neill, S. A. Sheikh and C. D. Ealy. (1997). "Design Method for Drilled Shafts in Soft Argillaceous Rock." *Journal of Geotechnical and Geoenvironmental Engineering*. Volume 123, Issue 3: pp. 272-280.

Hassan, K. M. and M. W. O'Neill. (1997) "Side Load-Transfer Mechanisms in Drilled Shafts in Soft Argillaceous Rock." *Journal of Geotechnical and Geoenvironmental Engineering.* Volume 123, Issue 2: pp. 145-152.

Holeyman, A., J. Maertens, C. Legrand, N. Huybrechts. (2000). "Results of an International Pile Dynamic Test Prediction Event." Proceedings of the 6th International Conference on the Application of Stress-Wave Theory to Piles: Sao Paulo, Brazil; 725-732.

Holloway, D. M., and G. A. Romig (1988). "CPT and Dynamic Pile Testing in Foundation Design." Proceedings of the 3rd International Conference on the Application of Stress Wave Theory to Piles: Vancouver, British Columbia, Canada; 889.

Holm, G. (1984). "Dynamic and Static Load Testing of Friction Piles in a Loose Sand." Proceedings of the 2nd International Conference on the Application of Stress Wave Theory to Piles: Stockholm, Sweden; 240-243.

Hooley, P. and S. R. L. Brooks (1993). "The Ultimate Shaft Frictional Resistance Mobilized by Bored Piles in Over-consolidated Clays and Socketed into Weak and Weathered Rock." *The Engineering Geology of Weak Rock*: Proceedings of the 26th Annual Conference of the Engineering Group Geological Society in Leeds, UK, September 1990, 447-455. A. A. Balkema.

Hsu, S. C., and P. P. Nelson. (1993). "Characterization of Cretaceous Clay Shales in North America." *Geotechnical Engineering of Hard Soils-Soft Rocks*: Proceedings of an International Symposium for ISSMFE, IAEG and ISRM in Athens, Greece, September 1993, 139-146. A. A. Balkema.

Huang, Shao-Ming (1988). "Application of Dynamic measurement on Long H-Pile Driven into Soft Ground in Shanghai." Proceedings of the 3rd International Conference on the Application of Stress-Wave theory to Piles: Stockholm, Sweden; 635-643.

Johnston, I. W. (1989). "Discussion Leaders Report: Material Properties of Weak Rock." Proceedings of the International Conference on Soil Mechanics and Foundation Engineering in Montreal, Canada: pp. 2831-2833.

Johnston, I. W., C. M. Haberfield and J. K. Kodikara. (1993). "Predicting the side Resistance of Piles in Soft Rock." *Geotechnical Engineering of Hard Soils-Soft Rocks*: Proceedings of an International Symposium for ISSMFE, IAEG and ISRM in Athens, Greece, September 1993, 969-976. A. A. Balkema.

Johnston, I. W. and E. A. Novello. (1993). "Soft Rocks in the Geotechnical Spectrum." *Geotechnical Engineering of Hard Soils-Soft Rocks*: Proceedings of an International Symposium for ISSMFE, IAEG and ISRM in Athens, Greece, September 1993, 177-184. A. A. Balkema.

Johnston, I. W. (1995). "Rational Determination of the Engineering Properties of Weak Rocks." *Geotechnical Engineering Advisory Panel*: Proceedings of the Institution of Civil Engineers, April 1995, 86-92.

Klingberg, D. J. and P. Mackenzie (2000). "Static and Dynamic Testing of the 'Campile" – A Displacement, Cast-In-Situ Pile." Proceedings of the 6th International Conference on the Application of Stress-Wave Theory to Piles: Sao Paulo, Brazil; 715-718.

Kormann, A. M., P. R. Chamecki, L Russo Neto, L. Antoniutti Neto, and G. Bernardes. (2000). "Behavior of Short CFA Piles in an Overconsolidated Clay Based on Static and Dynamic Load Tests." Proceedings of the 6th International Conference on the Application of Stress-Wave Theory to Piles: Sao Paulo, Brazil; 707-714.

Krauter, E. (1997). "General Co-report: Geological and Geotechnical Features, Investigation and Classification of Hard Soils." *Geotechnical Engineering of Hard Soils-Soft Rocks*: Proceedings of an International Symposium for ISSMFE, AEG and ISRM in Athens, Greece, September 1993, 1819-1826. A. A. Balkema.

Likins, G., J. Dimaggio, F. Rausche and W. Teferra. (1992). "A Solution for High Case Damping Constants in Sands." *Proceedings of the Fourth International Conference on the Application of Stress Wave Theory to Piles*: The Netherlands; 117-120.

Likins, G. and Rausche, F. (2004). "Correlation of CAPWAP with Static Load Tests." Proceedings of the 7th International Conference on the Application of Stress-wave Theory to Piles: Petaling Jaya, Selangor, Malaysia; 153-165.

Lima, H. M. (2000). "Analysis of Dynamic Load Tests on Steel Rail Piles." Proceedings of the 6th International Conference on the Application of Stress-Wave Theory to Piles: Sao Paulo, Brazil; 375-381.

Marinos, P. G. (1997). "General Report: Hard Soils-Soft Rocks: Geological Features with Special Emphasis to Soft Rocks." *Geotechnical Engineering of Hard Soils-Soft Rocks*: Proceedings of an International Symposium for ISSMFE, IAEG and ISRM in Athens, Greece, September 1993, 1807-1818. A. A. Balkema.

Mathias D., and M. Cribbs (1998). "DRIVEN 1.0: A Microsoft Windows Based Program for Determining Ultimate Static Pile Capacity." Federal Highway Administration.

Matsumoto, T., K. Fujita, O. Kusakabe, M. Okahara, N. Kawabata and S. Nishimura. (2002). "Dynamic Load Testing and Statnamic Load Testing for Acceptance and Design of Driven Piles in Japan." Proceedings of the 6th International Conference on the Application of Stress-Wave Theory to Piles: Sao Paulo, Brazil; 335-345.

Mayne, P.W. & Harris, D.E. (1993). Axial Load-Displacement Behavior of Drilled Shaft Foundations in Piedmont Residuum. Research Report No. E-20-X19 submitted to Federal Highway Administration by Georgia Tech Research Corp, 162 p.

Nevels, J., and J. G. Laguros. (1993). "Correlation of engineering Properties of the Hennessy Formation Clays and Shales." *Geotechnical Engineering of Hard Soils Soft Rocks*: Proceedings of an International Symposium for ISSMFE, IAEG and ISRM in Athens, Greece, September 1993, 215-222. A. A. Balkema.

Nguyen. T. T., B. Berggren and S. Hansbo (1988). "A New Soil Model for Driving and Drivability Analysis." Proceedings of the 3rd International Conference on the Application of Stress-Wave Theory to Piles: Vancouver, British Columbia, Canada; 353-367.

O'Neill, M. W., Townsend, F. C., Hassan, K. M., Buller, A., and Chen, P. S. (1996). *Load Transfer for Drilled Shafts in Intermediate Geomaterials*. U. S. Department of Transportation Publication No. FHWA-RD-95-172.

Oliveira, R. (1993). "Weak Rock Materials." *The Engineering Geology of Weak Rock*: Proceedings of the 26th Annual Conference of the Engineering Group Geological Society in Leeds, UK, September 1990, pp. 5-15. A. A. Balkema.

Papageorgiou, O. (1997). "Soft Rocks." *Geotechnical Engineering of Hard Soils-Soft Rocks*: Proceedings of an International Symposium for ISSMFE, IAEG and ISRM in Athens, Greece, September 1993, 1881-1883. A. A. Balkema.

Plesiotis, S. (1988). "Dynamic Testing for Highway Bridge Piling." Proceedings of the 3rd International Conference on the Application of Stress-Wave Theory to Piles; Vancouver, British Columbia, Canada; 668-678.

Rausche, F., L. Liang, R. C. Allin, D. Rancman. (2004). "Applications and Correlations of the Wave Equation Analysis Program GRLWEAP." Proc. 7th Intl. Conf. on the Application of Stress-wave Theory and Piles in Petaling Jaya, Selanqor, Malaysia 2004. 107-123.

Rausche, F., B. Robinson and G. Likins. (2004). "On the Prediction of Long Term Pile Capacity Form End-of- Driving Information." Current Practices and Future Trends in Deep Foundations, GSP No. 125 (2004): pp 77-95.

Reddy, E. S. and K. R. Sastri. (1993). "Geotechnical Investigation in Hard Soils of Hyderabad Region." *Geotechnical Engineering of Hard Soils-Soft Rocks*: Proceedings of an International Symposium for ISSMFE, IAEG and ISRM in Athens, Greece, September 1993, 243-252. A. A. Balkema.

Reese, L., W. M. Isenhower, S. Wang (2005). Analysis and Design of Shallow and Deep Foundations; John Wiley and Sons, Inc.

Reeves, G. M., J. Hilary and D. Screaton. (1993). "Site Investigations for Piled Foundations in Mercia Mudstones, Teesside, Cleveland County." *The Engineering Geology of Weak Rock*: Proceedings of the 26th Annual Conference of the Engineering Group Geological Society in Leeds, UK, September 1990, pp. 457-463. A. A. Balkema.

Riker, R. E. and B. H. Fellenius (1992). "A Comparison of Static and Dynamic Pile Test." Proceedings of the 4th International Conference on the Application of Stress Wave Theory to Piles: The Hague, Netherlands; 143-152.

Sanchez Del Rio, J. (1984). "Stress-Wave Measurements of Large Raymond-Type Piles." Proceedings of the 2nd International Conference on the Application of Stress Wave Theory to Piles: Stockholm, Sweden; 221-228.

Schmidt, H. H. and T. K. Rumpelt. (1993). "Pile Load Capacity in Pre-consolidated Keuper Marls of Southwest Germany." *Geotechnical Engineering of Hard Soils Soft Rocks*: Proceedings of an International Symposium for ISSMFE, IAEG and ISRM in Athens, Greece, September 1993, 1021-1028. A. A. Balkema.

Seidel, J. P., I. J. Haustorfer and S. Plesiotis (1988). "Comparison of Dynamic and Static Testing for Piles Founded into Limestone." Proceedings of the 3rd International Conference on the Application of Stress-Wave Theory to Piles: Vancouver, British Columbia, Canada; 717-723.

Seidel, J. P., G. D. Anderson and N. J. Morrison (1992). "The effects of Pile Relaxation on Toe Capacity and Stiffness." Proceedings of the 4th International Conference on the Application of Stress-Wave Theory to Piles: The Hague, Netherlands; 619-626.

Seidel, J. P. and D. J. Klingberg (1992). "The Instantaneous Liquefaction of Silty Soils During Installation of Displacement Piles." Proceedings of the 4th International Conference on the Application of Stress-Wave Theory to Piles: The Hague, Netherlands; 153-158.

Seidel, J. P. and C. M. Haberfield (1995). "The Axial Capacity of Pile Sockets in Rocks and Hard Soils." *Ground Engineering*. (March 1995): pp. 33-38.

Seidel, J. P. and M. Kalinowski (2000). "Pile Set-Up in Sands." Proceedings of the 6th International Conference on the Application of Stress-Wave Theory to Piles; 335-344.

Shibata, A., N. Kawabata, Y. Wakiya, Y. Yoshizawa, M. Hayashi and T. Matsumoto (2000). "A Comparative Study of Static, Dynamic and Statnamic Load Tests of Steel Pile Piles Driven in Sand." Proceedings of the 6th International Conference on the Application of Stress-Wave Theory to Piles: Sao Paulo, Brazil; 583-590.

Shioi, Y., O. Yoshida, T. Meta, and M. Homma. (1992). "Estimation of bearing Capacity of Steel Pipe Pile by Static Loading Test and Stress-Wave Theory." Proceedings of the 4th International Conference on the Application of Stress-Wave Theory to Piles: The Hague, Netherlands; 325 330.

Skov, R., and H. Denver (1988). "Time-Dependence of Bearing Capacity of Piles." Proceedings of the 3rd International Conference on the Application of Stress-Wave Theory to Piles: Vancouver, British Columbia, Canada; 879-888.

Smith, A. E. L. (1960). "Pile Driving Analysis by the Wave Equation." *Journal of the Soil Mechanics and Foundations Division*, ASCE, vol. 86, no. SM4, August.

Sorensen, T., S. E. Hansen and A. M. Myavang. (1993). "Stress influence on Rate ofPenetration." *Geotechnical Engineering of Hard Soils-Soft Rocks*: Proceedings of an International Symposium for ISSMFE, IAEG and ISRM in Athens, Greece, September 1993, 287-292. A. A. Balkema.

Spink, T. W. and D. R. Norbury. (1993). "The Engineering Geological Description of Weak Rocks and Over-consolidated Soils." *The Engineering Geology of Weak Rock*: Proceedings of the 26th Annual Conference of the Engineering Group Geological Society in Leeds, UK, September 1990, pp. 289-301. A. A. Balkema.

Svinkin, M. R. (2000). "Time Effect in Determining Pile Capacity by Dynamic Methods." Proceedings of the 6th International Conference on the Application of Stress-Wave Theory to Piles: Sao Paulo, Brazil; 35-40.

Svinkin, Mr. R., and R. Skov (2000). "Dynamic Pile Testing and Finite Element Calculations for the Bearing Capacity of a Quay Wall Foundation - Container Terminal Altenwerder, Port of Hamberg." Proceedings of the 6th International Conference on the Application of Stress-Wave Theory to Piles: Sao Paulo, Brazil; 249-274.

Svinkin, M. R. and R. Skov (2000). "Set-Up Effect in Cohesive Soil in Pile Capacity." Proceedings of the 6th International Conference on the Application of Stress Wave Theory to Piles: Sao Paulo, Brazil; 267-274.

Tanimoto, C. (1982). "Engineering Experience with Weak Rocks in Japan." *Issues in Rock Mechanics*: Proceedings of the 23rd Symposium on Rock Mechanics in Berkeley, California, August 1982, pp. 999-1014.Society of Mining Engineers of the American Mining, Metallurgical and Petroleum engineers, Inc.

Thompson, R. P. and M. Devata (1980). "Evaluation of the Ultimate Bearing Capacity of Different Piles." Proceedings of the 1st International Conference on the Application of Stress Wave Theory to Piles: The Hague, Netherlands; 163-195.

Thompson, R. P. and Goble (1988). "High Case Damping Constants in Sand." *Proceedings of the Third International Conference on the Application of Stress Wave Theory to Piles*: Ottawa, Canada; 555-564.

Thompson, R. P. and B. A. Leach. (1988). "The Application of the SPT in Weak Sandstones and Mudstone Rocks." Penetration Testing in the UK. London: Thomas Telford, 1988. pp. 83-86.

Tomlinson, M. J. (1977). "Preface." Piles in Weak Rock. London: Balkema.

Wakiya, Y., O. Hashimoto, M. Fukuwaka, T. Oki, H. Shinomiya and F. Ozeki. (1992). "Ability of Dynamic Testing and Evaluation of Bearing Capacity Recovery from Excess Pore Pressure measured in the Field." Proceedings of the 4th International Conference on the Application of Stress-Wave Theory to Piles: The Hague, Netherlands; 665-670.

Warrington, D. C. (1988). "A New Type of Wave Analysis Program." Proceedings of the 3rd International Conference on the Application of Stress-Wave Theory to Piles: Vancouver, British Columbia, Canada; 142-151.

Webb, D. L. (1977). "The Behavior of Bored Piles in Weathered Diabase." *Piles in Weak Rock.* London: The Institution of Civil Engineers. 63-72.

Wu, B., J. R. Marsden and J. A. Hudson. (1993). "Undrained Mechanical Behavior of Mudstone." *The Engineering Geology of Weak Rock*: Proceedings of the 26th Annual Conference of the Engineering Group Geological Society in Leeds, UK, September 1990, pp. 87-94. A. A. Balkema.

Yao, H. L., C. S. Shih, T. C. Kao and R. F. Wang. (1988). "Experiences of Dynamic Pile Loading Tests in Taiwan." Proceedings of the 3rd International Conference on the Application of Stress-Wave Theory to Piles: Vancouver, British Columbia, Canada; 805-813.

Yilmazer, I. (1993). "Engineering Geological properties of Caliche Consisting of Soft Pan and Hard Pan Levels." Geotechnical Engineering of Hard Soils-Soft Rocks: Proceedings of an International Symposium for ISSMFE, IAEG and ISRM in Athens, Greece, September 1993, 319-323. A. A. Balkema.

Zheng, Y. M., J. M. Zheng and B. Chen (2000). "Correlation Analyses of Dynamic and Static Load Tests for Nine Piles." Proceedings of the 6th International Conference on the Application of Stress-Wave Theory to Piles: Sao Paulo, Brazil; 651-656.

Zhou, L. B., and J. Wu (2000). "Comparative Analysis of Dynamic and Static Test of Foundation Pile." Proceedings of the 6th International Conference on the Application of Stress-Wave Theory to Piles: Sao Paulo, Brazil; 673-676.